

ANDRESSA DE ZAWADZKI

Improving meat quality through cattle feed enriched with mate  
extract: an integrated approach of the metabolic profile and  
redox chemistry of meat

Ph. D. Thesis submitted to the São Carlos Chemistry  
Institute from University of São Paulo for the degree  
of Doctor of Organic Chemistry and Biochemistry

Supervisors: Professor Daniel R. Cardoso, São Carlos Chemistry Institute,  
University of São Paulo  
Professor Leif H. Skibsted, Department of Food Science,  
University of Copenhagen

Co-supervisor: Luis Alberto Colnago, EMBRAPA Instrumentation, Brazilian  
Agricultural Research Corporation

São Carlos, June of 2017.

## Preface

The present PhD thesis is intended to fulfil the requirements for the PhD degree at São Carlos Chemistry Institute, University of São Paulo, Brazil, and at the Department of Food Science, University of Copenhagen, Denmark. The project has been done through the collaboration between Brazil and Denmark in the Food Science Research Program “BEAM - Bread and Meat for the Future” which involved University of Copenhagen, University of São Paulo, Embrapa Pecuária Sudeste and Embrapa Instrumentação. The research program was granted by FAPESP (Grant 2011/51555-7 and 2009/54040-8), by the Danish Research Council for Strategic Research (Grant 11-116064), by the Brazilian National Research Council - CNPq (Grants 305385/2009-7 and 141525/2013-4) and by CAPES – Coordenação de Aperfeiçoamento de Pessoal de Nível Superior (Science without Borders fellowship Grant 99999.008903/2014-00).

Initially, I would like to thank my supervisors Prof. Dr. Daniel Rodrigues Cardoso, from São Carlos Chemistry Institute, Prof. Dr. Leif Skibsted, from University of Copenhagen and Prof. Dr. Luiz Alberto Colnago, from Embrapa Instrumentação, for the helpful advice, patience, dedication, friendship and inspiration. I feel honoured for having the opportunity to enhance my knowledge through the collaboration with such brilliant minds.

I wish to particularly thank to CAPES for the Science without Borders fellowship that allow me the opportunity to do part of my research at University of Copenhagen (KU).

I would like to thank all the employees of the IQSC and of the KU that have done part of my work, specially, the Laboratory Technician Thiago Abrahão and the technicians of the IQSC’s NMR Lab. I would like to thank the academic staff of the KU, particularly, the secretaries Lisbet Christensen and Henriette Hansen. I would like to thanks Dr. Alberto

Grossi for providing advice on immunoblotting techniques and the master student Ceder Alloo for helping me to finish the Western Blot e Oxyblot experiments.

I wish to thank all the employees of Embrapa Pecuária Sudeste, particularly, Dr. Renata T. Nassu, Dr. Rymer R. Tullio, Dr. Alexandre Berndt, Marília P. Vidal and Maria Ligia Pacheco, for making possible the animal trials with cattle. I am thankful to Prof. Menten, from ESALQ, for the collaboration with the animal feeding trials with  $\beta$ -acids from hops as supplement. Centroflora Group is acknowledging for provide the mate extract.

I would like to thank Prof. Dr. Antonio G. Ferreira and his PhD student Clayton R. Oliveira for allowing me to use the NMR facilities at Federal University of São Carlos (UFSCar) and for the advice and the collaboration on untargeted NMR metabolomics.

I would like to thank to all of my colleges from Inorganic Chemistry and Food Chemistry at IQSC and from the Food Chemistry from KU for creating a social and motivating atmosphere. I would like to thank my Lab colleagues Papa, Silvia, Natália, Luíz, Marcella, Regina, Willy, Fernanda, Fernando, Eduardo, Augusto, Anna, Antônio, Carlos, Chen Hong, Dani Truzzi, Daniele, Ecem, Henrique, Inara, Jennifer, João, Marcella, Marcela Portes, Patrícia, Pedro, Silmara, Thiago japa, Zichen. A very special thank to my dear friend Martina who shared the office with me at the department of Food Science at University of Copenhagen and, to my Brazilian friendsat KU, André, Edelvan, Alan and Mari. I wish to thank my co-workers and friends Leandro and Carol.

A very special thank to all of my friends in São Carlos, specially, Igor and Ana for helping me with protein structures and, Heline and Alana. I also wish to thank all of the friends that I have made during my training sessions, particularly the colleges of my triathlon team Titan Sports Training and my coach Raphael.

Finally, I wish to thank very much my boyfriend Gustavo for sharing knowledge and good experiences with me along my PhD studies. I would like to thank my family, specially my

twin sister Krissia that has encouraged me to always move on and contributed with friendship and fruitful discussions on science topics.

“To myself I am only a child playing on the beach, while vast oceans of truth lie undiscovered before me”

(Isaac Newton)

## Resumo

O uso de extrato de plantas na suplementação tem sido considerado uma potencial alternativa para melhorar a estabilidade redox da carne. Alguns compostos bioativos presentes nos extratos de plantas atuam como antioxidantes e podem melhorar a saúde e o bem estar do animal e proteger a carne da oxidação. Propriedades farmacológicas e efeitos antioxidantes têm sido demonstrados em extratos de lúpulo e erva mate. Porém, os efeitos do uso de extrato de lúpulo e de erva mate como suplemento em dieta animal no perfil metabólico e na estabilidade redox da carne ainda não foram reportados. A adição de 0,5%, 1,0% e 1,5% de extrato de erva mate a uma ração composta de milho e soja destinada à alimentação de gado resultou no aumento da concentração de inosina monofosfato, creatina, carnosina e ácido linoléico conjugado na carne. A tendência à formação de radicais livres em homogenatos de carne diminuiu conforme aumentou o teor de erva mate na ração indicando um aumento da resistência da carne à oxidação. A adição de extrato de lúpulo (0, 30 ppm, 60 ppm e 240 ppm) à ração de frangos de corte promoveu efeitos significativos na concentração média de metabólitos polares que são de relevância para a qualidade da carne. As maiores diferenças nos perfis metabólicos entre o grupo controle (sem suplemento) e as amostras de carne de frango que foi alimentado com ração suplementada com  $\beta$ -ácidos foram obtidas usando 30 ppm de lupulonas na dieta. Como determinado pela técnica de spin-trapping, uma maior estabilidade redox foi observada nas amostras relacionadas aos animais alimentados com 30 ppm de lupulonas e podem ser relacionadas a um maior nível de antioxidantes endógenos, especialmente anserina, carnosina e NADH. Miosina e actina demonstraram ser os alvos principais da oxidação de proteínas em carne de frango. As proteínas miofibrilares de animais alimentados com  $\beta$ -ácidos mostraram ser menos susceptíveis à oxidação quando comparado ao grupo controle. Extratos de mate e de  $\beta$ -ácidos demonstraram ser aditivos promissores para dieta animal de gado e frango, respectivamente, e podem melhorar a estabilidade oxidativa, o valor nutricional, a qualidade sensorial e a aceitação da carne.

## Abstract

The use of plant extracts in animal feeding trials has been considered as a potential alternative to improve the redox stability of meat. Bioactive compounds from plant extracts can provide the antioxidative mechanisms required to improve animal health and welfare and, to protect meat against oxidation. Pharmacological properties and antioxidant effects have been associated to the extract of hops and to the extracts of yerba mate. However, the effects of hops and yerba mate as dietary supplement for animal feeding on the metabolic profile and the redox stability of meat have not been reported yet. Addition of extract of mate to a standard maize/soy feed at a level of 0.5, 1.0 or 1.5% to the diet of feedlot for cattle resulted in an increased level of inosine monophosphate, creatine, carnosine and of conjugated linoleic acid in the fresh meat. The tendency to radical formation in meat slurries as quantified by EPR spin-trapping decreased for increasing mate extract addition to feed especially after storage of the meat indicating an increased resistance to oxidation for meat. Addition of hops extract at different levels (0, 30 ppm, 60 ppm, 240 ppm) to the diet of broilers demonstrated to have significant effects on the averaged concentration of polar metabolites that are of relevance for meat quality. The major metabolic differences between control group (no supplements) and broilers fed different levels of  $\beta$ -acids were achieved using 30 ppm of supplement. As determined by EPR spin-trapping, increased redox stability was obtained in the samples referring to the animals fed 30 ppm of lupulones and may be related to the highest level of endogenous antioxidants, especially anserine, carnosine and NADH. Myosin and actin were recognized as the main targets of protein oxidation in meat. Myofibrillar proteins from animals fed with hops  $\beta$ -acids showed to be less susceptible to oxidation when compared to control group. Mate and hops  $\beta$ -acids extracts demonstrated to be promising additives to feedlot for, respectively, cattle and broilers and can improve the oxidative stability, nutritive value, sensory quality, and consumer acceptance of meat.

## List of Figures

<b>Figure 1.</b> Structure of horse heart deoxymyoglobin obtained from PDB 5d5r. Drawing was prepared with UCSF Chimera software.....	26
<b>Figure 2.</b> Proposed mechanism for the oxidation of myosin by H <sub>2</sub> O <sub>2</sub> -activated heme iron to yield protein radicals. Adapted from Lund et. al, 2008. ....	29
<b>Figure 3.</b> Lipid peroxidation cycle describing the three main reaction pathways related to the initiation of the oxidative processes in foods: I) Initiation of a free radical chain reaction from the activation of oxygen yielding hydroxyl radicals or from the production of free radicals by oxidants or by irradiation; II) Enzymatic formation of lipid hydroperoxides due to the activity of lipoxygenase; III) Photosensitized formation of lipid hydroperoxides through formation of singlet oxygen or through direct radical generation. Adapted from Carlsen et al, 2005. ....	30
<b>Figure 4.</b> Tumorigenesis and the role of inflammation in the cancer development. ROS = reactive oxygen species; RNS = reactive nitrogen species; NO = nitric oxide; PGs = prostaglandins; ODC = ornithine decarboxylase; MMP = matrix metalloproteinase; VEGF = vascular endothelial growth factor. Adapted from Pan et al., 2010. ....	31
<b>Figure 5.</b> Structure of the β-acids that are found in hops.....	35
<b>Figure 6.</b> Structure of the methylxantines caffeine, theophylline and theobromine. ....	36
<b>Figure 7.</b> Structure of ursolic acid and oleanolic acid. ....	36
<b>Figure 8.</b> Chemical structure of polyphenols found in yerba mate.....	37
<b>Figure 9.</b> Relationship between genome, transcriptome, proteome and metabolome. Adapted from Gerszten and Wang, Nature, 2008.....	39
<b>Figure 10.</b> Basic workflow for Foodomic analysis: NMR spectroscopy used for monitoring untargeted and targeted metabolomics in conjunction to statistical analysis. ....	40
<b>Figure 11.</b> Energy levels for a nucleus with spin quantum number $m = \frac{1}{2}$ . ....	41
<b>Figure 12.</b> Nucleus precession in the presence of a magnetic field. ....	42
<b>Figure 13.</b> Transition between two different spin states due to the absorption of radio frequency energy .....42	42
<b>Figure 14.</b> Schematic representation of the NMR spectrometer.....	44
<b>Figure 15.</b> Schematic representation of the NMR principle. ....	45
<b>Figure 16.</b> Energy levels splitting due to the application of increasing strength of magnetic field in an unpaired electron. ....	48
<b>Figure 17.</b> Conversion of the EPR absorbance spectrum of PBN adduct radical into the first derivative of the signal. ....	49
<b>Figure 18.</b> Energy-level diagram and corresponding EPR signals for an unpaired electron in an applied magnetic field that interacts with a <sup>14</sup> N nucleus in which the energy levels are additionally split by a nearby proton. ....	50
<b>Figure 19.</b> Trapping of a free radical by the spin trap PBN.....	51
<b>Figure 20.</b> Negative charge distribution in a protein upon addition of SDS.....	52

<b>Figure 21.</b> Principal steps of immunoblotting technique: (1) separation by size by gel electrophoresis, (2) transfer to a membrane by electrophoresis, and (3) visualization marking target protein using suitable antibodies. ....	53
<b>Figure 22.</b> Principal component score plots A) PC1xPC2, B) PC1xPC3, and C) PC2xPC3 and variable loading plots D) PC1, E) PC2, and C) PC3 for the full <sup>1</sup> H NMR spectra recorded for meat extracts from animals fed different levels of mate extract (none, 0.5%, 1.0%, and 1.5%). ....	72
<b>Figure 23.</b> Typical 600 MHz <sup>1</sup> H-RMN spectra for the metanol/water meat extract. Assignments: Ace (acetate); Ado (adenosine); Ala (alanine); Ans (anserine); Bet (betaine); Car (carnosine); Cho (choline); Crn (carnitine); Cre (creatine) Gln (glutamine); Gly (glycine); GLY (glycerol); Glc (glucose); Ile (isoleucine); Lac (lactate); Leu (leucine); Met (methionine); Val (valine). ....	74
<b>Figure 24.</b> <sup>1</sup> H NMR metabolite concentration ( $\mu\text{mol g}^{-1}_{\text{meat}}$ ) changes during meat ageing at 5 °C (0 and 14 days). ....	79
<b>Figure 25.</b> Principal Component Analysis (PCA) of the quantitative metabolite profile for animals fed with different levels of mate extract. A color-coded number according to mate extract level in the diet represents each meat sample and a letter was used to differentiate animals with the same treatment. Metabolite concentrations determined by <sup>1</sup> H-NMR and ESI-HRMS were selected as variables. A: Two-dimensional plot of samples using the principal components one and two (PC1xPC2) capturing most of the variance in the original dataset (total variance 66.07%). B: Loading plots for PC-variables correlations. ....	82
<b>Figure 26.</b> Typical EPR spectra of meat slurry added of PBN (400 mmol L <sup>-1</sup> ) recorded for different period of incubation at 65 °C. ....	83
<b>Figure 27.</b> Radical formation as measured by the relative intensity of PBN radical adduct by electron paramagnetic resonance (EPR) in slurry incubated at 65°C made from fresh meat and in meat stored at 5°C for 14 days, PBN concentration of 400 mM. A: EPR intensity was calculated by double integration of EPR signal and expressed as the ratio $\text{Area}_{T=X_{\text{min}}}/\text{Area}_{T=0}$ . Rates for radical formation were determined by linear regression of relative EPR intensity plots and shown in B for each set of condition. ....	85
<b>Figure 28.</b> <sup>1</sup> H-RMN spectra of metanol/water meat extracts containing the polar metabolites of meat from broilers fed with no supplements (black) and from broilers fed with 240 ppm of lupulones (red). Major peak assignments: (A) leucine/isoleucine/valine; (B) lactate; (C) alanine; (D) carnosine; (E) creatine; (F) anserine; (G) ATP/ADP/AMP; (H) carnosine; (I) adenine/hypoxantine; (J) adenosine/ inosine/carnosine; (K) phosphoglycerate; (L) carnitine. ....	90
<b>Figure 29.</b> <sup>1</sup> H-RMN spectra of metanol/water meat extracts containing the polar metabolites of meat from pigs fed with no supplements (black) and from broilers fed with 360 ppm of lupulones (red). Major peak assignments: (A) leucine/isoleucine/valine; (B) lactate; (C) alanine; (D) carnosine; (E) creatine; (F) anserine; (G) ATP/ADP/AMP; (H) carnosine; (I) adenine/hypoxantine; (J) adenosine/ inosine/carnosine; (K) phosphoglycerate; (L) carnitine; (M) sugar region. ....	91
<b>Figure 30.</b> Principal component score plots A) PC1xPC2, B) PC1xPC3, and C) PC2xPC3 and variable loading plots D) PC1, E) PC2, and C) PC3 for the full <sup>1</sup> H NMR spectra recorded for meat extracts from broilers fed different levels of lupulones (none, 30 ppm, 60 ppm, and 240 ppm). ....	94

<b>Figure 31.</b> Principal component score plots A) PC1xPC2, B) PC1xPC3, and C) PC2xPC3 and variable loading plots D) PC1, E) PC2, and C) PC3 for the full <sup>1</sup> H NMR spectra recorded for meat extracts from pigs fed different levels of lupulones (none, 120 ppm, 240 ppm, and 360 ppm). .....	96
<b>Figure 32.</b> Principal component score plots A) PC1xPC2, B) PC2xPC3, and variable loading plots associated to C) PC1xPC2 and D) PC2xPC3 for the quantitative metabolite profile for meat extracts from broilers fed different levels of lupulones (none, 30 ppm, 60 ppm, and 240 ppm). .....	97
<b>Figure 33.</b> Principal component score plots A) PC1xPC2, B) PC2xPC3, and variable loading plots associated to C) PC1xPC2 and D) PC2xPC3 for the quantitative metabolite profile for meat extracts from pigs fed different levels of lupulones (none, 120 ppm, 240 ppm, and 360 ppm). .....	99
<b>Figure 34.</b> Typical EPR spectrum for the PBN radical adduct produced during incubation of chicken meat slurries at 65 °C. ....	101
<b>Figure 35.</b> Radical formation as measured by the relative intensity of PBN radical adduct in meat slurry incubated at 65° C during different time intervals. (A) broilers and (B) pigs. EPR intensity was calculated by double integration of EPR signal and the ratio $Area_{T=X_{min}}/Area_{T=0}$ . ....	101
<b>Figure 36.</b> Characterization of the sarcoplasmic proteins (SC) and myofibrillar protein (MP) by SDS-Page in gel NuPAGE® Novex® 10% Bis-Tris. Protein concentration was determined spectrophotometrically using a NanoDrop system. ....	103
<b>Figure 37.</b> EPR spectra of hydroxyl-DMPO radicals produced under different levels of myofibrillar proteins. Reactions were carried out in 50 mM phosphate buffer pH 6.8 at room temperature. Conditions: DMPO (5.0 mM), FeSO <sub>4</sub> ·7H <sub>2</sub> O (1.0 mM), H <sub>2</sub> O <sub>2</sub> (1.0 mM), control (no protein [black]) and MP (8.0 mM [red], 32.0 mM [blue] and 64.0 mM [green]). ....	103
<b>Figure 38.</b> Effect of oxidation on the structural integrity of myofibrillar proteins incubated in the presence of: (i) Fe <sup>2+</sup> /H <sub>2</sub> O <sub>2</sub> ; (ii) Fe <sup>2+</sup> /H <sub>2</sub> O <sub>2</sub> and DMPO; (iii) Fe <sup>2+</sup> /H <sub>2</sub> O <sub>2</sub> and DTT; (iv) Fe <sup>2+</sup> /H <sub>2</sub> O <sub>2</sub> and DTT and DMPO). The table presents the components that are present (+) and absent (-) in the samples. Two concentrations of DMPO were used: 2.5 mM (grey) and 25.0 mM (salmon). ....	105
<b>Figure 39.</b> Formation of cross-link in protein via oxidation of cysteine residues. ....	106
<b>Figure 40.</b> DMPO trapping thyl radicals. ....	106
<b>Figure 41.</b> Immunoblotting assay of myofibrillar protein radicals incubated with (i) Fe <sup>2+</sup> /H <sub>2</sub> O <sub>2</sub> ; (ii) Fe <sup>2+</sup> /H <sub>2</sub> O <sub>2</sub> and DMPO; (iii) Fe <sup>2+</sup> /H <sub>2</sub> O <sub>2</sub> and DTT; (iv) Fe <sup>2+</sup> /H <sub>2</sub> O <sub>2</sub> and DTT and DMPO. The table on the top presents the components that are present (+) and absent (-) in the samples. Two concentrations of DMPO were used: 2.5 mM (grey) and 25.0 mM (salmon). ....	107
<b>Figure 42.</b> Principle for the detection of protein carbonyls by spectrophotometric and immunoblotting methods derivatized with 2,4-dinitrophenylhydrazine (DNPH). Reproduced with permission from Törnvall, 2010. <sup>161</sup> .....	108
<b>Figure 43.</b> SDS-Page gel electrophoresis and Oxyblot results for myofibrillar proteins from chicken that were incubated with Fe <sup>2+</sup> /H <sub>2</sub> O <sub>2</sub> , DNPH and control solution. MP were incubated at 4 °C with (i) Fe <sup>2+</sup> /H <sub>2</sub> O <sub>2</sub> ; (ii) Fe <sup>2+</sup> /H <sub>2</sub> O <sub>2</sub> and DNPH; (iii) Fe <sup>2+</sup> /H <sub>2</sub> O <sub>2</sub> and solution control. The table on the top presents the components that are present (+) and absent (-) in the samples. ....	109
<b>Figure 44.</b> Effect of the storage on the formation of carbonyl groups in myofibrillar proteins from broilers fed with different levels of hops β-acids. MP were incubated at 4 °C with (i) Fe <sup>2+</sup> /H <sub>2</sub> O <sub>2</sub> ; (ii) Fe <sup>2+</sup> /H <sub>2</sub> O <sub>2</sub> and	

DNP; (iii) $\text{Fe}^{2+}/\text{H}_2\text{O}_2$ and solution control. The table on the top presents the components that are present (+) and absent (-) in the samples. ....	110
<b>Figure 45.</b> Pathways of purine catabolism in humans. ....	114
<b>Figure 46.</b> Acid/base equilibrium between uric acid/urate and one-electron oxidation of urate coupled to proton loss. Adapted from Telo, 2003. ....	115
<b>Figure 47.</b> Heme pocket and Tyr 103 as redox-active centres for electron transfer in ferryl myoglobin. Drawing was prepared with UCSF Chimera software from PDB 5d5r. ....	119
<b>Figure 48.</b> Single mixing SX20 stopped-flow spectrometer. ....	120
<b>Figure 49.</b> Spectral changes for (A) Soret band and (B) Q bands indicating reduction of MbFe(IV)=O by uric acid. (C) Stopped-flow kinetic traces at 405 nm (Soret Band) for the reduction of ferryl myoglobin by uric acid and dependence of $k_{\text{obs}}$ on uric acid concentration at 25 °C. Conditions: $5 \times 10^3 \text{ mol L}^{-1}$ acetate buffer pH 4.7 containing $1 \times 10^3 \text{ mol L}^{-1}$ of EDTA; $[\text{MbFe(IV)=O}]_0 = 15 \times 10^6 \text{ mol L}^{-1}$ . Second-order rate constants found by linear regression was $775 \pm 109 \text{ L mol}^{-1} \text{ s}^{-1}$ . (D) Stopped-flow kinetic traces at 580 nm (Q band) for conditions as for (C). Second-order rate constant found by linear regression was $791 \pm 133 \text{ L mol}^{-1} \text{ s}^{-1}$ . ....	124
<b>Figure 50.</b> Dependence of second-order rate constant, $k'$ , on pH for the reduction of ferrylmyoglobin by uric acid in aqueous $0.067 \text{ mol L}^{-1}$ NaCl at $25.0 \pm 0.1 \text{ }^\circ\text{C}$ with full line calculated by non-linear regression according to eqn (26). ....	126
<b>Figure 51.</b> Temperature dependence of pH-profile for second-order rate constant, $k'$ , for reduction of ferryl myoglobin by uric acid in aqueous $0.067 \text{ mol L}^{-1}$ NaCl at varying temperature. ....	128
<b>Figure 52.</b> (A) Total protein charge $Z_{\text{H}}$ as function of pH for horse heart myoglobin calculated with Protein Calculator v3.4 ( <a href="http://protecalc.sourceforge.net/cgi-bin/protecalc">http://protecalc.sourceforge.net/cgi-bin/protecalc</a> ), sequences taken from pdb files (P68082.2). (B) Acid/base equilibrium distribution of uric acid and ferryl myoglobin as function of pH. ....	129
<b>Figure 53.</b> Eyring plots for reduction of ferrylmyoglobin by uric acid/urate for each possible reaction path, see Scheme 1. ....	131
<b>Figure 54.</b> A possible mechanism for the proton coupled electron transfer from uric acid to non-protonated ferrylmyoglobin. ....	132

## List of Tables

<b>Table 1.</b> Animal performance parameters for animals fed different levels mate extract. ....	69
<b>Table 2.</b> Carcass characteristics for animals fed different levels mate extract.....	70
<b>Table 3.</b> Concentration of the major phenolic compounds identified in the mate extract as determined by UPLC–ESI-HRMS (n = 3, mg·g <sup>-1</sup> extract). ....	71
<b>Table 4.</b> Mean concentration of the polar metabolites (n = 3 per feeding treatment, μmol·g <sup>-1</sup> meat) as obtained by quantitative <sup>1</sup> H-NMR of the methanol/water extract of meat from animals fed different levels mate extract. ....	75
<b>Table 5.</b> Mean concentration of the polar metabolites (n = 12 per feed treatment, μmol·g <sup>-1</sup> meat) as obtained by ESI-HRMS of the methanol/water extract of meat from animals fed different levels of extract.....	76
<b>Table 6.</b> Meat quality for meat from animals fed different levels of mate extract.....	87
<b>Table 7.</b> Sensory descriptive analysis of meat from animals fed different levels of mate extract. ....	89
<b>Table 8.</b> Sensory acceptance of meat from animals fed 1.5% mate extract as compared to meat from no supplementation. A non-trained panel of 100 panelists were used. ....	89
<b>Table 9.</b> Mean concentration of the polar metabolites (n = 3 per feeding treatment, μmol·g <sup>-1</sup> meat) as obtained by quantitative <sup>1</sup> H-NMR of the methanol/water extract of meat from broilers fed different levels hops β-acids.....	91
<b>Table 10.</b> Average concentration of polar metabolites (n=3, μmol. g <sup>-1</sup> of meat) as determined by <sup>1</sup> H-NMR in meat from pigs fed with different levels of β-acids.....	92
<b>Table 11.</b> Second-order rate constants, activation enthalpy and activation entropy for possible reaction path of importance for the reduction of MbFe(IV)=O by uric acid/urate in aqueous 0.067 M NaCl as calculated by non-linear regression at each temperature (see Figure 51) together with pK <sub>a</sub> values of protonated ferryl myoglobin and uric acid as estimated from the temperature dependence of the pH-reduction profile.....	130
<b>Table 12.</b> Rate constant and activation parameters for reduction of ferrylmyoglobin and protonated ferrylmyoglobin in aqueous solution by physiological relevant reductants at 25 °C.....	133

# TABLE OF CONTENT

<b>INTRODUCTION</b> .....	<b>16</b>
<b>CHAPTER I: IMPACT OF ANIMAL FEEDING REGIMES ON MEAT METABOLOMICS AND REDOX STATIBLY OF MEAT</b> .....	<b>19</b>
<b>1. INTRODUCTION</b> .....	<b>19</b>
<b>1.1. Redox processes in meat</b> .....	<b>20</b>
1.1.1. Composition and biochemistry of meat in relation to the redox stability.....	21
1.1.2. Post mort changes and the conversion of muscle in meat .....	24
1.1.3. The role of myoglobin in oxidative physiological processes .....	25
1.1.4. Formation of reactive species and radicals in meat .....	27
1.1.5. Prooxidant activity of myoglobin and diseases (colorectal cancer).....	31
<b>1.2. Nutritional strategies for improving meat quality</b> .....	<b>32</b>
1.2.1. Plant extracts as novel feed additives .....	33
1.2.2. Hops $\beta$ -acids.....	34
1.2.3. Yerba mate .....	35
<b>1.3. Methods for investigation of meat quality: mebolomics, NMR, Chemometrics, EPR spin trapping and protein oxidation</b> .....	<b>38</b>
1.3.1. Metabolomics .....	38
1.3.2. Nuclear Magnetic Resonance NMR .....	40
1.3.3. Chemometrics.....	46
1.3.4. EPR spin trapping.....	47
1.3.5. Protein oxidation .....	51
<b>2. GOALS</b> .....	<b>53</b>
<b>3. MATERIALS AND METHODS</b> .....	<b>54</b>
<b>3.1. Animals and sampling</b> .....	<b>54</b>
3.1.1. Supplementation with yerba mate .....	54
3.1.2. Supplementation with hops $\beta$ -acids.....	55
<b>3.2. Animal performance and carcass trait evaluation</b> .....	<b>56</b>
3.2.1. Cattle fed yerba mate.....	56
3.2.2. Broilers and pigs fed $\beta$ -acids.....	57
<b>3.3. Mate extract characterization and analysis of polyphenols in beef</b> .....	<b>57</b>

3.4.	Extraction of polar metabolites and CLA from meat .....	58
3.5.	Untargeted polar metabolites screening of meat extract by <sup>1</sup> H-NMR spectroscopy .....	59
3.6.	Quantitative polar metabolite profile of meat extract by <sup>1</sup> H-NMR spectroscopy .....	60
3.7.	Quantitative determination of polar metabolites and CLA in beef extract by high-resolution accurate ESI and APCI mass spectrometry .....	61
3.8.	Principal component analysis of the quantitative metabolite profile .....	62
3.9.	EPR spin-trapping technique and redox stability of beef.....	62
3.10.	Low-field <sup>1</sup> H NMR spectroscopy for fat amount of beef .....	63
3.11.	Meat quality parameters of beef.....	63
3.12.	Sensory descriptive analysis and consumer acceptance of beef .....	64
3.13.	Investigation of the oxidation of myofibrillar proteins in chicken meat .....	65
3.13.1.	Extraction and characterization of myofibrillar proteins of chicken meat.....	66
3.13.2.	Induction of oxidative conditions .....	66
3.13.3.	Electron paramagnetic resonance (EPR).....	66
3.13.4.	SDS-Page to determinate the formation of cross-link due oxidation of proteins and Western Blot.....	67
3.13.5.	SDS-Page and Oxyblot: investigation of the formation of carbonyl groups in amino acids of proteins.....	68
<b>4.</b>	<b>RESULTS AND DISCUSSION .....</b>	<b>68</b>
4.1.	Mate extract as Feed Additive for Improvement of Beef Quality .....	68
4.1.1.	Animal performance and carcass trait evaluation .....	69
4.1.2.	Mate extract characterization and analysis of polyphenols in beef.....	70
4.1.3.	<sup>1</sup> H-NMR metabolite untargeted sample screening: Principal components analyses (PCA) of full <sup>1</sup> H NMR spectra.....	71
4.1.4.	Quantitative <sup>1</sup> H NMR and High-resolution Accurate Mass Spectrometry .....	73
4.1.5.	Principal component analysis of targeted profiling metabolomics .....	81
4.1.6.	EPR spin-trapping and oxidative stability of beef .....	83
4.1.7.	Intramuscular and CLA content.....	85
4.1.8.	Meat quality parameters.....	87
4.1.9.	Sensory descriptive analysis and acceptance .....	88
4.2.	Hops β-acids as feed additive for improvement of meat from broiler and pigs .....	90

3.1.1.	<sup>1</sup> H-NMR metabolic profile of meat extracts of broilers and pigs fed with different levels of lupulones in the diet.....	90
3.1.2.	<sup>1</sup> H-NMR metabolite untargeted of meat from broilers and pigs fed β-acids: Principal components analyses (PCA) of full <sup>1</sup> H NMR spectra .....	93
3.1.3.	<sup>1</sup> H-NMR targeted metabolomics of meat from broilers and pigs fed β-acids: Principal components analyses (PCA) .....	97
3.1.4.	Redox stability of meat from animals fed with different levels of hops β-acids as determined by EPR 100	
3.1.5.	Investigation of myofibrillar protein oxidation in chicken meat through immuno spin-trapping	102
<b>5.</b>	<b>CONCLUSION .....</b>	<b>111</b>
<b>CHAPTER II: REDUCTION OF FERRYLMYOGLOBIN BY URIC ACID .....</b>		<b>113</b>
<b>1.</b>	<b>INTRODUCTION.....</b>	<b>113</b>
1.1.	Uric acid and oxidative stress.....	114
1.2.	Pseudo peroxidise activity and redox mechanisms of heme proteins .....	116
1.3.	Kinetics investigation of the redox reactions involving myoglobin by stopped-flow spectroscopy .....	119
<b>2.</b>	<b>GOALS .....</b>	<b>120</b>
<b>3.</b>	<b>MATERIALS AND METHODS.....</b>	<b>121</b>
3.1.	Chemicals .....	121
3.2.	Kinetic experiments .....	121
3.3.	Kinetic Calculations.....	122
<b>4.</b>	<b>RESULTS AND DISCUSSION .....</b>	<b>123</b>
<b>5.</b>	<b>CONCLUSION .....</b>	<b>135</b>
<b>REFERENCES.....</b>		<b>136</b>

# Introduction

Oxidation of lipids and proteins is recognized as the major non-microbiological cause of quality deterioration of meat and meat products.<sup>1-4</sup> The balance between prooxidants and antioxidants has a direct effect in the resistance of muscle tissue and meat to oxidation. The content of endogenous antioxidants together with the fatty acid profile are considered the most important internal factors accounting for the redox stability of meat. Improvements in the oxidative stability of poultry meat as a result of supplementation with natural antioxidants via feeding have been widely reported.<sup>5</sup> Nevertheless, the use of underexplored plant extracts rich in antioxidants still seems very attractive in order to diversify the existing alternatives and to discover novel antioxidants with potential technical or economical advantages.<sup>6</sup>

As a consequence of the increase in the global population growth in companion with the growing demand for meat in the developing countries, over the next decades the world's meat consumption is expected to be double by around 2050 (FAO, 2013).<sup>7,8</sup> Considering the international market, nowadays Brazil exports 1.8 million megaton of beef and 3.9 million megaton of chicken meat. The Ministry of Agriculture – Brazil and EMBRAPA (Brazilian Agricultural Research Corporation) forecast the Brazilian production of chicken, beef and pork would grow up to 30% in the next decade according to a recent study. The expectations are that before 2020, Brazil will become responsible for 44.5% of the beef international market and around 48% for the chicken meat market worldwide (The Ministry of Agriculture – Brazil, 2010).<sup>9</sup>

The competitive global market system increases the necessity for improving the Brazilian meat quality to ensure the world leadership in the international market. The optimization of meat production needs a wide variety of antimicrobial agents and feeding preservatives aiming to act as growth promoters and to increase the safety and the quality of food. However, owing to the broad and indiscriminate use of antibiotics, some banned by EU regulations which inhibit the exportations, there is a worldwide problem of pathogenic bacteria resistance to a vast number of antimicrobial agents. Thus, an urgent need to find alternatives emerges. Plant extracts such as mate (*Ilex paraguariensis*) and  $\beta$ -acids from hops are potential alternatives for replacement of synthetic antioxidants and antimicrobial agents for acting as food and feed preservatives and animal growth promoters.<sup>10</sup> The prevention of oxidative deterioration leads to an increased productivity, which reduces the environmental impact contributing to achieve the global sustainability.

Hop  $\beta$ -acids have been added to the animal food aiming to enhance the absorption of nutrients and, consequently, can increase the production of eggs in broilers and the production of propionate and lactate in milk from cattle.<sup>11-13</sup>  $\beta$ -acids from hops do not need to be isolated for oral administration in animals and can be directly mixed to the animal food. Earlier studies have shown that plant leaves from the native Brazilian plants, mate (*Ilex paragariensis*) have antioxidant properties. Mate extract have been shown to improve the stability of poultry meat from broilers raised on feed supplemented with 0.5% mate of aqueous extract.<sup>10</sup> Plant extracts, as a source of natural antioxidants, can modulate the meat composition improving the redox stability of meat and consequently, improving meat quality. Any development of a reliable method to predict oxidative stability based on the biochemical composition will be a breakthrough in meat quality and production. The effect of adding these plant extracts to animal feed on animal metabolism has not been previously reported in literature.

The epidemiological evidence of an increased risk of colorectal cancer for a high intake of red meat seems also related to the oxidative stability of meat and especially to the high content of bioavailable iron as a prooxidant.<sup>14</sup> Red meat includes meat from pigs and cattle, and since the relationship between feed intake and meat stability is better documented for pigs, it seems timely to investigate the effect of the addition of plant rich in bioactive components to feed for cattle.

The aim of the present Thesis is to investigate the impact of animal feeding diet supplemented with natural antioxidants on the metabolic profile of meat and its relation to the redox stability of meat. Different animals and supplements has been investigated in this study: i) Nellore's cattle fed different levels of fed mate (*Ilex paraguariensis* A. St.-Hil.), ii) broilers fed different levels of  $\beta$ -acids from hops, and iii) pigs fed different levels of  $\beta$ -acids from hops. Meat metabolomics studies will provide further evidence and molecular basis of the effect of these plant materials on animal metabolism and its influence on redox stability of meat. The characterization of the biochemical composition affecting oxidative stability has been undertaken by the use of modern analytical methodologies such as NMR and HRMS. The redox stability of meat has been investigated by the use of the EPR spin-trapping technique in order to obtain kinetic information of the radical formation in meat. The study of redox stability of meat has been also extended to the trend of oxidation in proteins. Finally, chemometrics of the metabolomic profile in companion with the redox stability will provide a selection of target metabolites that effectively enhance the redox stability of meat.

Additionally, the present PhD thesis proposes to investigate uric acid as a potential antioxidant in biological systems focusing on oxidative reactions mediated by hypervalent myoglobin species, perferryl myoglobin and ferryl myoglobin. The role of hypervalent myoglobin species in the initiation of oxidative damage in meat and biological system has been further investigated by many researchers.<sup>2,3,15-22</sup> Hypervalent meat pigments, ferryl myoglobin (MbFe(IV)=O) and perferrylmyoglobin ( $\bullet$ MbFe(IV)=O), are generated from the activation of metmyoglobin (MbFe(III)) with H<sub>2</sub>O<sub>2</sub> and/or organic hydroperoxides present in foods, initiating the pseudoperoxidase catalytic cycle of myoglobin.<sup>23</sup> Both perferryl myoglobin and ferryl myoglobin are strong oxidant species known to initiate lipid and protein oxidation in muscle tissues, and meat products.<sup>15,19,20,23</sup> Thus, the knowledge of the reaction kinetics and mechanisms for the deactivation of hypervalent myoglobin species by dietary antioxidants is of relevance to improve human health and to the prevention of diseases.

The present PhD thesis includes an introductory literature review with relevant information about redox processes in meat and their relationship to the meat composition, nutritional strategies to improve meat quality, the role of natural antioxidants as animal supplements, the role of myoglobin in initiating oxidative processes and, the protective effect of uric acid against the hypervalent meat pigment species mediated oxidative damage. Brief descriptions of the methodology used in the present study are presented in the next chapters as well. Experimental results and discussion with an introductory related content are divided in two chapters. The impact of animal feeding regimes on meat metabolomics and redox stability of meat are the subject of Chapter I which is divided in two sections: A) yerba mate as feed additive for cattle and B) hops  $\beta$ -acids as feed additive for broilers and pigs. Chapter II focuses on the reactivity of the hypervalent meat pigment, ferryl myoglobin, towards natural antioxidants and, particularly, towards uric acid.

# CHAPTER I: Impact of animal feeding regimes on meat metabolomics and redox stability of meat

Parts of this chapter content has been published in the journal article: A. Zawadzki; L.O.Arrivetti; M.P. Vidal; J.R. Catai; R.T. Nassu;, R.R. Tullio; A. Berndt; C.R. Oliveira; A.G. Ferreira; L.F. Neves-Junior; L.A. Colnago; L.H. Skibsted; D. R. Cardoso. (2017). Mate extract as feed additive for improvement of beef quality. *Food Research International* (in press). DOI:10.1016/j.foodres.2017.05.033

## 1. Introduction

The oxidative stability of meat from non-ruminant animals like poultry and pigs may be improved by adding antioxidants to the feed or by increasing the content of plant rich in natural antioxidants in the feed.<sup>24</sup> The lipid profile of meat from non-ruminants may likewise be made healthier by changing the lipid composition of the animal feed towards higher degree of unsaturation.

For broilers and pigs, several studies demonstrated that the diet has effective impact on animal performance, intestinal health, fat content and lipid metabolism, meat composition and oxidative stability of meat.<sup>10,25–28</sup> Phytogetic additives for non-ruminant animal feed have been receiving an increasing attention due to their pharmacological properties and for potentially replacing antimicrobial agents and growth promoters.<sup>10,25,28</sup> Widely recognized for their use in beer manufacturing, hops (*Humulus lupulus*) are one example of phytogetic additives with antimicrobial activity that have been studied as a dietary supplement to enhance animal performance, especially for broilers.<sup>28</sup> Despite the fact that many reports in literature have been focused in the bacteriostatic efficacy of hops  $\beta$ -acids in comparison with synthetic antibiotics in animal feeding for improvement of animal performance, there is little information regarding the metabolic effects due to the use of hops as supplement for animal diet. Herein, we report the impact of increasing levels of hops  $\beta$ -acids in the diet of broilers and pigs on the metabolic profile and redox stability of meat.

For ruminant, the rumen microbiota may decrease the degree of lipid unsaturation prior to absorption and the effect of the feed composition on the meat may be modulated. An increase in content of plant rich in bioactive compounds like antioxidants for

ruminant feed may, however, affect the microflora of the rumen subsequently affecting meat composition and quality.<sup>24,29,30</sup>

Mate is generally recognized as safe (GRAS status) and is native to the South America region with the highest beef production and also with the highest beef consumption. Mate has a high content of alkaloids, saponins, and phenolic acids<sup>31</sup> and has been shown to increase the oxidative stability of chicken meat both when added to the meat during cooking and when added as an extract to the drinking water of broilers.<sup>10,25</sup> In this study, we report results for oxidative stability of meat from Nellore cattle's, the most common cattle breed in Brazil, fed mate (*Ilex paraguariensis* A. St.-Hil.).

### 1.1. Redox processes in meat

Redox processes in the animal muscles are the major non-microbiological factors involved in quality deterioration of meat. Many oxidative reactions are involved in these processes. Lipid oxidation in meat is responsible for the production of undesirable off flavour compounds and rancidity.<sup>2</sup> Oxidation of meat proteins leads to intra and inter-molecular cross-linking of proteins which affects negatively the tenderness of meat.<sup>3,22</sup> Many pathways for lipid and protein oxidation in meat involve the activation of the heme pigments myoglobin and hemoglobin.

Besides decrease eating quality and stability of foods, oxidation reactions are further associated with negative consequences for human health. Oxidative stress has been reported as involved in the development of many pathogenic conditions like diabetes<sup>32</sup>, cardiovascular diseases<sup>32,33</sup>, Parkinson's disease<sup>34</sup>, Alzheimer's disease<sup>35</sup> and cancer<sup>36</sup>. Elevated red meat intake is recognized for increasing oxidative stress markers and inflammatory processes.<sup>14,34,36-39</sup> Therefore, the investigation of oxidative processes in meat and their involvement in some diseases arising from oxidative stress are interesting subjects discussed in the next sections of the present thesis.

Meat as a complex structure has a wide range of compounds with prooxidant and antioxidant activity. The balance between these species influences the meat resistance to oxidation or redox stability of meat. Identifying which compounds affect the redox stability of meat is necessary to understand how to inhibit oxidation reactions and, consequently, prevent quality deterioration. Thus, the next section briefly describes the meat composition highlighting the compounds with relevance for oxidation and protection against oxidation. The following sections describe the main oxidation processes in meat, like the production of

free radicals and reactive species and the role of heme iron and endogenous antioxidants for the redox status of meat.

#### **1.1.1. Composition and biochemistry of meat in relation to the redox stability**

The study of meat composition is substantial to comprehend the oxidation reactions that can occur in meat. Muscle is composed by water, proteins, lipids, polar metabolites, vitamins, inorganic compounds and carbohydrates. Several post-mortem biochemical and structural changes take place after slaughter to convert muscle in meat. These post-mortem changes have an effect on the individual concentrations of meat compounds and considerably affect the meat quality.<sup>40</sup>

Meat is known as the most important nutritional source of high quality proteins. Meat proteins can be further classified into sarcoplasmic, myofibrillar and connective tissue.<sup>41</sup> Insoluble proteins like collagen and elastin compose the connective tissue and have structural function. Myofibrillar proteins are salt soluble proteins organized into thick and thin filaments (myofilaments) responsible for muscle contraction. Myofilaments are composed by long proteins actine, myosin and tinin. Myosin is a thiol-rich protein and an easily oxidizable constituent of muscle.<sup>3,22</sup> Sarcoplasmic proteins constitute water-soluble globular proteins mostly with enzymatic function. Hemoglobin and myoglobin are examples of sarcoplasmic proteins and deserve attention considering their function as oxygen carrier and their involvement in oxidation.

Lipids are present in meat as phospholipids of cell membrane, fat between the muscles (intermuscular fat) and subcutaneous fat (intramuscular fat).<sup>42</sup> The content and the profile of meat fatty acids depend on the cut and the degree of trimming. Intramuscular fat of meat contributes to the juiciness, tenderness and aroma of meat and has been considered of relevance for human health.<sup>43-45</sup> In this respect, many studies reported in the literature have focus on the composition of intramuscular fatty acids of meat. Intramuscular fat is composed by saturated fatty acids (SFA), mono unsaturated fatty acids (MUFA) and poly unsaturated fatty acids (PUFA).<sup>44,46</sup> Dietary fat intake, especially the high consumption of SFA, has been associated with high cholesterol levels and the incidence of cardiovascular diseases.<sup>44</sup> On the other hand, several studies have demonstrated the potential benefits of n-3 PUFA supplementation for health.<sup>29,43-45</sup> Omega-3 poly unsaturated fatty acids, eicosapentaenoic acid (EPA,20:5n3) and docasahexaenoic acid (DHA; 22:6n3) have shown importance for the maintenance of brain and visual tissues function as well as for the prevention of

cardiovascular diseases, inflammatory diseases and cancer. These Omega-3 PUFAS are found in meat fish, fish oils and eggs.<sup>42-44</sup> In beef, conjugated linoleic acid (CLA) is an important PUFA and has demonstrated health-promoting effects due to its antioxidant, anticholesteremic and antitumoral properties.<sup>6,44,45,47-50</sup>

Amino acids, peptides, nucleotides and sugars correspond to meat polar metabolites and, many of them are water-soluble precursors of meat flavour.<sup>51-54</sup> The presence of nucleotides in meat is important not only for the flavour but also because some nucleotides are considered biomarkers for relevant metabolic pathways.<sup>52,55,56</sup> For example, inosine monophosphate (IMP), inosine and hypoxanthine are related to the purine degradation pathway which yields uric acid as end product. IMP is converted to inosine and inosine to hypoxanthine during the post mortem metabolism of meat when degradation pathways take place. Inosine and hypoxanthine are biomarkers for stress and both contribute for an undesirable bitter taste in meat whereas IMP is an important flavour enhancer.<sup>54,55,57,58</sup>

Carbohydrates and phosphate forms of sugar can produce important flavour precursors in meat during cooking through the Maillard reaction.<sup>51</sup> Moreover, the Maillard reaction has been identified as a source of compounds with antioxidant activity. These Maillard reaction products are thermally produced from the reaction between reducing sugars, amino acids and proteins and have demonstrated to be effective inhibitors of lipid oxidation in meat.<sup>59,60</sup>

Amino acids are the building blocks of proteins and small peptides and are highly concentrated in meat. The free amino acid composition of meat confers nutritional quality to the food product. For example, the branched chain amino acids (BCAA) leucine, isoleucine and valine have been widely used as supplement in sports nutrition. The concentration of free amino acids in meat depends on the animal metabolism before slaughter and on the activity of proteolytic enzymes during the post mortem metabolism.<sup>40,53,61</sup> Hence, many metabolic pathways in muscle tissue have specific free amino acids as biomarkers. The physiological pathways that are necessary for maintenance, growth, reproduction, and immunity, called key metabolic pathways, are regulated by functional amino acids (arginine, cysteine, glutamine, leucine, proline, and tryptophan).<sup>62</sup> Furthermore, some amino acids like cysteine are important antioxidants in biological systems and meat. Cysteine, methionine, tyrosine, thryptophan, histidine, phenylalanine, proline, lysine and arginine correspond to the amino acids that are more susceptible to oxidation.<sup>3</sup> The oxidative stability of amino acid residues influences the maintenance of the protein conformation and hydrophobicity. In meat,

oxidation of residues of cysteine, tyrosine and tryptophan is responsible for the formation of cross-linking in proteins.<sup>3,22,63,64</sup>

Peptides constitute short sequences of 2-30 amino acids. Meat peptides can be naturally produced in the muscle tissue or during the post mortem metabolism. Peptides from beef, chicken, pork and fish muscle proteins have been demonstrated to be bioactive compounds. Antioxidant, antimicrobial, antithrombotic, hypocholesteromic and antihypertensive effects have been ascribed to the therapeutic use of these bioactive peptides.<sup>65-68</sup> The function of a bioactive peptide relies on its amino acid composition and sequence. Glutathione, carnosine and anserine are examples of peptides that have been largely reported as radical scavengers and reducing agents.<sup>69,70</sup> Besides the commercial interest to produce functional foods through the incorporation of bioactive peptides, there is an increasing concern to stimulate the production of these peptides in meat just by manipulating the animal diet.<sup>71</sup>

Certain nutrients are exclusively found in animal sources, specially meat, which has been recognized as a substantial source of many nutrients like zinc, cooper, heme iron (the most bioavailable form of iron),  $\alpha$ -tocopherol (vitamin E) and B vitamins.<sup>72-74</sup> Meat is the primary source of Vitamin B<sub>12</sub> (cobalamine) which is essential for the proper functioning of the nervous system and the production of red cells.<sup>74-76</sup> Regarding the complex B vitamins, riboflavin deserves attention for its role in light-induced quality deterioration of foods. Photosensitization of riboflavin yields a triplet-excited state that induces the formation of long lived protein radicals in muscle tissues. These primary radical photoproducts can potentially initiate vitamin and lipid oxidation resulting in quality and nutritional losses in meat.<sup>77,78</sup> Notably, riboflavin photosensitized oxidation of myoglobins has been reported by Grippa et al.<sup>78</sup> On the other hand, some vitamins present in meat can protect muscle against oxidation. High levels of  $\alpha$ -tocopherol in fresh meat have been associated with improved redox stability. Indeed, several studies have demonstrated that vitamin E enhances the non-enzymatic antioxidant activity in muscle tissue maintaining the stability of colour and consequently, abrogating lipid oxidation. Considering that vitamin E dietary supplemented diet increases the content of  $\alpha$ -tocopherol and other relevant antioxidants in meat, supranutritional vitamin E supplementation has been widely applied in the diet of cattle, pigs and broilers to study its positive effects on meat quality.<sup>79-81</sup>

In muscle tissues, minerals are found in the sarcoplasm, cellular compartments and extracellular. Most part of minerals found in meat are metallic ions that are important for

the maintenance of the neutrality of tissues and organic fluids and for the regulation of the muscular and nervous activities.<sup>82,83</sup> Potassium, sodium, phosphorous, chloride, magnesium, calcium, iron, cooper, manganese, zinc, molibdenium, cobalt and iodide constitute essential minerals that can be obtained from the consume of meat.<sup>84</sup>

The combination of all the meat components in suitable concentrations may provide the consumer requirements in relation to the meat sensory aspects. Meat composition is not only essential for consumer acceptance, but a particular attention has been given to the nutritional value of meat, especially regarding the presence of functional components for health concerns.<sup>46,65,66,71</sup> In this context, the scientific community has been collaborating with the food industry in the study of which factors affect the meat composition in order to develop new differentiated products. Many researchers have been reporting that composition of meat can be manipulated by nutritional and genetic strategies and is affected by maturation and processing as well. Mainly genetic and diet effects on the fatty acid composition of meat have been thoroughly studied.<sup>29,44-47,79-81,85-87</sup> However, considering that genetic selection is not the focus of the present thesis, only the contributions of the animal diet and the post-mortem changes for meat composition are further discussed, respectively, on the sections 1.2 and 1.1.2 of the present thesis. Oxidation of proteins and lipids has also been discussed in relation to their influence for meat composition change and for meat quality, as presented in section 1.1.4. Considering the relevance of myoglobin in the production of reactive species, its oxidant activity has been further discussed in the section 1.1.3 highlighting the production of hypervalent iron species and their involvement in the development of diseases.

### **1.1.2. Post mort changes and the conversion of muscle in meat**

*Post mortem* changes in meat correspond to the biochemical events that occur after the slaughter of the animal and are of exceptional importance for meat quality. As the oxygen supply gradually decreases upon slaughter, meat *post mortem* metabolism is different from living tissue metabolism. The change from oxidative to glycolytic metabolism lead to the accumulation of latic acid and, consequently, the pH dramatically decreases from 7.4 to approximately 5.5. Loss in water holding capacity (WHC) and in calcium release as consequence of acidification promotes the formation cross-bridges between myosin and actin filaments. The depletion in glycogen levels also occurs upon slaughter leading to the decrease of the available energy which is required to maintain the muscle in a relaxed form. Such alterations in energy metabolism result in further pH decrease and, consequently, lead to loss

of muscle flexibility. At this stage, known as the onset of *rigor mortis*, muscle is converted to meat.<sup>40,88,89</sup> *Post mortem* changes continue to happen during meat storage. The aging period of meat is also known as maturation.

The role of the *post mortem* metabolism in meat tenderization and development of flavour has been further investigated in literature.<sup>40,53,61,88-90</sup> The activity of proteolytic enzymes is enhanced after *rigor mortis* and affects key myofibrillar proteins. Titin, nebulin, filamin, desmin, vinculin, troponin-T, myosin heavy chain, and actin have been identified as the proteins that can be degraded due to proteolysis. Calpains and cathepsins have been considered the main proteolytic systems involved in meat tenderization. However, meat tenderization involves multienzymatic processes that have not been fully elucidated. Additionally, age, genotype/breed, castration, muscle type, nutritional treatment or technological factors (like electrical stimulation) are known for affecting the conversion of muscle into meat.<sup>40,53</sup> Studies on proteomics have been receiving attention for providing insights on potential biomarkers for meat tenderization.<sup>40,88,89</sup>

The protein breakdown during proteolysis releases peptides and free amino acids that are of importance to yield a range of flavour precursors. Besides that, *post mortem* changes can induce the enzymatic breakdown of nucleotides into free ribose, phosphate and hypoxanthine. The decrease in glycogen levels yields a range of sugar derivatives. All of these compounds may react to each other giving rise to the characteristic aroma and flavour of roast meat during cooking.<sup>40,53,54,61,85,91</sup>

The loss of muscle compartmentalization together with protein denaturation and proteolysis during the *post mortem* process are responsible for the release of potential reactants for the initiation of non-physiological reactions related to oxidation processes. Therefore, muscle components that are highly susceptible to oxidation can interact with reactive species resulting in meat quality deterioration.

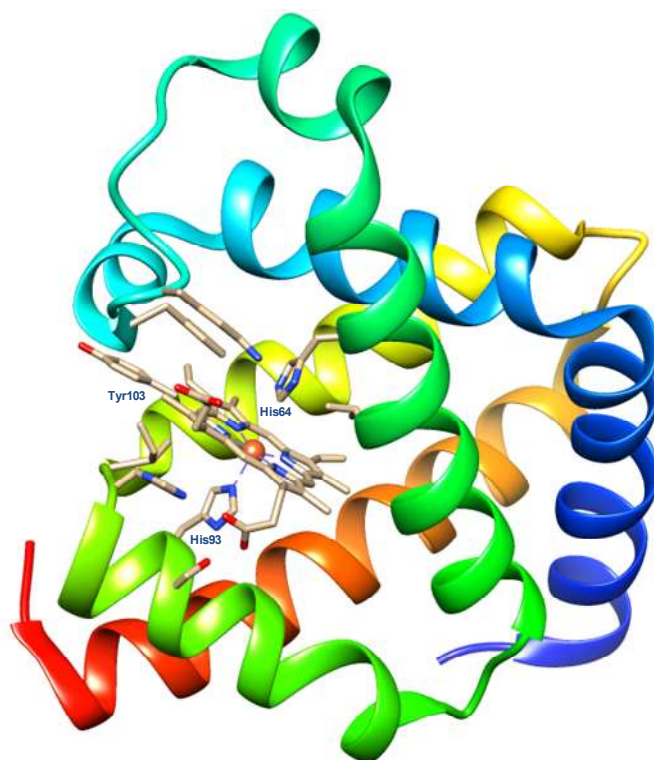
### **1.1.3. The role of myoglobin in oxidative physiological processes**

The iron heme porphyrin pigment of red meat, myoglobin (Figure 1, PDB 5d5r), is the most abundant heme protein in the muscle cell and a physiological oxygen carrier. Myoglobin and haemoglobin reversibly binds oxygen to the heme iron which constitutes a redox active center also being involved in many redox processes including the prooxidative catalytic activity and the formation of reactive oxygen species (ROS), free radicals and

cytotoxic derivatives of these proteins.<sup>20</sup> In this context, myoglobin has been thoroughly studied as one of the main initiators of oxidative processes.<sup>15</sup>

The dynamic conversion between different redox states of heme iron in myoglobin is directly connected to its prooxidant activity. Features of reductants and oxidants are substantial for the cycle colour of meat as illustrated in Scheme 1. Deoxymyoglobin (MbFe(II)) is the active physiological form of myoglobin that has the iron in the ferrous oxidation state and can bind molecular oxygen to yield oxymyoglobin (MbFe(II)O<sub>2</sub>). Since molecular oxygen is an oxidant agent, oxymyoglobin can be converted to metmyoglobin (MbFe(III)) through an auto-oxidation reaction.<sup>92</sup> Subsequent oxidations of the ferric state of myoglobin can occur via H<sub>2</sub>O<sub>2</sub>-activation producing hypervalent iron species, ferryl myoglobin (MbFe(IV)=O) and perferrylmyoglobin (<sup>•</sup>MbFe(IV)=O).<sup>2</sup> These hypervalent iron forms of myoglobin exhibit pseudo peroxidase activity and have received special attention in the past decades due to their involvement in pathological conditions.<sup>2,78,93,94</sup> Among various red meat derived oxidants, it is believed that hypervalent iron species from myoglobin are the main oxidizing species promoting the redox unbalance overwhelming cellular defenses.<sup>36-39</sup>

**Figure 1.** Structure of horse heart deoxymyoglobin obtained from PDB 5d5r. Drawing was prepared with UCSF Chimera software.



Source: Figure elaborated by the author.



produce free radicals include enzyme-catalysed reactions and Fenton reaction which is described as an one-electron Fe(II)/Fe(III) cycling mechanism mediated by hydrogen peroxide<sup>95</sup>, as shown in Equation 1. For meat systems, metal-catalyzed production of radicals has been found to occur rather than through irradiation and light exposure.



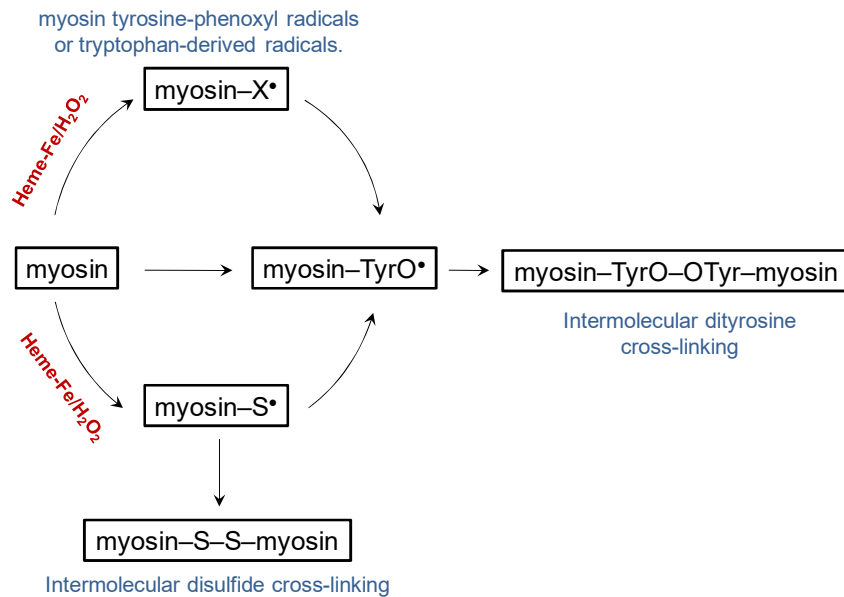
Radicals are extremely reactive when compared to non-radical species because their unpaired electrons are available to react with biological substrates, like lipids, proteins and DNA. Hydroxyl ( $\text{HO}^\bullet$ ), superoxide ( $\text{O}_2^{\bullet-}$ ), nitric oxide ( $\text{NO}^\bullet$ ), nitrogen dioxide ( $\text{NO}_2^\bullet$ ), peroxy ( $\text{ROO}^\bullet$ ) and LOO $^\bullet$  (lipid peroxy) are examples of radicals found in biological systems and in meat.

Excessive levels of hydrogen peroxide are critical for the production of free radicals in biological systems. The presence of hydrogen peroxide concomitant with transition metals increases the pro-oxidant activity of the system. The non-enzymatic production of hydrogen peroxide is enhanced in meat compared to *in vivo* conditions because *post mortem* conditions have lower pH. The conversion of  $\text{HO}_2^\bullet$  to  $\text{H}_2\text{O}_2$  is favoured at low pH when compared to the conversion of  $\text{O}_2^{\bullet-}$  to  $\text{H}_2\text{O}_2$  which occur through the enzymatic disproportionation reaction catalyzed by superoxide dismutase (SOD) since the activity of this enzyme decreases gradually during *post mortem* conditions.<sup>23</sup> Hydrogen peroxide has an important role in the activation of myoglobin producing hypervalent species ferryl and perferryl myoglobin as discussed in the previous section.

Myoglobin and haemoglobin are involved in the production of free radical processes in meat by catalysing reactions with small molecules including  $\text{O}_2$ , NO, HNO and  $\text{H}_2\text{O}_2$ .<sup>20</sup> The initiation of oxidation reactions by myoglobin involves three main pathways: i) auto-oxidation of oxymyoglobin with subsequently enzymatic reduction of metmyoglobin, ii) catalytic degradation of lipid hydroperoxides, and iii) pseudoperoxidase activity.<sup>23</sup> One and two-electron transfer processes have been identified as the catalytic mechanisms from which heme-iron takes part in oxidation reactions. The activation of myoglobin by  $\text{H}_2\text{O}_2$  has also been shown to stimulate the production of long-lived protein radicals and, consequently, protein-cross-linking.<sup>3,22,97</sup> Østdal et al. have demonstrated that  $\beta$ -lactoglobulin can be oxidized by an electron transfer to ferrylmyoglobin that can result in inter or intramolecular dityrosine formation via a radical mechanism. In meat, myosin has been demonstrated to be oxidized by hypervalent iron yielding tyrosyl and thiyl radicals ( $\text{R-TyrO}^\bullet$  and  $\text{R-S}^\bullet$ , respectively) that

promptly react to each other producing dityrosyl and disulfide cross-linking (Figure 2).<sup>22</sup> The formation of intermolecular cross-linking in myosin has been associated with tenderness loss as a consequence of the decreasing in the gel-forming ability, in the protein solubility and in the water-holding capacity.

**Figure 2.** Proposed mechanism for the oxidation of myosin by H<sub>2</sub>O<sub>2</sub>-activated heme iron to yield protein radicals. Adapted from Lund et. al, 2008.



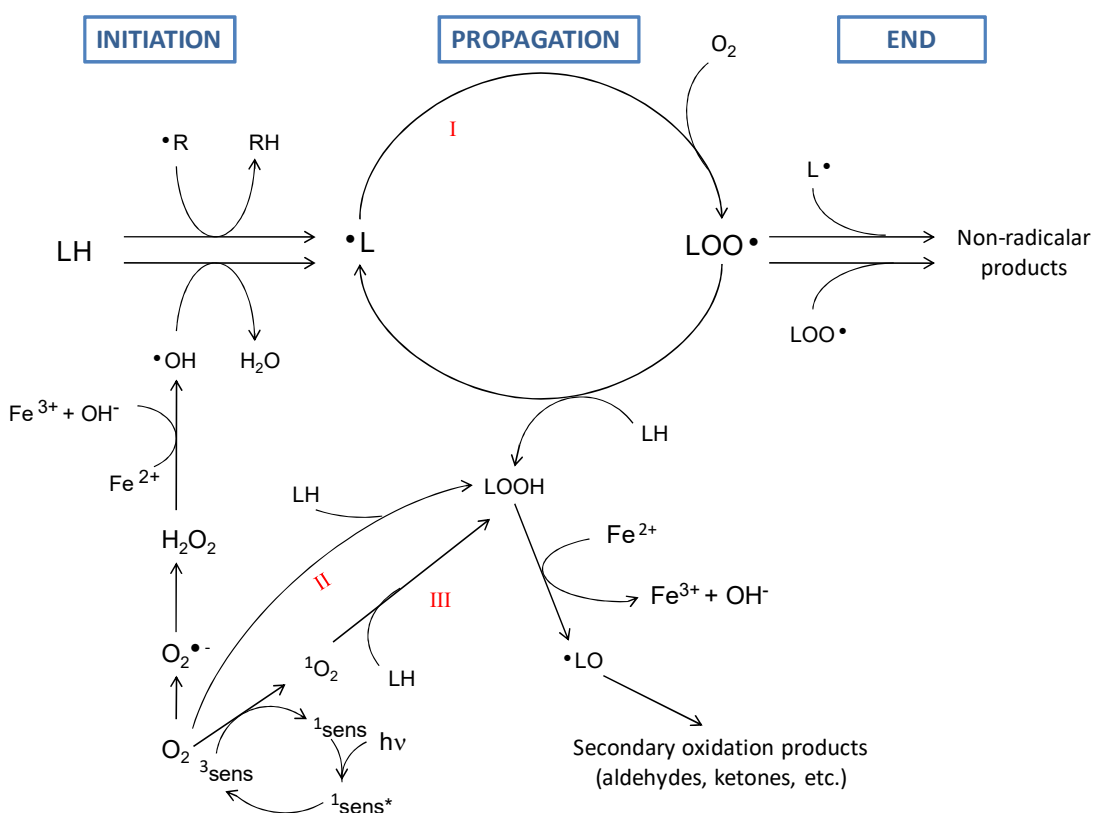
Source: LUND, M. N.; LUXFORD, C.; SKIBSTED, L. H; DAVIES, M. J. *Biochem. J.* (2008) 410, 565–574.<sup>22</sup>

Protein oxidation is not only important for quality deterioration of meat but has been related to some pathologies and aging.<sup>3</sup> Tyrosine, tryptophan and cysteine have been identified as the amino acid residues most susceptible to be oxidized yielding radicals in the protein structure. These radicals can result in intra and intermolecular cross-linking changing the protein structure and, consequently, loss of protein functionality. Besides that, free radicals can react with protein and peptides in the presence of oxygen to induce oxidative changes including cleavage of peptide bonds and modification of amino acid side chains. Formation of protein carbonyl groups have been identified as one of the most common modifications on amino acid residues. Especially, arginine, lysine and proline have been demonstrated to be easily oxidized via metal-catalyzed reactions to yield carbonyl residues. The extension of protein oxidation can be evaluated from the content of carbonyl groups in biological samples.<sup>3</sup>

The production of radicals in the aqueous phase of meat which concentrates the sarcoplasmic proteins (including myoglobin) have been considered to occur prior the

oxidation of lipids. However, lipids are very sensitive to the presence of traces of metals and metalloproteins and their oxidation mechanism involves either the participation of free radicals or the production of free radicals intermediates (Figure 3). The primary oxidation products of the lipid peroxidation cycle are hydroperoxides that can be further cleaved to produce peroxy radicals or alkoxy radicals. New chain reactions can be initiated by peroxy radicals and alkoxy radicals. Secondary lipid oxidation products can also react with proteins damaging their structure. Hence, lipid peroxidation may initiate the propagation free radical chain reactions, affecting negatively other meat components. The oxidation of meat lipids has been shown to produce unacceptable rancidity and *off flavour* compounds. Lipid oxidation and protein oxidation are coupled processes responsible for quality deterioration that have been investigated in meat models and meat.

**Figure 3.** Lipid peroxidation cycle describing the three main reaction pathways related to the initiation of the oxidative processes in foods: I) Initiation of a free radical chain reaction from the activation of oxygen yielding hydroxyl radicals or from the production of free radicals by oxidants or by irradiation; II) Enzymatic formation of lipid hydroperoxides due to the activity of lipoxygenase; III) Photosensitized formation of lipid hydroperoxides through formation of singlet oxygen or through direct radical generation. Adapted from Carlsen et al, 2005.<sup>4</sup>



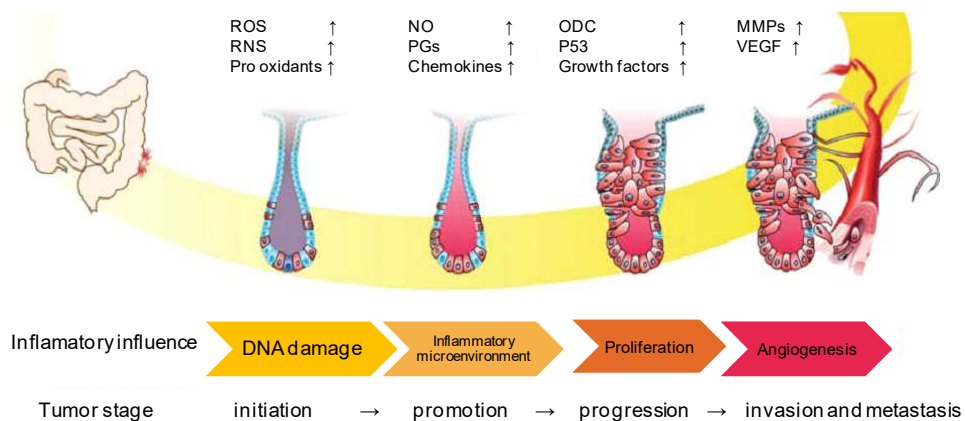
Source: CARLSEN, C. U.; MØLLER, J. K. S.; SKIBSTED, L. H. Heme-iron in lipid oxidation. *Coordination Chemistry Reviews* (2005) 249, 485-498.

Non-radical reactive species are also of importance for the study of oxidative processes that occur in meat and includes hydrogen peroxide (H<sub>2</sub>O<sub>2</sub>), ozone (O<sub>3</sub>), singlet oxygen (<sup>1</sup>O<sub>2</sub>), hypochlorous acid (HOCl), nitrous acid (HNO<sub>2</sub>), peroxyxynitrite (ONOO<sup>-</sup>), dinitrogen trioxide (N<sub>2</sub>O<sub>3</sub>), LOOH (lipid peroxide).<sup>34,98</sup> These reactive species may take part into oxidation reactions leading to free radical reactions. Peroxyxynitrite has been shown to react with desoxyribose, α-tocopherol and proteins and, also, can initiate lipid oxidation.<sup>99</sup>

#### 1.1.5. Prooxidant activity of myoglobin and diseases (colorectal cancer)

Myoglobin is believed to be one of the main causes for colorectal cancer since the heme content of red meat is 10 fold higher compared to white meat. The epidemiological evidence of an increased risk of colorectal cancer for a high intake of red meat seems also related to the oxidative stability of meat and especially to the high content of bioavailable iron as a prooxidant.<sup>14</sup> During digestion, myoglobin may become activated and cleave lipid hydroperoxides. Intracellular reactions including hypervalent iron and ROS can result in the initiation and progression of carcinogenesis by induction of gene mutations, chromosomal damage and other cytotoxic effects. Since ROS regulate the expression of genes active during cell differentiation and proliferation, it can probably play an important role in the promotion phase of tumor generation (Figure 4).<sup>100</sup>

**Figure 4.** Tumorigenesis and the role of inflammation in the cancer development. ROS = reactive oxygen species; RNS = reactive nitrogen species; NO = nitric oxide; PGs = prostaglandins; ODC = ornithine decarboxylase; MMP = matrix metalloproteinase; VEGF = vascular endothelial growth factor. Adapted from Pan et al., 2010.<sup>100</sup>



Source: PAN, M.-H; LAI, C.-S.; HO, C.-T. Food Functions (2010), 1, 15–31.<sup>100</sup>

Nitrite is another carcinogenic agent in the gastro-intestinal (GI) tract. Besides its role as a source of Reactive Nitrogen Species (RNS), nitrite can promote nitrosation of important biomolecules leading to oxidative modifications, DNA damage and mutations. Nitrite is found in processed and cured meat. Recent meta-analysis studies have shown that high consumption of cured and red meat is related to increased risk of around 20 – 30% colorectal cancer.<sup>38</sup> Colorectal cancer is the second leading cancer related - deaths 500.000 deaths per year. In this direction, aiming to reduce the risk in account, the World Cancer Research Fund makes the recommendation to limit the intake of red meat and specially to avoid processed meat.

Dietary patterns, foods, nutrients and other constituents of the diet are strongly associated with the risk and incidence of various types of cancer, and in this respect, it is estimated that 35% of all cancers deaths are related to nutritional patterns.<sup>37,38</sup> Consume of antioxidants is of relevance to ensure the health maintenance. Some antioxidants obtained from the feed are directly absorbed and transferred to the cells where they act scavenging radicals and preventing oxidative reactions. However, other antioxidants can be produced endogenously via bioconversion of compounds obtained through the diet. Antioxidants either produced endogenously or externally supplied by nutrition are essential to repair the damage caused by ROS and RNS and to the enhancement of the cellular defenses against the development of diseases.<sup>34,101</sup>

## **1.2. Nutritional strategies for improving meat quality**

Nutritional strategies have been used by the meat industry in order to increase the meat production and to improve quality aspects of meat.<sup>27,29,30,44,47,80,102</sup> Together with the increasing demand for high quality meat, there is an increasing public concern to propose a more humane production of meat, and for alternatives to prevent environmental impact due to intensive livestock farming. Diet manipulation has the advantages to naturally induce changes in the meat composition avoiding the use of antibiotics and hormones. Such factors increase the safety of the product and provide a more sustainable animal production and to contribute to the animal welfare.<sup>44</sup> Novel animal feeding regimes can enhance the absorption of nutrients and the disease resistance, improving animal health and, consequently increase the production and benefit the biochemical properties of the product.<sup>6</sup>

Many studies have been investigating changes in the fatty acid composition of meat through the design of diets with vitamins, combinations of grains and grass, lipids or

increased content of plant rich in natural antioxidants.<sup>44</sup> Especially for beef, a particular attention is given to the intramuscular fat (IMF) and several supplements have been studied to potentially increase the content of polyunsaturated fatty acids (PUFA) and conjugated linoleic acid (CLA) that are considered beneficial for health maintenance and disease prevention.<sup>44</sup> Vitamin E has shown to be effective in decreasing the rate of lipid peroxidation in meat while used as supplement for pigs, broilers and cattle.<sup>81</sup> Vitamin D is another meat nutrient that deserves attention. It is also known that grain and grass-fed have different metabolic pathways associated to the muscle development and to the meat quality.<sup>102</sup> Moreover, the use of protected lipid supplements in the animal diet has been used in order to induce the production of lipids with higher degree of unsaturation in the meat.<sup>87</sup>

Not only the fatty acid composition of the animal diet influences the lipid profile of the meat, but also, some metabolites have an import role for the lipid metabolism. Methionine and betaine are examples of amino acids that have been investigated by their effect on the fat distribution, carcass composition and growth performance of broilers and ducks, indicating improvement of animal performance and carcass quality.<sup>26,103</sup> L-carnitine is another amino acid studied as supplement for broilers in order to modulate the fat distribution since this metabolite promotes the mitochondrial  $\beta$ -oxidation of long-chain fatty acids. The products of this oxidation can be easily transferred across the inner mitochondrial membrane, preventing the accumulation of short-chain and medium-chain fatty acids produced through normal and abnormal metabolism.<sup>27,104</sup> Moreover, L-carnitine has been also studied for improving growth performance of pigs, fish, quail (*Coturnix coturnix*) and foals.

Despite the fact that vitamins, amino acids, peptides and lipids have been widely studied in this field, there are few studies reporting the use of plant extracts in animal feeding trials for the improvement of animal welfare or meat quality.

### **1.2.1. Plant extracts as novel feed additives**

Plant extracts have been shown to be effective to protect food products against lipid and protein oxidation. Many studies in literature have demonstrated that extracts offruits (grapes, pomegranate, date, kinnow), vegetables (potato, drumstick, pumpkin, curry, nettle) and herbs and spices (green tea, rosemary, oregano, aloe vera, cinnamon, sage, thyme, mint, ginger, clove, onion, garlic) can inhibit lipid oxidation in a wide variety of meat products. Especially phenolic-rich plant extracts have been added to meat based products and fresh meat. The antioxidant mechanisms of the phenolic compounds include radical scavenging and

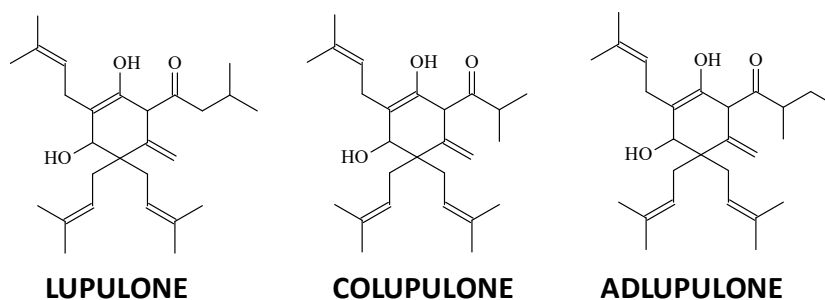
metal chelating activity.<sup>105,106</sup> Considering that the addition of plant extracts directly to the meat can affect the consumer acceptance, there is an interest to use these extracts in animal feeding trials in order to improve the redox stability of meat. When added to the animal diet, the absorbed antioxidant active compounds from plant materials can follow two routes: i) they can directly reach the muscle tissue or ii) they can be metabolized into biological precursors of endogenous antioxidants. In both cases, phenolic compounds can provide the antioxidative mechanisms required to improve animal health and welfare and, to protect meat against oxidation.

### 1.2.2. Hops $\beta$ -acids

One example of a plant extract with pharmacological properties is the extract of hops that is used in beer production. The extract of hops has two principal classes of compounds:  $\beta$ -acids (lupulones, colupulones and adlupulones) and  $\alpha$ -acids (humulones and isohumulones). In beer,  $\alpha$ -acids are responsible for the bitter flavour and  $\beta$ -acids are responsible for beer stability since they have antimicrobial activity. The concentration of these compounds in the beer depends on the degree of isomerization reactions provided by the conditions of the brewing process.

Lupulones are the most important compound found in the fraction of the  $\beta$ -acids and, like the other compounds in this fraction, has three prenyl side chains and allyl which confer hydrophobicity to these compounds (Figure 5). The hydrophobic nature of the  $\beta$ -acids ensures their antimicrobial effect on gram negative and gram-positive bacteria, fungi and yeast. Because of the antibacterial activity of the  $\beta$ -acids, hops have been used in the food industry for the production of beverages like herbal teas and soft drinks, and in herbal medicine as well. Besides that, some studies have demonstrated that  $\beta$ -acids act as antioxidants. Almeida et al. studied the antioxidant activity of  $\beta$ -acids toward 1-hydroxyethyl radical that can prevent beer oxidation. Authors found that lupulones are easily oxidizable, reacting with 1-hydroxyethyl radical close to the diffusion control ( $k = 2.6 \cdot 10^8$  and  $2.9 \cdot 10^8 \text{ L mol}^{-1} \text{ s}^{-1}$  at 25 °C) and, the prenyl side chains were recognized as the main reaction centers for the electron transfer.<sup>107</sup>

**Figure 5.** Structure of the  $\beta$ -acids that are found in hops.



Source: Figure elaborated by the author.

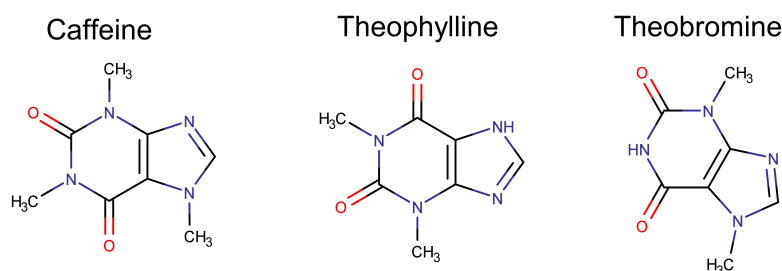
In this perspective, hops have potential to be used as a novel feed additive in broilers and pigs enhancing the absorption of nutrients and consequently, acting as growth promoter. In literature, there is a report regarding the effect of hops on performance and intestinal health of broiler chickens and weanling pigs. In these studies, positive effects on the productive performance of the animals were demonstrated.<sup>28,108</sup> Other studies comparing the use of hops as antibacterial performance enhancers to synthetic antibiotics, like penicillin and avilamycin, have shown that  $\beta$ -acids can be potential alternatives to antibiotics in animal feeding supplementation.<sup>28</sup>

### 1.2.3. Yerba mate

Another example of plant extract is the extract of yerba mate or *Ilex Paraguariensis*. Mate is a native plant found in South America from the family Aquifoliaceae. Brazil has approximately 80% of the area of occurrence of yerba mate which is also found in Argentina, Bolivia, Paraguay, Uruguay and Chile. The southern regions of Brazil (Paraná, Santa Catarina and Rio Grande do Sul) are leaders in the yerba mate production and consume. Yerba mate is traditionally consumed in these regions as the beverage called mate (chimarrão, tererê and other variations). Brazil is a leader of exportation of mate considering the international market that has demonstrating an increasing interest to consume this plant due to its phytotherapeutic properties. Mate became popular worldwide as a supplement for weight loss. According to the popular medicine, mate has positive effects on arthritis, rheumatism, constipation, and retention of liquid, fatigue, hypertension, diabetes and obesity. Many studies have been carried out to probe the benefits of yerba mate to the human health with potential applications in treatment of many diseases, like cancer, diabetes and obesity.<sup>11,109,110</sup>

Yerba mate is composed by a high amount of phytochemical compounds, which major compounds are phenolics, saponins and methylxantines. Caffeine, theobromine and theophylline (Figure 6) are examples of methylxantines that are found in mate being recognized as nervous system stimulants (Alikaridis, 1987). These three compounds are also considered the main purine alkaloids found in plants.<sup>109</sup>

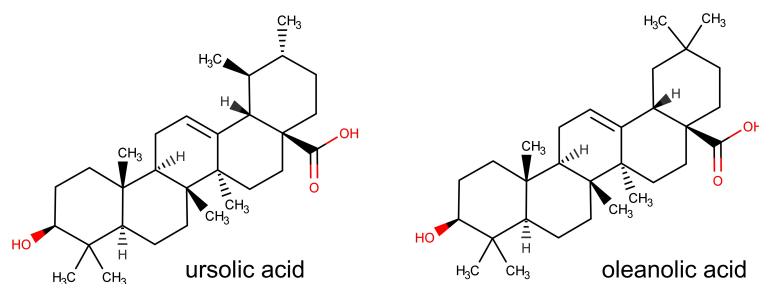
**Figure 6.** Structure of the methylxantines caffeine, theophylline and theobromine.



Source: Figure elaborated by the author.

Saponines are amphiphatic glycosides that are responsible for the bitter flavour and for the foam formation of the beverages made of mate. Besides that, the anti-inflammatory, antifungal, antibacterial, antitumoral and antimutagenic activities of yerba mate have been assigned to the presence of saponines. Yerba mate leaves has significant amounts of the triterpenoid saponines ursolic and oleanolic acids (Figure 7).<sup>109</sup>

**Figure 7.** Structure of ursolic acid and oleanolic acid.



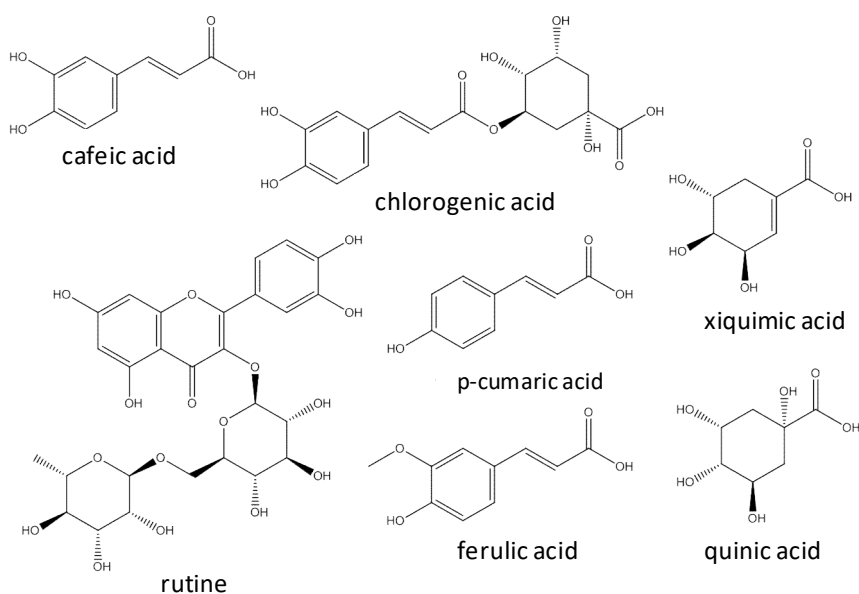
Source: Figure elaborated by the author.

Present in the leaves of yerba mate, phenolic compounds are responsible for the astringent properties and the antioxidant activity of the plant. The most important phenolic compounds that are present in yerba mate have their structure presented in Figure 8. Chlorogenic acid and its isomers (CGAs) are important examples of phenolic compounds

found in mate. CGAs derivatives, series of trans-phenyl-3-propenoic acids differing in their ring substitution, are widely distributed in the plant as ferulic, caffeic, sinapic and *p*-coumaric acids. Many studies have shown the efficient antioxidant activity of CGAs. The CGAs ability to act as electron or hydrogen atom donors is responsible for their powerful free radical scavenger activity. Moreover, these polyphenols can prevent free radical formation by chelating transition metal ions.<sup>109</sup> Phenolic compounds have demonstrated efficacy in the prevention of lipid oxidation.

Yerba mate also contains flavonoids as examples of the phenolic compounds that have been associated to the prevention of age-related chronic conditions. Rutin, quercetin, a diglycosyl derivative of luteolin, tannins and caffeoyl glucose are also present in the extract of yerba mate.

**Figure 8.** Chemical structure of polyphenols found in yerba mate.



Source: Figure elaborated by the author.

Yerba mate has been widely used as supplement in human nutrition, indicating potential achievements in the medicinal field: anti-diabetic action, protection of the cells against mutagenesis, hypocholesterolemic effect, improvement of the circulatory system, digestion improvement, antioxidant and anti-ageing effect and, anti-fatigue action.<sup>31,109</sup> These results suggest that yerba mate may influence human metabolism enhancing the balance that is necessary for health maintenance. Therefore, yerba mate can potentially be used as

supplement for animal nutrition in order to provide improvement of animal health, consequently, benefiting the quality of meat.

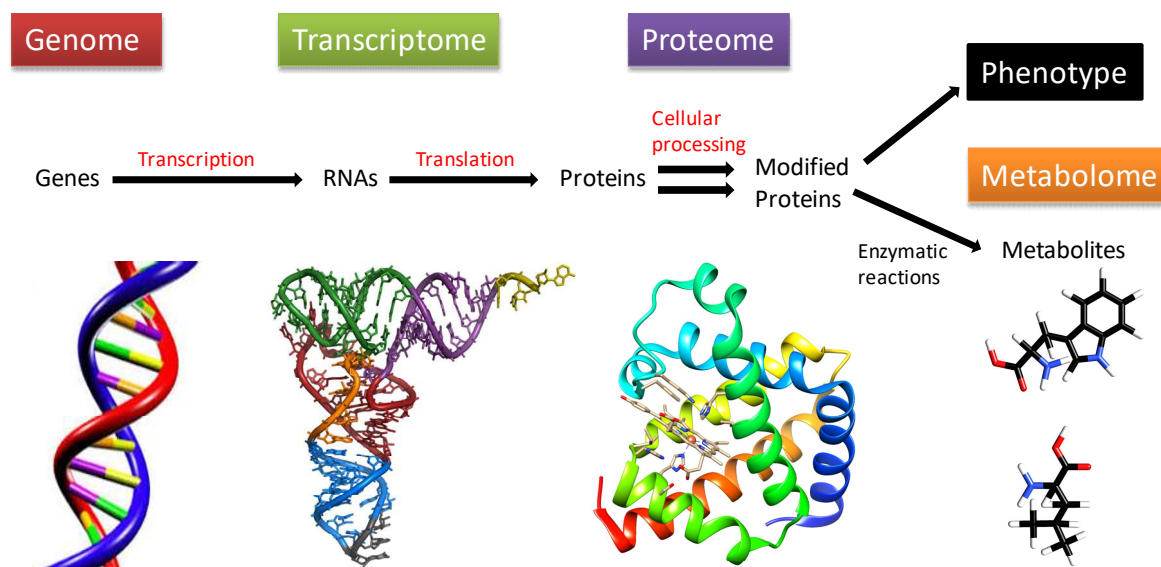
### **1.3. Methods for investigation of meat quality: metabolomics, NMR, Chemometrics, EPR spin trapping and protein oxidation**

#### **1.3.1. Metabolomics**

Food science and nutrition have been receiving increasing attention considering the potential role of the diet in the occurrence of diseases. Many researches in this field became possible due to the development of the Omics science that aims to investigate the composition of a system of interest. There are four main “omics” analysis: genomics, transcriptomics, proteomics and metabolomics.<sup>111</sup> Metabolomics has been widely applied in the study of drug-induced toxicology<sup>112</sup>, disease development and disease diagnostics<sup>113</sup>, biomarker discovery<sup>114</sup>, metabolite signatures and nutrition science.<sup>115,116</sup> The characterization of complex matrixes (i.e. foods) can be done under omics approaches permitting the determination of the “metabolite or metabolic profile”. Metabolomics analyses are based on the use of analytical procedures required to identify and to quantify all the metabolites with low molecular weight (MW lower than 1500 dalton) that are synthesized or modified by a living cell or organism, the metabolome.<sup>111</sup> Metabolome is the final product of the biological events that reflects the combination between genetic and environmental effects on the organism. Numerous studies based on metabolomics analysis reported in literature aim to obtain a global metabolic overview of the system through the determination of metabolic patterns or profiles (known as “metabolic fingerprinting”) and, then, search discriminant attributes through statistical methods.<sup>112,114,116</sup>

Foodomics appears as the study of food composition and uses the combination of the analytical tools from transcriptomics, proteomics and metabolomics.<sup>117,118</sup> These three methodologies are related to each other, as represented in Figure 9. The characterization of the biochemical composition affecting oxidative stability of food may be undertaken by the use of modern analytical methodologies such as Nuclear Magnetic Resonance and High Resolution Accurate Mass Spectrometry (HR-MS).

**Figure 9.** Relationship between genome, transcriptome, proteome and metabolome. Adapted from Gerszten and Wang, Nature, 2008.<sup>119</sup>

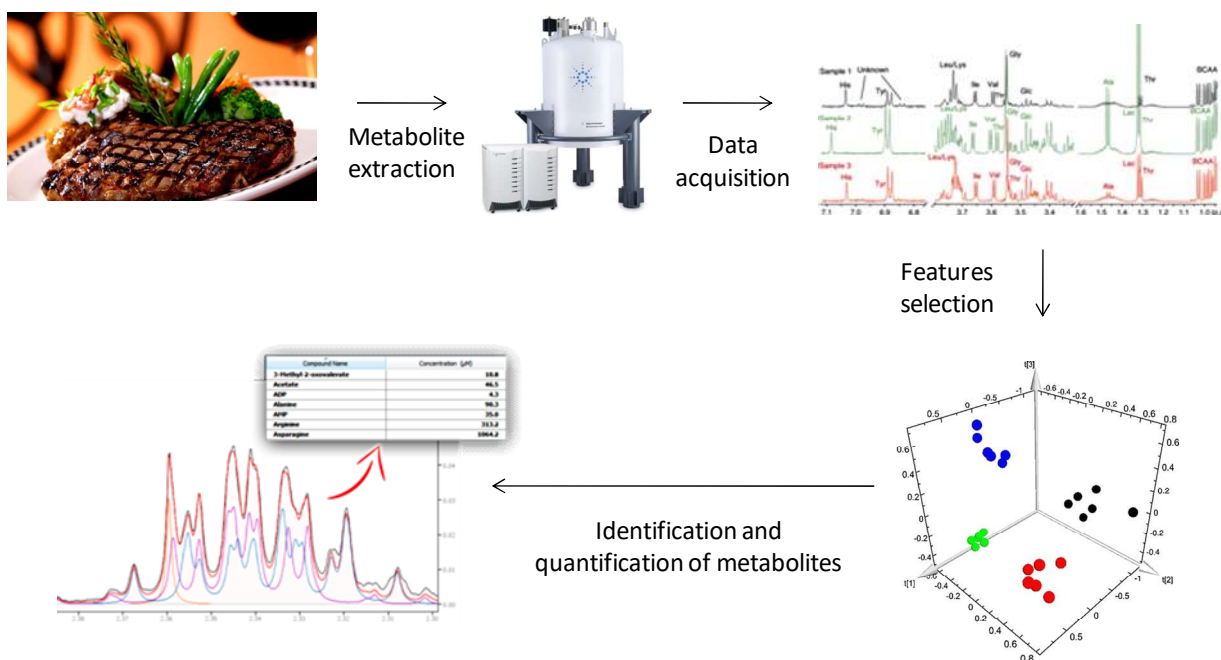


Source: Figure elaborated by the author.

Metabolomics and foodomics methodologies have been divided into two different approaches: untargeted and targeted metabolomics. Untargeted metabolomics consists in the comprehensive analysis of all the measurable analytes in a sample by the observation of the full profile of this sample, with no identification of each one of these unknown chemical compounds in the sample. Due to the high complexity of the datasets used for untargeted metabolomics, advanced chemometric methods need to be performed in order to reduce the overall dataset into a smaller and simple set of signals. On the other hand, targeted metabolomics corresponds to the measurement of specific metabolites that have their identity previously established through a quantitative or semi-quantitative approach. Targeted metabolomics allows the discovery of novel associations between metabolites and the understanding of biochemical pathways to which they participate.<sup>115</sup> A basic workflow illustrating the use of targeted and untargeted metabolomics in Foodomics is shown in Figure 10.

Considering that HR-MS has not been the focus of the present thesis, the following sections describe the use of NMR, Chemometrics, EPR spin-trapping technique and methods for the investigation of protein oxidation.

**Figure 10.** Basic workflow diagram for Foodomic analysis: NMR spectroscopy used for monitoring untargeted and targeted metabolomics in conjunction to statistical analysis.



Source: Figure elaborated by the author.

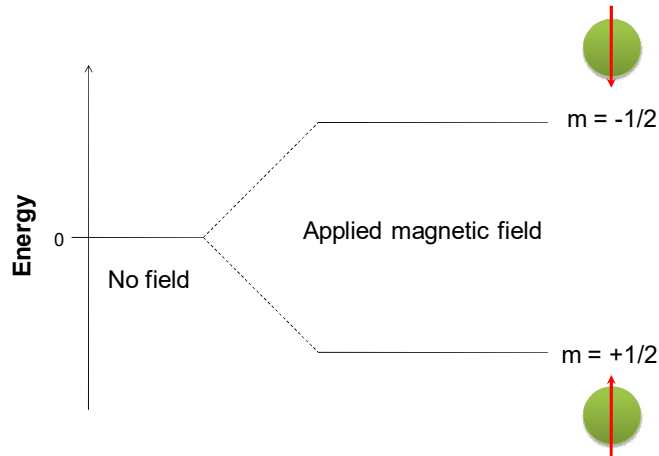
### 1.3.2. Nuclear Magnetic Resonance NMR

Nuclear Magnetic Resonance (NMR) is a powerful analytical technique to study metabolism and “metabolic profile”. The first report on Nuclear Magnetic Resonance was described by Isidor Rabi in 1938. In this study, Rabi et al. observed that molecular beams of hydrogen could absorb radiofrequency (RF) energy when placed in a magnetic field and when subjected to a specific frequency of RF which is known as resonance frequency. However, the visibility of the NMR technique has increased when Edward Mills Purcell and Felix Bloch used liquid and solid samples, for which they were awarded the 1952 Nobel Prize in Physics.<sup>120</sup>

The principle behind NMR is based on a physical phenomenon of absorption and re-emission of electromagnetic radiation by nuclei in the presence of a magnetic field. The nuclei of all the elements have charge ( $q$ ), mass ( $m$ ), magnetic momentum ( $\mu$ ) and an intrinsic angular momentum since they are spinning on their axes. It is a quantum property called spin ( $I$ ). Due to the existence of spin, nuclei experience a rotational motion without a specific orientation. When these spins are paired against each other, the overall spin is zero. The NMR phenomenon occurs when the overall nuclear spin is different of zero ( $I \neq 0$ ) and, when an external magnetic field ( $B_0$ ) is applied to a nucleus, producing a splitting

of the energy levels. Consequently, this nucleus admits  $2I + 1$  possible orientations (Figure 11). Such energy level splitting due to the application of a magnetic field is known as Zeeman Effect.<sup>120</sup>

**Figure 11.** Energy levels for a nucleus with spin quantum number  $m = \frac{1}{2}$ .



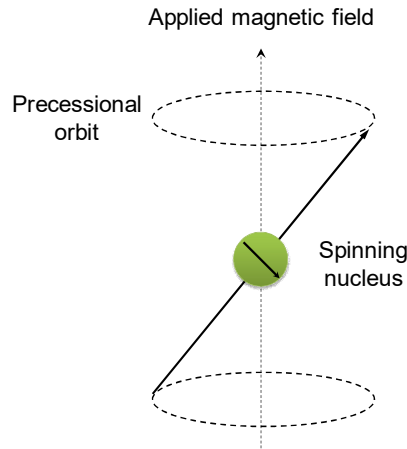
Source: Figure elaborated by the author.

The initial populations of the energy levels of a nucleus are determined by thermodynamics according to the Boltzmann distribution. Therefore, levels of lower energy tend to be more occupied by nuclei than the energy levels with higher energy. In the presence of an applied magnetic field, the nuclei axis of rotation precesses around the external magnetic field (Figure 12) with a precession frequency denoted by the Larmor frequency, which is identical to the frequency that is required for the transition to the upper energy level. There is a potential energy ( $E_p$ ) associated to the precession of the nucleus:

$$E_p = \mu B \cos \theta \quad (2)$$

where  $\mu$  is the magnetic momentum;  $B$  is the magnetic field and  $\theta$  is the angle between the direction of the applied field and the axis of nuclear rotation.<sup>120</sup>

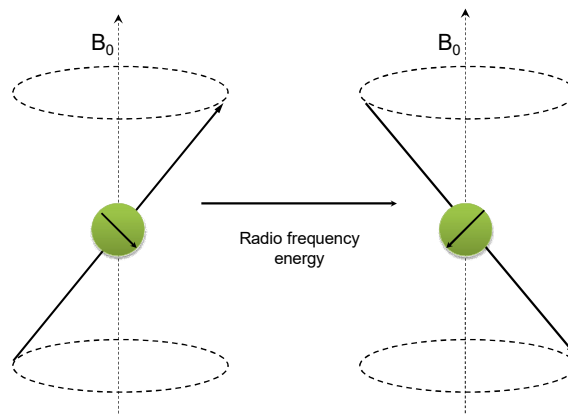
**Figure 12.** Nucleus precession in the presence of an external magnetic field.



Source: Figure elaborated by the author.

The angle of precession can be changed due to the absorption of RF energy making the magnetic momentum flips toward the opposite direction of the magnetic field, changing the spin state,  $m$  (Figure 13).

**Figure 13.** Transition between two different spin states due to the absorption of radio frequency energy.



Source: Figure elaborated by the author.

The application of electromagnetic radiation in a frequency of radiation corresponding to the difference in energy between the energy levels allows the excitation of the nuclei to the higher energy level. This frequency of radiation is the frequency of resonance. The corresponding energy associated to this process can be described by the Bohr Equation:

$$\Delta E = h\nu \quad (3)$$

where  $\Delta E$  corresponds to the difference of energy between the two states;  $h$  is the Planck's constant and  $\nu$  is the frequency of resonance.

To calculate the energy involved in the transition between these different states, it is necessary to consider that the nucleus possesses positive charge and is spinning on its axes, producing a small magnetic field. As consequence, the nucleus has a magnetic momentum ( $\mu$ ) which is proportional to its spin ( $I$ ), according to the follow equation:

$$\mu = \frac{\gamma I h}{2 \pi} \quad (4)$$

where  $\gamma$  is fundamental nuclear constant called the magnetogyric ratio which has a different value for every nucleus and  $h$  is Planck's constant.

Considering a particular energy level, the energy is given by:

$$E = -\frac{\gamma h}{2 \pi} m B_0 \quad (5)$$

where  $B_0$  corresponds to the strength of the magnetic field at the nucleus and  $m$  corresponds to the spin state.

The transition energy between two states  $\alpha$  and  $\beta$  can be, accordingly, calculated by:

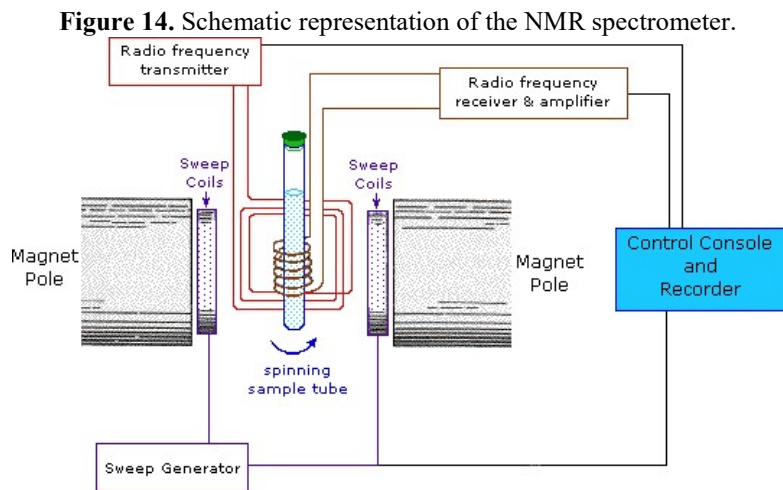
$$\Delta E = E_\alpha - E_\beta = \frac{\gamma h B_0}{2 \pi} \quad (6)$$

A NMR signal arises from the absorption or the emission of energy due to the transition of the nuclear spins between different states and the return of the magnetization to the ground state, which is known as relaxation process. There are two main relaxation processes: spin - lattice (longitudinal) relaxation and spin - spin (transverse) relaxation.<sup>120</sup>

In Figure 14 is shown a schematic representation of the NMR spectrometer instrumentation. The detection of the NMR signal is possible because during the relaxation process, the oscillating magnetization induces a current in a nearby pickup coil of the NMR equipment. This current creates an electrical signal oscillating at the NMR frequency.

The observable NMR signal produced through the relaxation processes is called Free Induction Decay (FID) and is expressed as a time-domain function. The magnetic resonant absorption that is detected in NMR can be converted to a spectrum representing the intensity of the NMR signal as a function of frequency by the application of the Fourier Transform (FT). FT is a mathematical method that decomposes the time-

domain function FID into a function representing the dependence of the signal amplitude on frequency. The most common nuclei analysed by NMR are  $^1\text{H}$  and  $^{13}\text{C}$ .<sup>120</sup>



Source: <https://www2.chemistry.msu.edu/faculty/reusch/virttxtjml/spectrpy/nmr/nmr1.htm>

Considering a specific molecule, each nucleus presents a particular resonant frequency because the electrons around the nucleus provide a nuclear shielding. It means that the magnetic field at the nucleus is different from the applied magnetic field. The nuclear shielding depends on the chemical environment of the nucleus and represents the influence of the other atoms in a molecule on a specific nucleus. Electron density, polar effects, type of chemical bond and hyperconjugation are important factors determining the chemical environment and the nuclear shielding of a nucleus. The nuclear shielding is usually expressed as chemical shift that represents the nuclear resonance frequency in relation to a standard in a magnetic field. The frequency of resonance expressed in hertz (Hz) can be converted to the chemical shift ( $\delta$ ) expressed in parts per million (ppm) by frequency, as calculated from:

$$\delta = \frac{\nu_s - \nu_{ref}}{\nu_{ref}} \quad (7)$$

where  $\nu_s$  and  $\nu_{ref}$  correspond, respectively, to the absolute resonance frequency of the sample and the absolute resonance frequency of a standard reference compound, measured in the same applied magnetic field  $B_0$ .<sup>120</sup>

$\delta$  is expressed in ppm because the numerator is usually expressed in hertz, and the denominator in megahertz. The chemical shift in a NMR spectrum is essential for the elucidation of molecular structures. However, other two aspects are highlighted as important determinant factors for structure diagnostic: the intensity and the multiplicity of the signal. The intensity of the signal has a straight relation to the number of nuclei that

experience the same resonant frequency. The multiplicity of the signal is associated to the coupling between equivalent protons and its neighbors. Small interactions (coupling) between different groups of protons are observed through the splitting of one peak into two or more peaks in the NMR spectrum. The result of this splitting is denoted by hyperfine splitting.<sup>120</sup> The number of peaks or multiplicity (M) produced by hyperfine splitting can be calculated as follow:

$$M = 2 n I + 1 \quad (8)$$

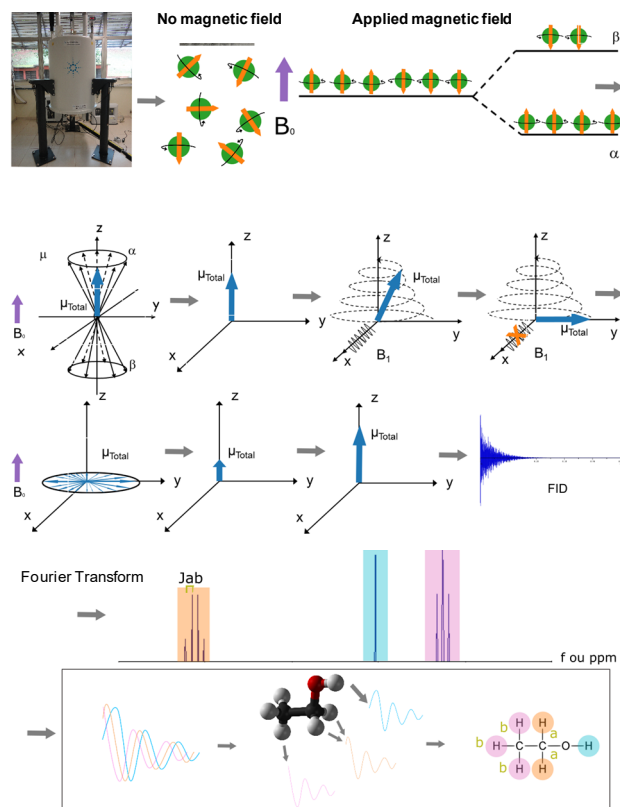
where n is the number of neighboring atoms and I is the spin number of the analyzed nucleus.

The coupling between two neighboring atoms (a and b) can be measured by the difference between their respective resonance frequency ( $f_a$  and  $f_b$ ) as denoted by the hyperfine coupling constant ( $J_{ab}$ ):

$$J_{ab} = f_a - f_b \quad (9)$$

A representative scheme of the principles of NMR spectroscopy, taking into account the theoretical principles behind it, is shown in Figure 15.

**Figure 15.** Schematic representation of the NMR principle.



Source: Figure provided by Caroline Ceribeli.

Methods of  $^1\text{H}$ -nuclear magnetic resonance ( $^1\text{H}$ -NMR) spectroscopy,  $^{13}\text{C}$ -nuclear magnetic resonance ( $^{13}\text{C}$ -NMR) spectroscopy, gas chromatography-mass spectrometry (GC-MS), gas chromatography-flame ionization detection (GC-FID), direct infusion-mass spectrometry (DI-MS) and liquid chromatography-mass spectrometry (LC-MS) were essential to the initiation of the omic sciences. As NMR sensitivity has improved with the evolution of higher magnetic fields and magic-angle spinning (MAS), NMR continues to be a leading analytical tool in this area.<sup>121</sup>

### 1.3.3. Chemometrics

Statistical methods, especially multivariate analysis, have been largely used to analyze variations indicated by NMR regarding the composition of complex systems. The use of mathematical and statistical methods to a better understanding of a chemical system by correlating its physical and chemical properties to analytical instrument data is known as Chemometrics. The aim of this method is to identify patterns in the data in order to set a model that can be routinely applied to future data for predicting the same physical and chemical parameters and for the design of novel experiments. Chemometrics consists in an interdisciplinary science that comprehends studies in chemistry, biochemistry, physics, medicine, biology and chemical engineering.<sup>122</sup>

Spectroscopic analysis has been using a chemometric approach to solve problems of calibration during the analysis of spectral data sets. The reduction and the correction of interferences in the spectral data, including overlapped bands, baseline drifts, scattering and path length variation, can be done by data pre-processing using chemometric methods. The chemometric methods mostly used by spectroscopists are: Principal Component Analysis (PCA); Regression (PLS, PCR, MLR, 3-way PLS) and Prediction; SIMCA and PLS-DA Classification; Design of Experiments; ANOVA and Response Surface Methodology, Multivariate Curve Resolution (MCR); Clustering (K-Means). PCA deserves attention as it is considered one of the most important and powerful chemometric methods used in chemical analysis.<sup>123</sup>

PCA is a very useful method to represent graphically clustering of data sets. The basis of PCA is the use of a linear transform or orthogonal transformation to determine suitable linear combinations of uncorrelated variables. Through this method, the sum or the average of all the variables is converted into a new variable that can replace the original variables. This new variable is composed by a weighted average of all the random

variables and is represented by a unit vector that indicates the variance of the original variables. The weight is necessary to describe the contribution of each variable for this new variable. The new variable that includes the defining weights and is the most suitable variable to explain the main variation in the whole data set is called the first principal component (PC1). Usually, the number of components necessary to accurately describe the original data set is chosen to represent more than 75% of the latter. A previous data processing is required to perform PCA. Normalization methods are applied to the data sets in order to scaling the data. Then, data is converted into a matrix  $X$  with the size  $I \times J$ , where  $I$  corresponds to the number of rows ( $i = 1, \dots, I$ ) representing samples/objects and,  $J$  corresponds to the number of columns ( $j = 1, \dots, J$ ) representing variables. For normalized eigenvalues, the projective dimension yielded by PCA is set by the sum of the eigenvalues of the principal components. Although it is not a rule, we set the sum to be 0.75, a value which typically accounts for 2 or 3 components and yields bi or tridimensional projections.<sup>122,123</sup>

#### **1.3.4. EPR spin trapping**

Under oxidative conditions, food components can produce short-lived free radicals that are strongly reactive species. Reactions involving radicals and antioxidants in foods are essential for understanding the quality and flavor stability of food products. Spectroscopic methods have been efficiently used to evaluate the redox stability of food compounds subjected to oxidative conditions from which Electron Paramagnetic Resonance (EPR) can be highlighted. EPR spectroscopy has been successfully used for the determination of radical scavenging activity of antioxidants from foods (like phenolic compounds, catechins, flavonoids, carotenoids) and for the investigation of the redox stability of beer, tea, wine, milk and meat based products. The redox stability as determined by EPR can be used to predict shelf life of foods.<sup>124</sup>

Electron Paramagnetic Resonance (EPR) or Electrons Spin Resonance (ESR) is a spectroscopic method to study chemical species with unpaired electrons. The principle behind EPR phenomenon is analogous to NMR, since both phenomena are based on the Zeeman effect and the property of the atomic particles to interact with electromagnetic radiation absorbing or emitting energy.<sup>124</sup> However, instead of nuclei in NMR, unpaired electrons are monitored in the case of EPR. As well as the nuclei, unpaired electrons have a magnetic moment ( $\mu$ ) and spin quantum number ( $I$ ) that admits certain spin states. When

unpaired electrons are placed in an external magnetic field ( $B_0$ ), there is an alignment of their spins in two different ways producing two different spin states. This alignment of the electron magnetic moment along the direction of the magnetic field  $B_0$  can be parallel ( $m_s = -1/2$ ) or antiparallel ( $m_s = +1/2$ ). Each alignment has a specific energy that is given by the Zeeman effect and the Bohr equation, according to:

$$E = h\nu = m_s g_e \mu_B B_0 \quad (10)$$

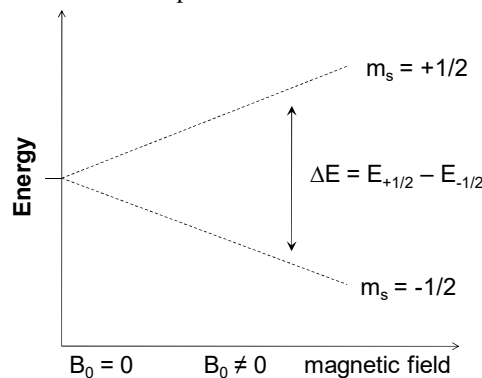
where  $h$  is the Planck's constant;  $\nu$  is the frequency of radiation;  $m_s$  is the the spin state;  $g_e$  is the g-factor (a proportionality constant that relates the observed magnetic moment  $\mu$  of a particle to its angular momentum quantum number and a unit of magnetic moment);  $\mu_B$  is the Bohr magneton.

The difference between the two different states of energy is given by:

$$\Delta E = h\nu = E_{+1/2} - E_{-1/2} = g_e \mu_B B_0 \quad (11)$$

According to this equation, the separation between the lower and the upper state shows that the splitting of the energy levels is directly proportional to the strength of the magnetic field (Figure 16).<sup>125</sup>

**Figure 16.** Energy levels splitting due to the application of increasing strength of magnetic field in an unpaired electron.

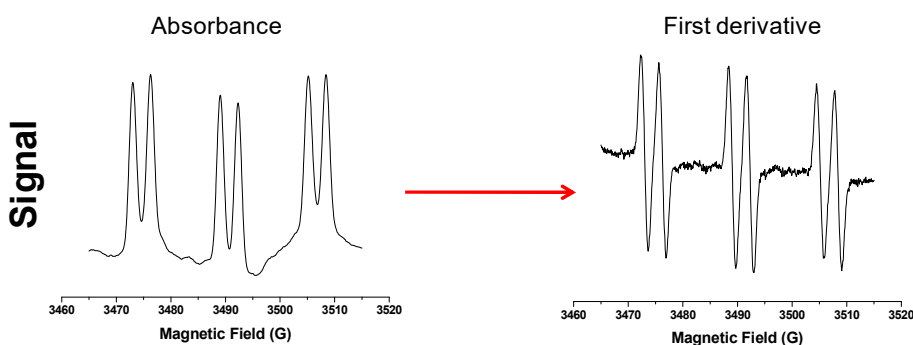


Source: Figure elaborated by the author.

To reach the upper state of energy, an unpaired electron can absorb energy with a frequency  $\nu$ . To reduce the gap between the two different states, the magnetic field is increased until the energy required for the transition matches the energy of the microwaves. In the majority of the EPR experiments, microwaves in the range of 9000–10000 MHz (9–10 GHz) are used as the frequency. EPR experiments are continuous wave (CW) methods, since the samples are continuously irradiated with microwave radiation at a fixed frequency, sweeping the external magnetic field and monitoring the microwave

absorption for each field value. The absorption of energy can be measured and converted into a spectrum that can be plotted as a first derivative spectrum of the absorption spectra (Figure 17). The first derivative of the absorption spectra is most usual way to report an EPR spectra.<sup>125</sup>

**Figure 17.** Conversion of the EPR absorbance spectrum of PBN adduct radical into the first derivative of the signal.



Source: Figure elaborated by the author.

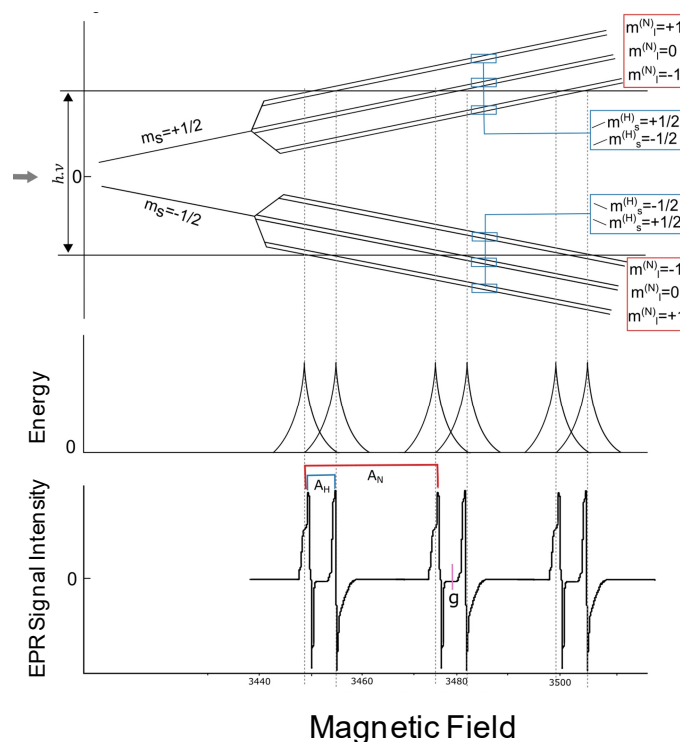
ERP spectra of free radicals have particular patterns that allow their identification. The main characteristic parameters of an EPR spectrum are the g-factor and the hyperfine splitting. The g-factor is a dimensionless constant that measures the gyromagnetic ratio and the magnetic momentum of an atom. The hyperfine splitting is related to the interaction between the electronic spin of an unpaired electron and its nearby nuclear spins. Hyperfine coupling results in the creation of additional allowed energy states that may be observed as multi-lined spectra (Figure 18). The interaction between electrons and nuclei can occur by Fermi contact interaction and by bipolar interaction. The number of lines in the EPR spectrum of a radical can be determined by:

$$M = 2I + 1 \quad (12)$$

where I corresponds to nuclear spin referring to the nearby nucleus.

The linespacing of a signal provides anisotropic hyperfine coupling constants (B) and isotropic hyperfine coupling constants (A) that are also of importance to characterize free radicals. Isotropic hyperfine coupling constants can be denoted by  $A_N$  and  $A_H$  (Figure 18).  $A_N$  is related to the coupling between the spin of an unpaired electron and the nucleus where this unpaired electron is associated.  $A_H$  represents the coupling between the spin of an unpaired electron and the nuclear spin of its neighbor nucleus.<sup>125</sup>

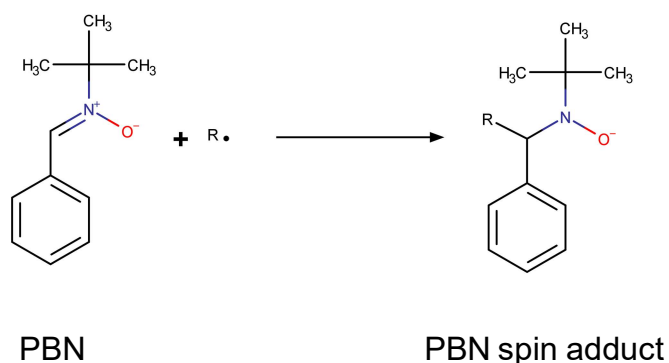
**Figure 18.** Energy-level diagram and corresponding EPR signals for an unpaired electron in an applied magnetic field that interacts with a  $^{14}\text{N}$  nucleus in which the energy levels are additionally split by a nearby proton.



Source: Figure elaborated by the author.

Most part of radicals produced in food products and other systems is strongly reactive, having short lifetimes of less than seconds. Hence, there is a high difficulty in measuring these free radicals. The spin-trapping technique was developed in order to solve these difficulties. Free radicals can be chemically added to spin-trap double bonds producing long-lived adduct radicals (spin adducts) that can be monitored at room temperature by Electron Paramagnetic Resonance (Figure 19). The resulting EPR spectra of the spin adduct have characteristic profiles of hyperfine splitting and g-values that allow the identification of the type of radical trapped by the spin-trap. 5,5-dimethyl-1-pyrroline-N-oxide (DMPO);  $\alpha$ -(4-pyridyl-1-oxide)-N-tertbutylnitron (POBN) and  $\alpha$ -phenyl-N-tert-butyl nitron (PBN) are examples of nitron spin traps that are generally used to determine the redox stability of systems with radicals.<sup>124,125</sup> Nitron spin traps scavenge free radicals via addition to the carbon located in an alpha position relative to the nitrogen as exemplified in Figure 19.

**Figure 19.** Trapping of a free radical by the spin trap PBN.



Source: Figure elaborated by the author.

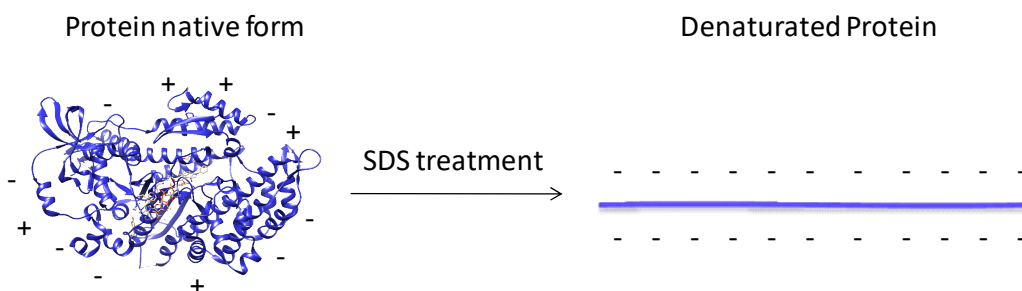
### 1.3.5. Protein oxidation

Oxidative stress can induce reversible and irreversible modifications in proteins, leading to cellular damage. Since protein structure has fundamental role for enzymatic catalysis, it is necessary to know how oxidative reactions in proteins can modify important biological pathways. For meat, protein oxidation promotes not only changes in the sensorial attributes which directly affect its acceptance and consume as well as it is related to initiation of some diseases as previously discussed. Oxidative reactions in proteins from meat may lead to the formation of protein radicals and cross-links.<sup>3</sup> Gel electrophoresis combined with immunoblotting techniques have been largely used for the study of such modifications in proteins.<sup>126,127</sup>

Polyacrylamide Gel Electrophoresis (SDS-Page) is an analytical technique used to separate macromolecules (proteins and nucleic acids) according to their size. Proteins, as charged molecules, experience electrostatic effects when an electric field is applied. Therefore, proteins can migrate in an electric field towards an electrode with opposite sign. Considering that the electrophoretic mobility of a molecule depends on its charge and size, the use of a denaturant like sodium dodecyl sulphate (SDS) is necessary to achieve an uniform negative charge on the protein surface (Figure 20), making the electrophoretic mobility depends primarily on the molecular size. A protein negatively charged due to presence of SDS on its surface can be loaded onto a gel that corresponds to a cross-linked polymer with suitable composition and porosity. The networks of the polymer can achieve a specific porosity according to the gel composition and the concentration of the pre-polymer (before crosslinking). Polyacrylamide gels are widely used for protein separation by electrophoresis because they are chemically inert,

electrically neutral, hydrophilic, and transparent for optical detection at wavelengths greater than 250 nm. When an electric current is applied, proteins will migrate through gel towards the positively charged electrode (anode). Proteins with high molecular weight tend to migrate less than those ones with low molecular weight, so they can be separated according to their size.<sup>128</sup>

**Figure 20.** Negative charge distribution in a protein upon addition of SDS.

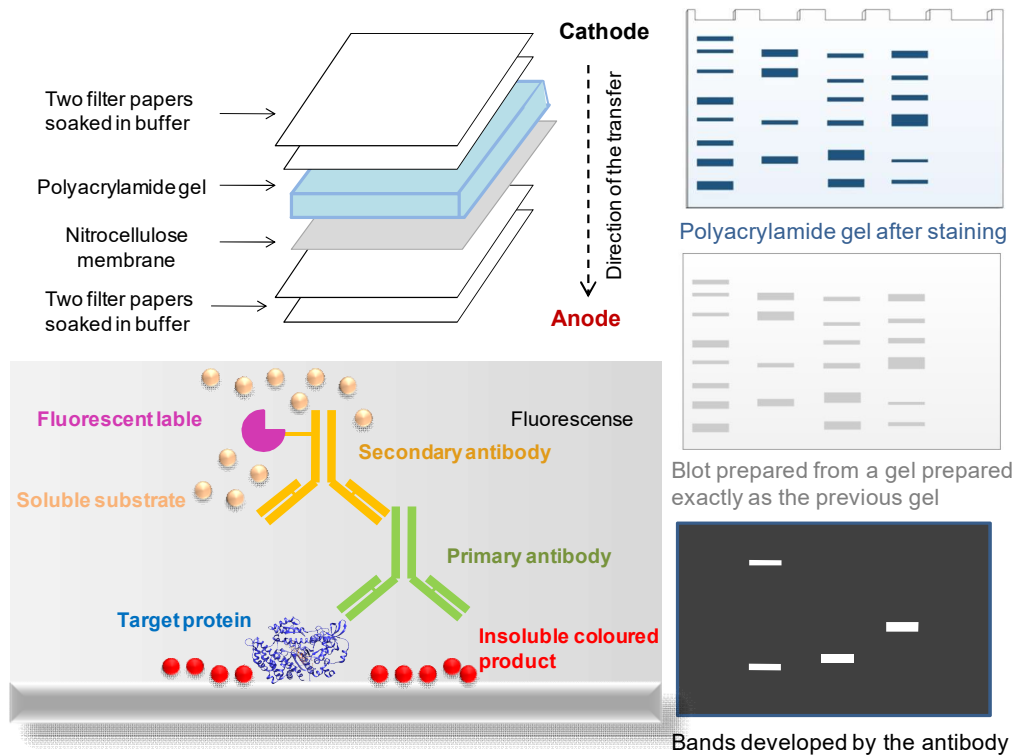


Source: Figure elaborated by the author.

Western blotting technique has been used in conjunction to the SDS-Page to separate and identify proteins. Both techniques separate a mixture of proteins according to their molecular weight by gel electrophoresis. However, Western blotting uses the gel resulting from a previous SDS-page experiment to additionally transfer the separated proteins to a membrane producing a band for each protein. Since these bands are not visible, the incubation of the membrane with label antibodies specific to the protein of interest is necessary. These antibodies bond to a targeted protein producing an insoluble colored product that can be visualized as band by fluorescence, chemiluminescence and colorimetric techniques.<sup>126</sup> The principal steps to perform Western blotting are present in Figure 21.

Western blotting is also called protein immunoblotting considering that detection of a specific antigen requires particular antibodies. Derivatizations of Western Blot techniques have been applied to the detection of carbonyls and radicals in proteins.<sup>127</sup>

**Figure 21.** Principal steps of immunoblotting technique: (1) separation by size by gel electrophoresis, (2) transfer to a membrane by electrophoresis, and (3) visualization marking target protein using suitable antibodies.



Source: Figure elaborated by the author.

## 2. Goals

Chapter I of the present PhD thesis aim to investigate the impact of adding supplements to the animal diet in the metabolic profile of meat in relation to its redox stability and its sensory aspects. Specifically, the present research aims to:

- Determinate the metabolic profile of meat from animals fed with different levels of natural supplements (hops  $\beta$ -acids and yerba mate) via NMR and ESI-MS and compare the results with animals fed without supplements;
- Verify if the addition of supplements in the diet promoted significant changes in the metabolic profiles using statistical methods of analysis;
- Investigate the redox stability of meat from animals control and animals fed with natural supplements by EPR spin-trapping technique and the relation between redox stability and metabolic profile;

- Investigate the oxidation of myofibrillar proteins in meat and the influence of diet to prevent protein oxidation;
- Investigate the effect of the supplements in the sensory properties of meat.

## 3. Materials and methods

### 3.1. Animals and sampling

#### 3.1.1. Supplementation with yerba mate

Animals used for the present study were raised at Embrapa Pecuária Sudeste (São Carlos, SP, Brazil). Animal treatment was in agreement with Ethical Principles of Animal Experimentation of Embrapa Southeast Livestock.

Forty-eight Nellore steers (*Bos indicus*, minimal genetic variation due to common semen donor) with an average age of 21 months and an initial weight of 419 kg were individually fed during 94 days with the same basic diet, differing by mate extract levels (0%, 0.5%, 1.0%, and 1.5% w/w). Diets were composed of grounded corn grain (51.3% w/w), corn silage (43.0% w/w), mineral supplement (1.2% w/w), soybean meal (1.0% w/w), urea (1.0% w/w), sodium bicarbonate (1.0% w/w), and Moensin (0.030% w/w). The final diet was composed of 11% crude protein and 72% of total digestible nutrients. Diets were balanced using 0%, 0.5%, 1.0% and 1.5% w/w of food grade kaolin as an inert ingredient. Mate extract (particles of 40 mesh, maximum of 6% water content, 6% of organic matter, and a maximum caffeine content of 6%) without addition of excipient was the product of Centroflora Group (Botucatu – SP, Brazil) produced from fresh leaves of mate (*Ilex paraguariensis* A. St.-Hil.) by water:ethanol 75:25 v/v extraction at 90 °C.

Animals were shipped one day before the slaughter to a commercial abattoir and held overnight with access to water. Animals were slaughtered and carcasses were chilled overnight at 2° C. All dietary treatments and experimental procedures were approved by the EMBRAPA Southeast Livestock Animal Care Committee (CEUA protocol 06/2014) and animals were cared and stunned by captive bolt and exsanguinated in accordance with guidelines established by the Brazilian Ministry of Agriculture. After twenty-four hours post mortem the left half-carcass between the 12 and 13th rib was removed and 2.5 cm steaks (*Longissimusthoracis et lumborum* muscle) were collected for

sensory analysis and chemical investigations. Steaks were placed in plastic bags, vacuum-packed and stored at  $-20\text{ }^{\circ}\text{C}$  and  $-80\text{ }^{\circ}\text{C}$  for sensory evaluation and for chemical profiling, respectively.

### 3.1.2. Supplementation with hops $\beta$ -acids

Hops  $\beta$ -acids, porlupulone ( $\text{C}_{27}\text{H}_{38}\text{O}_4$ ), colupulone ( $\text{C}_{26}\text{H}_{37}\text{O}_4$ ), and adlupulone ( $\text{C}_{27}\text{H}_{38}\text{O}_4$ ), were microencapsulated with cellulose to contain 30% hops  $\beta$ -acids (Hopsteiner, New York, EUA). Animal feeding trials were carried out at Luiz de Queiroz College of Agriculture (ESALQ, Piracicaba-SP, Brazil) in collaboration with Prof. J. F. M. Menten. The institutional animal care and use committee of the Luiz de Queiroz College of Agriculture, University of Sao Paulo, approved all the procedures for the animal experiment. Experimental diet and water were provided on an *ad libitum* basis throughout the experiments.

#### 3.1.2.1. Pigs fed $\beta$ -acids

Sixty four newly weaned (BW of  $5.48 \pm 0.42$  kg) were randomly allotted into one of the four different feeding regimes with four repetitions for treatment and four animals for experimental unity. Pigs were fed *ad libitum* for 35 days with basal diets with different levels of  $\beta$ -acids: T1 – negative control basal diet (no additives); T2 – basal diet supplemented with  $\beta$ -acids at 120 mg/kg; T3 – basal diet supplemented with  $\beta$ -acids at 240 mg/kg; T4 – basal diet supplemented with  $\beta$ -acids at 360 mg/kg. Considering that hops  $\beta$ -acids have a bitter flavor, their levels were established on the basis of preliminary animal trials for acceptance in order to get similar food consume for all the feeding regimes. A three-phase feeding program was used as follow: pre-starter (1 to 7 d), starter 1 (7 to 21 d), and starter 2 (21-35 d). Each phase provided, respectively, 3,400; 3,375 and 3,230 kcal / kg of metabolizable energy; 20.9; 19.5; and 17.5 of crude protein; and 1.45; 1.30; 1.10 % of lysine. For each phase, a basal diet was formulated with corn, soybean meal, and the inclusion dairy products meal, plasma and 20 mg of  $\alpha$ -tocopherol acetate/kg of food as a source o vitamin E, attending to the nutritional requirements of pigs.

After 35 days of feeding trials, one castrated male (BW of  $19.3 \pm 0.95$  kg) per replicate was euthanized by electrical stunning followed by bleeding. After slaughter, *Longissimus*

*thoracis et lumborum* muscle was sampled and stored at -80 °C until metabolomics analysis and redox stability experiments.

### **3.1.2.2. Broilers fed $\beta$ -acids**

1440 one-day-old male Cobb 500 broiler chicks (initially averaging  $42.3 \pm 0.4$  g in weight) were randomly distributed into five treatments with six repetitions for treatment and forty animals for experimental unity. Birds were fed ad libitum during 42 days according to the four experimental treatments: T1 – negative control basal diet; T2 – basal diet supplemented with  $\beta$ -acids at 30 mg/kg; T3 – basal diet supplemented with  $\beta$ -acids at 60 mg/kg; T4 – basal diet supplemented with  $\beta$ -acids at 240 mg/kg. The nutritional program was divided into four-phase feeding program: prestart (1–7 d), starter (7–21 d), grower (21–35 d), and finisher (35–42 d), providing, respectively, 2,950; 3,000; 3,100 and 3,150 kcal / kg of metabolizable energy; 23.3; 21.5; 20.0; and 19.0% of crude protein; and 1.31; 1.17; 1.08; and 1.01% of lysine. The basal diets consisted of corn, soybean meal, and the inclusion of 5% poultry by-products meal and 5% wheat bran, in agreement to the proposed nutritional requirements of the broilers (Rostagno et al., 2011). Also, 20 mg of  $\alpha$ -tocopherol acetate/kg of food were added to a pre-mixture of vitamins in order to provide the levels of vitamin E that are required for broilers.

After 42 days of feeding trial, 1 broiler per replicate was euthanized by cervical dislocation. After slaughter, *pectoralis* major muscle was collected, deboned and the samples was vacuum-packed and stored at a freezer at -80 °C until proceed to the analyses used in this study.

## **3.2. Animal performance and carcass trait evaluation**

### **3.2.1. Cattle fed yerba mate**

Animal performance evaluation was carried out at Embrapa Pecuária Sudeste (São Carlos, SP, Brazil) in collaboration with Prof. Dr. Renata Nassu, Prof. Dr. Alexandre Berndt and Prof. Rymer Tullio, whom were responsible for conducting the experiments described in this section. Dry matter intake was calculated by weighting offer and leftover daily. Samples were collected for analysis of dry matter, performed in a ventilated oven at 60 ° C for 72 hours. Animal live weights were obtained every 28 days to calculate daily weight gain.

Carcasses were weighed immediately after slaughter to obtain hot carcass weight (HCW) and then were split into sides and were chilled overnight at 2 °C. Carcass yield (CY) was obtained by multiplying the hot carcass weight by 100, divided by final live weight.

The loin eye area (LEA) was evaluated in *longissimus* muscle between the 12th and 13th ribs. The outer perimeter of *longissimus* muscle was directly traced on tracing paper, and the loin eye area was measured using a transparent scale. Back-fat thickness (BFT) was measured in *longissimus* muscle, in millimeters, using a ruler.

The experimental design was completely randomized with four treatments and twelve replications, with analysis of variance and regression depending on the levels of mate extract added to the animal diet. The statistical model included the fixed effect under study: diet. For statistical analysis, XLSTAT (Addinsoft, Paris, France) software was employed.

### **3.2.2. Broilers and pigs fed $\beta$ -acids**

Methods for evaluation of animal performance of broilers and pigs fed  $\beta$ -acids as well as the results of animal trials are, respectively, reported by Bortoluzzi et al.<sup>28</sup> and Sbardella et al.<sup>108</sup>

### **3.3. Mate extract characterization and analysis of polyphenols in beef**

The extract of yerba-mate leaves was obtained from Centroflora Group (Botucatu, SP – Brazil, Dr. Ricardo Luiz Araujo Dias). The mate extract was prepared from fresh leaves by extraction with water:ethanol 75:25 (v/v) at 90 °C. The extract was dried in spray-dry tower.

Ultra performance liquid chromatography (UPLC) coupled to high-resolution accurate mass spectrometry (HRMS) were used for the characterization of the phenolic compounds of yerba mate extract. The PhD student Leandro Arrivetti at São Carlos Chemistry Institute carried out UPLC-HR-ESI-MS experiments. 10 mg of mate extract was homogenized for 1 min using a commercial cell disruptor (Fast Prep®, MP Biomedicals, Solon, OH, USA) with 1.5 mL of cold methanol/water solution (1:1 v/v) in homogenization tubes containing ceramic beads at a speed of 5.0 ms<sup>-1</sup> during 120 s, after that samples were filtered using nylon membranes of 0.45  $\mu$ m and stored at -20°C until the UPLC-HRESI-MS analysis. 10  $\mu$ L of the sample extract were injected into an Accela 1250 HPLC system coupled

with an auto sampler Accela AS and a high-resolution accurate mass spectrometer LTQ OrbitrapVelos (Thermo Fisher Scientific, Bremen, Germany), which was equipped with an electrospray source (HESI-II) operating in the negative ion detection mode. The mobile phase at a flow rate of 0.5 mL min<sup>-1</sup> consist of a linear gradient from 5% of mobile phase B (methanol containing 0.1% formic acid) and 95% of mobile phase A (0.1% aqueous formic acid) to 80% of mobile phase B over 30 min and then from 80 % to 95 % of mobile phase B in 5 min which was held 5 min isocratic and then from 95% of the mobile phase B to 5% of B in 7 min.

The analysis of phenolic compounds in beef were carried out by taking a sample of 500mg of frozen beef which was homogenized for 1 min at 5 m s<sup>-1</sup> using a commercial cell disruptor (Fast Prep®, MP Biomedicals, Solon, OH, USA) with 1.0 mL of cold isopropanol containing 2% v/v of trichloroacetic acid in homogenization tubes containing ceramic beads. Samples were kept on ice throughout the procedure. The supernatant was collected using a micropipette and transferred to 2 mL micro-tube. Tubes were placed into a speed-vac for 12 hours until dryness. After complete dryness, 500 µL of a solution of 50:50 (v/v) water-methanol was added and each tube was vortexed for 2 min. Tubes were again centrifuged and the supernatant was passed L of the resulting extract injected through a 0.22 µm hydrophilic filter and 10 in the UPLC system for phenolic analyses.

### **3.4. Extraction of polar metabolites and CLA from meat**

Approximately 0.20 g of frozen beef was homogenized for 1 min using a commercial cell disruptor (Fast Prep®, MP Biomedicals, Solon, OH, USA) with 1.0 mL of cold methanol/water solution (1:1 v/v) for polar metabolites or cold chloroform for CLA<sup>48</sup>(only from beef) in homogenization tubes containing ceramic beads. Samples were kept on ice throughout the procedure. Then, the homogenates were centrifuged for 10 min at 10,000×g at 10 °C to remove precipitated protein, fat and connective tissue. Supernatants were carefully collected, transferred to Eppendorf tubes and dried in a centrifugal concentrator (Speed-Vac, Thermo Savant, Holbrook, NY, USA). The dried extract containing the polar metabolites of beef was re-suspended with deuterium oxide phosphate buffer (0.10 M, pD 7.3) containing 0.050% w/w of the internal chemical shift standard sodium 3-trimethylsilyl-2,2,3,3-d4-propionate (TMSP-d4, from Cambridge Isotopes, Leicestershire, UK), and transferred to a 5mm NMR precision tube (Vineland, NJ, USA). The same extraction was performed in chicken and pork meat and, in beef samples after 14 days of

storage at 4 °C to investigate changes during ageing. Extraction procedures were carried out at São Carlos Chemistry Institute.

### **3.5. Untargeted polar metabolites screening of meat extract by <sup>1</sup>H-NMR spectroscopy**

Untargeted metabolomics were performed on the NMR spectra of the meat extracts in order to investigate possible clustering of the samples as function of the diet. High-resolution <sup>1</sup>H-NMR spectroscopy was performed on the extracts of beef and chicken meat. The experiments were performed on a 9.4 T BrukerAvance III spectrometer (BrukerBioSpin, Rheinstetten, Germany) equipped with a 5 mm PABBI probe head with gradients, automated tuning and matching accessory (ATMATM), BCU-I for regulation of temperature, and a Sample-Xpress sample changer. The experiments were acquired at 300 K in fully automatic mode without sample rotation. Before the <sup>1</sup>H NMR spectra acquisition, a delay of 5 min was ensured for each sample inserted in the magnet for temperature equilibration. Automatic tuning, matching (ATMATM), locking (LOCK), phase, shimming (TOPSHIM), and a saturation pulse (25 Hz) were achieved using standard Bruker routines by ICON-NMR interface. Thirty-two scans and four prior dummy scans of 65536 data points were acquired with a spectral width of 20.5524 ppm, a receiver gain of 90.5, an acquisition time of 3.98 s, a recycle delay of 4 s, and mixing time was set to 10 ms. The water suppression was achieved using the NOESY-presaturation pulse sequence (Bruker 1D noesygprr1d pulse sequence) with irradiation at the water frequency (O1 = 1881.95 Hz) during the recycle and mixing time delays. FIDs were multiplied by a 0.3 Hz exponential multiplication function prior to Fourier transformation, only a zero order phase correction was allowed, and the TMSp-d4 signal was calibrated at 0.0 ppm.

Untargeted metabolites screening of beef was carried out at Universidade Federal de São Carlos (São Carlos, SP, Brazil) in collaboration with Prof. Dr. Antônio Gilberto Ferreira and the PhD student Clayton Oliveira, who was responsible for conducting the NMR experiments described in this section. The spectral data were exported to Amix version 3.9.3 for screening of samples. A bucketing was done within 0.90 – 9.00 ppm, dividing the region into 400 sequential segments or “bins”, obtaining an integral for each. The regions of carnosine (8.50–8.30 ppm), residual water (5.00–4.65 ppm), and both the left (9.00–15.00 ppm) and right (0.90– -5.00 ppm) empty regions have been excluded (those regions are irrelevant for the present investigation or exclude in order to minimize pH variations). Principal components analyze (PC's) was performed by different pre-processing

methods (scaling to unit variance and Pareto) as well as no scaling. The best results of PC's analyses were achieved using no scaling method with buckets width of 0.05 ppm.

Extracts of pork were analyzed by high-resolution  $^1\text{H}$ -NMR spectroscopy using an Agilent DD2 spectrometer (Agilent Technologies) with magnetic field of 11.7 T (499.84 MHz for hydrogen frequency) that is located at São Carlos Chemistry Institute. NMR experiments were performed using a pulse of  $\pi/6$  and 64 transients were collected into 32768 complex points spanning a spectral width of 14 ppm and relaxation delay of 4 s, and the pulse sequence with water presaturation PRESAT (Agilent Technologies) was employed to suppress the water peak. Spectra were processed by phase and baseline correction and by the calibration of the internal chemical shift standard TMSP-d4 at 0 ppm using the software VnmrJ 4.0 software (Agilent Technologies, USA).

NMR datasets reported as time-domain FID were converted into a frequency-amplitude table by the use of the complete reduction to amplitude frequency table (CRAFT) technique, which corresponds to a Bayesian approach for NMR spectral analysis provided as a toolbox included in the packages of the VnmrJ 4.0 software (Agilent Technologies, USA). Multivariate data analyses were performed on Statistica software (version 12, StatSoft, Tulsa, OK, USA) using the correlation method on the data taken from the table of frequency, amplitude and line-width as extract from CRAFT software.

### **3.6. Quantitative polar metabolite profile of meat extract by $^1\text{H}$ -NMR spectroscopy**

For beef, quantitative  $^1\text{H}$ -NMR spectra were acquired on a BrukerAvance III spectrometer (BrukerBioSpin, Rheinstetten, Germany), which is located at Embrapa Instrumentação (São Carlos, Brazil). A standard solvent suppression pulse sequence zgcppr was used to saturate the residual water peak, using a  $90^\circ$  pulse, a SW of 20.55 ppm, 256 scans, 32K total acquired complex points, and a relaxation delay of 4 s. The data were phase corrected, baseline corrected and the TMSP-d4 was calibrated using TopSpin 2.1 (BrukerBioSpin, Rheinstetten, Germany). The assignment of peaks in the spectra was based on the database present in the Chenomx NMR suite 7.7 software (Chenomx Inc., Edmonton, AB, Canada) in order to identify the polar metabolites in beef extract.

For beef with 14 days of maturation, quantitative  $^1\text{H}$ -NMR spectra were acquired on an 11.7 T Agilent DD2 500 MHz NMR Spectrometer. For solvent suppression, the pulse sequence PRESAT was used to saturate the residual water peak, using a  $90^\circ$  pulse

width of 7.9 $\mu$ s, a SW of 20.55 ppm, 256 scans, 32K total acquired complex points, and a relaxation delay of 4 s. The data were phase corrected, baseline corrected and the TMSP-d4 was calibrated using VnmrJ 4.0 software (Agilent Technologies, USA). The data were phase corrected, baseline corrected and the TMSP-d4 was calibrated using VnmrJ 4.0 software (Agilent Technologies, USA).

From the database information, a spectral fingerprinting of metabolites composed by a Lorentzian peak shape model matching the actual spectrum was generated. Individual metabolite concentrations were determined using the 600-MHz library from Chenomx NMR Suite 7.7 by referencing the TMSP-d4 concentration (1mM). The average metabolite concentration according to the animal diet was calculated using the values of three replicate beef samples. Assignment of the  $^1\text{H}$  NMR spectra was obtained by literature data<sup>61,129</sup> or by adding standard compounds. Furthermore,  $^1\text{D}$  JRES, 2D  $^1\text{H}$ - $^1\text{H}$  TOCSY and 2D  $^1\text{H}$ - $^{13}\text{C}$  HSQC experiment were performed on selected samples in order to confirm the assignment of metabolites.

### **3.7. Quantitative determination of polar metabolites and CLA in beef extract by high-resolution accurate ESI and APCLmass spectrometry**

Mass spectrometry analyses were done at São Carlos Chemistry Institute in collaboration with the PhD student Leandro Arrivetti. Mass spectrometry analyses of the methanol/water extract of beef were performed by flow-injection, using an Accela 1250 HPLC system coupled with an auto sampler Accela AS and a high resolution mass spectrometer LTQ Orbitrap Velos (Thermo Fisher Scientific, Bremen, Germany), which was equipped with an electrospray source operating in the positive and negative ion modes. The injection volume of 10  $\mu\text{L}$  was injected at a flow rate of 300  $\mu\text{L min}^{-1}$  of anisocratic mobile phase consisting of methanol/water (1:1 v/v) with 0.1% formic acid for polar metabolites. Sample cleanup was performed on-line by using a RAM BSA-octyl column (Hypersil phase, 100  $\mu\text{m}$  particle size; 5 cm x 5 mm) to prevent matrix effect. Metabolite identification was carried out by high-resolution MS and MS/MS spectra assignment and by standard addition. Positively identified metabolites were then quantified by external standard calibration curves.

For conjugated linoleic acid (CLA) the mass spectrometer was equipped with an atmosphere pressure chemical ionization source operating in the positive mode. The injection

volume of 10  $\mu\text{L}$  was injected at a flow rate of 300  $\mu\text{L min}^{-1}$  of a mobile phase consisting of acetonitrile and the quantification was carried out by external standard calibration curves. Sample cleanup was performed on-line by using a RAM BSA-octyl column (Hypersil phase, 100  $\mu\text{m}$  particle size; 5 cm x 5 mm) to minimize matrix effect.

### **3.8. Principal component analysis of the quantitative metabolite profile**

Multivariate data analyses were performed on Statistica software (version 12, StatSoft, Tulsa, OK, USA) using the correlation method on the data taken from the quantitative metabolomics approach as determined by combined NMR spectroscopy and ESI-MS. Variables were pre-selected based on variability of the data values using one-way analysis of variance (ANOVA,  $p = 0.05$ ). Principal Component Analysis (PCA) was carried out by use of the mean-centered data for metabolite concentrations determined in the methanol/water meat extract as x-variables. Three animals representing each treatment were selected as samples to investigate any clustering of the data.

### **3.9. EPR spin-trapping technique and redox stability of beef**

The redox status of meat was investigated by the spin-trapping EPR technique<sup>1,130</sup> probing PBN radical adduct formation in meat slurries incubated at 65 °C. 0.5 g of fresh meat or meat aged for 14 days at 4 °C were homogenized in 5.0 mL of 50 mM 2-(N-morpholino)-ethane-sulfonic acid (MES, Sigma-Aldrich, Stenheim, Germany) buffer pH 5.7 under ice bath cooling using an Ultra Turrax homogenizer (Janke & Kunkel, Staufen, Germany). Then, 450  $\mu\text{L}$  of 400 mM of  $\alpha$ -tert-butyl-phenyl-nitron (PBN, Sigma-Aldrich, Stenheim, Germany) dissolved in ethanol were added to the homogenate. Samples were vortexed briefly and centrifuged for 10 min at 10,000 rpm and 10 °C. Aliquots of 1.0 mL of the centrifuged solutions were incubated over 4–5 hours in water bath at 65° C before recording the EPR spectra. Every 1 hour, one aliquot was collected, cooled at room temperature and transferred to a 50 mL micropipette (Blaubrand Intramark, Wertheim, Germany) located in the EPR cavity through a flowing system. The X-band EPR spectra of the slurries were obtained at room temperature in an EPR spectrometer Bruker EMXplus (Bruker BioSpin, Rheinstetten, Germany). The EPR parameters were: microwave power 1mW, sweep width 50.00 Gauss, center field 3940.00 Gauss, modulation frequency 100.00

kHz, modulation amplitude 2.00 G, 16 scans. EPR experiments were carried out at São Carlos Chemistry Institute.

### 3.10. Low-field $^1\text{H}$ NMR spectroscopy for fat amount of beef

Low field NMR was carried out at Embrapa Instrumentação in collaboration with the PhD student Luíz Neves-Jr. One cylindrical sample, 8 mm in diameter and 1 cm in height, was collected from each forty-eight beef slice, as described by Correa et al.<sup>131</sup>. The relaxometric time measurements ( $T_1$  and  $T_2$ ) were performed in a bench top time-domain NMR Bruker spectrometer Minispec MQ 20 (Bruker BioSpin, Rheinstetten, Germany), equipped with a permanent magnet of 0.47 T (19.9 MHz for  $^1\text{H}$ ), a heater module Bruker N<sub>2</sub> Temperature Controller, and 10 mm probe. Analyses were performed at controlled temperature  $25.0 \pm 0.1^\circ\text{C}$ . The longitudinal relaxation time ( $T_1$ ) values were obtained using inversion-recovery pulse sequence, applied  $\pi/2$  and  $\pi$  pulses with duration of 2.42  $\mu\text{s}$  and 4.68  $\mu\text{s}$ , respectively, recycle time of 4 s and 8 scans. CP-CWFP sequence has been performed with a train of  $\pi/2$  pulses with duration of 2.42  $\mu\text{s}$ , separated by an interval time  $T_p = 300 \mu\text{s}$ , recycle time of 4 s, 8 scans and number of echoes 500, and the acquisition time was 0.02 ms. The rate  $M_c/M_0$  was obtained after normalizing the values of  $M_0$  using  $M_c$  as obtained from eq. (15).  $T_1$  and  $T_2$  were calculated using eq. (13) and (14) combined with the magnitude of NMR signals after the pulse ( $M_0$ ), in steady state ( $M_c$ ). The  $T^*$  was obtained by mono-exponential fitting of decay after the quasi-stationary state (QSS), eq. (15).

$$T_1 = \frac{T^*/2}{M_z M_0} \quad (13)$$

$$T_2 = \frac{T^*/2}{1 - (M_z/M_0)} \quad (14)$$

$$M_c = \frac{M_0 \times T_2}{(T_1 + T_2)} \quad (15)$$

### 3.11. Meat quality parameters of beef

The collaborator group from Embrapa Pecuária Sudeste conducted the determination of meat quality parameters out. For objective color determination, steaks were exposed to atmospheric air for thirty minutes at room temperature prior to the analyses, and CIE tristimulus values coordinates  $L^*$ ,  $a^*$  and  $b^*$  were measured at three different locations

across the surface of the steaks randomly selected using a Hunter Lab colorimeter model MiniScan XE (Hunter Associates Laboratory, Reston, VA, USA). Then, the pH was measured also at three different locations across the surface using a Testo pH-measuring instrument, model 230 (Testo Limited, Hampshire, UK). Water holding capacity was obtained by the difference between the weights of a meat sample of approximately 2g, before and after submission to a pressure of  $10 \text{ kgf cm}^{-2}$  for 5 minutes as described by Hamm (Hamm, 1986). For cooking loss and shear force measurements, the same steak of 2.5 cm thickness was weighed and cooked in a Tedesco combination oven at  $170 \text{ }^\circ\text{C}$  (Tedesco, Caxias do Sul, RS, Brazil) until the temperature at the center of the sample reached  $70 \text{ }^\circ\text{C}$ , controlled by a thermocouple. Samples were then cooled at room temperature and weighed again. Cooking loss was calculated by difference between the weights before and after cooking, and expressed as percentage. Steaks were transferred to a cooler and held for 24 hours, after which, eight cores (1.27 cm in diameter) were removed per steak, parallel to the fiber grain. Peak shear force was determined on each core perpendicular to the fiber grain using a 1.016 mm Warner Bratzler probe in a TA-XT Plus Texture Analyzer (Stable Micro Systems, Surrey, UK) with a calibration weight of 10kg. Full peak shear force was recorded and maximum shear force calculated as the average of the eight cores. The experimental design was completely randomized with four treatments and twelve replications, with analysis of variance and regression depending on the levels of mate extract added to the animal diet. The statistical model included the fixed effect under study, diet. For statistical analysis, XLSTAT (Addinsoft, Paris, France) software was employed.

### **3.12. Sensory descriptive analysis and consumer acceptance of beef**

The collaborator group carried out sensory descriptive analysis and consumer acceptance of beef trials at Embrapa Pecuária Sudeste. A ten-member trained test panel was used to perform the descriptive sensory analysis. Frozen samples were placed in a refrigerator at  $5 \text{ }^\circ\text{C}$  overnight prior to the sensory analysis. Steaks were removed from the refrigerator and cooked according to each type of sensory test. For descriptive analysis, five steaks per treatment were evaluated and cooked in the Tedesco combination oven model TC 06 at  $170 \text{ }^\circ\text{C}$ , until it reached an internal temperature of  $75^\circ\text{C}$ . Steaks each cut into cubes of 1.5 cm of each side and were salted with 1.0 g of salt each, and pan-fried with soybean oil until they reached an internal temperature of  $75^\circ\text{C}$ . Samples were presented for each panelist in a

balance design assigned by Fizz Software version 2.41 (Biosystemes, Couternon, France). Eight samples were evaluated per session. Attribute ratings were electronically collected using a nine-point descriptive scale for beef characteristic aroma/flavor (1 = extremely bland; 9 = extremely intense), strange aroma/flavor (1 = extremely intense; 9 = none), tenderness (1 = extremely tough; 9 = extremely tender) and juiciness (1 = extremely dry; 9 = extremely juicy).

Concerning the sensory acceptance, samples were randomly assigned to a non-trained panelist, who analyzed two traits (control and 1.5% mate extract). A pool of samples was made combining steaks, which came from 10 animals of each treatment. Attribute ratings were collected using nine-point hedonic scales for flavor, texture and overall acceptance (1 = dislike extremely; 9 = like extremely). Experimental design was completely randomized with four treatments and 12 replicates, with diet as fixed factor. The data were analyzed by ANOVA using XLSTAT software. Trained and consumer panels were conducted at Meat Analysis Laboratory at Embrapa Pecuária Sudeste and Dietetic Techniques Laboratory at Centro Universitário Central Paulista (UNICEP), respectively. Human Research Ethical Committee from Federal University of São Carlos approved the protocol and written consent (CAEE 08551012.3.0000.5504) which participants were required to complete.

### **3.13. Investigation of the oxidation of myofibrillar proteins in chicken meat**

Oxidative modification of proteins from chicken meat was investigated by electrophoretic methods (SDS-Page) and by immunoblotting technique (Western Blot, Oxyblot and immuno-spin trapping). These trials were carried out at University of Copenhagen (Denmark) in collaboration with Prof. Dr. Alberto Grossi and master student Ceder Alloo.

Initially, myofibrillar proteins were extracted, and then, their characterization was carried out using SDS-Page electrophoresis. Oxidative conditions were imposed to the fraction of myofibrillar proteins containing DMPO (a spin-trap reagent) in order to evaluate the development of radicals on the protein structure by the use of immuno-spin trapping technique. Myofibrillar proteins were also incubated in the presence of DNPH to detect the formation of carbonyl groups via Oxyblot.

### **3.13.1. Extraction and characterization of myofibrillar proteins of chicken meat**

The fraction containing myofibrillar proteins (MP) from chicken was separated from the fraction of sarcoplasmic proteins according to extraction methods reported in literature.<sup>132</sup> Approximately 2 g of muscle tissue (excluding parts containing fat or conjunctive tissue) were homogenized in 10 mL of 20 mM phosphate buffer pH 7.5 containing 0.1 M de NaCl and 1.0 mM EDTA using an UltraTurrax homogenizer. The resulting supernatant was carefully collected and centrifuged for 30 min at 20,000 g at 1° C. Supernatant containing the fraction corresponding to the sarcoplasmic proteins (SP) was collected for further characterization. Pellets containing the fraction of myofibrillar proteins were collected, re-suspended in 10 mL of phosphate buffer pH 7.5 containing NaCl 0.6 M and then, kept under magnetic stirring overnight. The resulting suspension was centrifuged at 20,000g for 30 min at 1° C. The supernatant consisting in myofibrillar proteins was collected and the pellet containing fat and connective tissue was discarded. Total protein concentration of the extract of MP was spectrophotometrically determined using the absorbance at 280 nm (A<sub>280</sub>) and a calibration curve obtained from standard solutions of bovine serum albumin (BSA) with known concentrations. Spectra were recorded on a NanoDrop spectrophotometer (ThermoScientific). After separation, MP and SP were characterized by SDS-Page.

### **3.13.2. Induction of oxidative conditions**

Solutions of hydrogen peroxide (H<sub>2</sub>O<sub>2</sub>) and ferrous sulfate (FeSO<sub>4</sub>) were used to induce the oxidation of myofibrillar proteins from chicken meat through Fenton reaction. Both aqueous fractions of MP and SP were incubated in the presence of H<sub>2</sub>O<sub>2</sub> and Fe<sup>2+</sup> and were analyzed by different techniques as will be discussed as follow.

### **3.12.3. Electron paramagnetic resonance (EPR)**

Initially, DMPO (5,5-dimethyl-pirrolone N-oxide) was used as spin-trap to investigate the formation of radicals in solutions containing different concentrations of the extract of myofibrillar proteins of chicken meat.

Accordingly, 50 µL of FeSO<sub>4</sub> and different volumes of the extract of MP were added to 1 mL of a DMPO stock solution. Finally, 50 µL of H<sub>2</sub>O<sub>2</sub> were added to the resulting mixture that has been submitted to magnetic stirring. For all the samples

containing iron and hydrogen peroxide, the final concentration of these two reactants was 1.0 mM. A control solution was prepared with no addition of MP solution.

Solutions were then; transferred to quartz capillary (i.d. = 0.75mm) and the EPR spectra were recorded in a MiniScope MS200 EPR spectrometer at room temperature after 2 min 30s of the addition of H<sub>2</sub>O<sub>2</sub>. The following parameters were used: power of 4mW; center field of 3364G; sweep width of 60 G; sweep time 30 s; modulation amplitude of 4 G; 8 scans.

#### **3.12.4. SDS-Page to determinate the formation of cross-link due oxidation of proteins and Western Blot**

SDS-Page in conjunction with Western Blot was used to evaluate protein oxidation in meat. Cross-linking of myosin was examined by SDS-PAGE and the development of radicals in myofibrillar proteins was analyzed by the immuno-spin trapping technique, which consists in a derivatization of the Western Blot technique.

Extracts of MP dissolved in phosphate buffer pH 7.5 containing NaCl 0.6 M were incubated in the presence or in the absence of DMPO, under oxidative conditions or not for 12 hours at 1 °C. Samples were dissolved in LDS buffer, heat at 80 °C for 10 min and, transferred to a NuPAGE® Novex® 3–8% Tris-Acetate gel, following the recommended protocol provided by the company. Two identical gels were prepared to simultaneously perform SDS-Page and, after separation of the proteins by electrophoresis, one was dyed with Coomassie Brilliant Blue and other gel was used for Western Blot. Dithiothreitol (DTT; 0.1 M) was used when reducing conditions were required. After electrophoresis, the second gel was transferred to a nitrocellulose membrane 0.45 µm at 40 mV for 2 hours. Then, membranes were blocked in 1% BSA in 80 mM phosphate buffer pH 7.5 containing 0.05% Twen-20 and 145 mM de NaCl for 1 hour at room temperature. The membrane was washed three times with TBST buffer (20 mM Tris pH 7.5 containing 0,05% Twen-20 and 100 mM NaCl). The membrane was incubated with an affinity-purified antibody to DMPO (anti-DMPO; 1:100) for 12 hours. The membrane was washed again with TBST buffer and, then, was incubated with the antibody Rabbit Anti-Goat IgG (GE Healthcare, Little Chalfont, U.K.) for 1 hour. After the membrane was washed three times in TBST buffer, the proteins were visualized using chemiluminescent system model ECL-plus.

### **3.12.5. SDS-Page and Oxyblot: investigation of the formation of carbonyl groups in amino acids of proteins**

The Oxyblot technique is based on the use of DNPH (2,4-Dinitrophenylhydrazine) and consists in a derivatization of the colorimetric method most often used for the detection of carbonyl groups combined to the immunoblotting technique (Kezler et al., 2006).<sup>127</sup>

Samples with the extract of MP were incubated for 12 hours under oxidative conditions or not and, then, subjected to the reaction with DNPH or control solution as described in the protocol provided by the OxyBlot™ Protein Oxidation Detection Kit (Millipore). As described in the previously section, two identical set of samples were applied to two NuPAGE® Novex® 10% Bis-Tris gels. One of these gels were dyed in Coomassie Brilliant Blue G-250 (BioRad) and the other gel was subjected to a new step of electrophoresis in order to transfer the proteins from the gel to a nitrocellulose membrane which will be further analysed by Oxyblot technique.

Initially, the detection of carbonyl groups was done only for fresh meat samples (0 days of storage). Then, the same chicken meat samples were stored for 1 and 7 days at 4° C allowing the contact with molecular oxygen to stimulate the increase in the oxidation reactions and, then, to evaluate the redox stability of the different samples.

## **4. Results and discussion**

In order to enhance the organization of the results, data sets and discussion were divided in two different sections according to the animal diet. Therefore, all the results referring animals fed yerba mate have been discussed in the section 4.1. and, the results of trials involving animals fed  $\beta$ -acids have been presented in the section 4.2.

### **4.1. Mate extract as Feed Additive for Improvement of Beef Quality**

Following feeding of 48 Nellore steers during their finishing for the last 94 days prior to slaughter with a feed supplemented with mate extract, which was characterized for content of bioactive compounds, meat from *Longissimus thoracis et lumborum* muscle was collected and extract of meat samples from different feeding treatment subjected to <sup>1</sup>H-NMR

screening for untargeted metabolomics. Having identified approximately 30 compounds in the meat extracts, 17 compounds of relevance for meat quality and significantly influenced by the feeding treatment, was selected as targeting compounds for a quantitative analysis by a combination of <sup>1</sup>H-NMR and high-resolution accurate mass spectrometry. Meat from the different feeding groups was further characterized by content of conjugated linoleic acid, relative amount of intramuscular fat by time domain low-field <sup>1</sup>H-NMR and by resistance to oxidation by EPR spectroscopy using the spin trapping technique. The acceptability and the sensory quality of meat from the different feeding groups were evaluated by a consumer and trained panel, respectively, and by objective meat quality parameters like water holding capacity and color. All in all, the effect of adding extract of mate as a source of bioactive compounds including antioxidants at increasing levels to cattle feed was followed through changes in metabolite profile and resistance to oxidative changes to eating quality and to possible effect on nutritive value and finally to consumer acceptance.

#### 4.1.1. Animal performance and carcass trait evaluation

Animal performance parameters such as dry matter intake, average daily gain, and feed conversion are collected in Table 1. According to the values reported in Table 1, there was no significant difference ( $p > 0.05$ ) in animal performance between control feed group and the feedlots supplement with different levels of mate extract. Dry matter intake, average daily gain, and overall feed conversion are in agreement with literature values reported for Nellore (*Bosindicus*) steers.<sup>133,134</sup>

**Table 1.** Animal performance parameters for animals fed different levels mate extract.

	mate extract supplementation (%)				p-value	SEM
	none	0.5	1	1.5		
<b>dry matter intake (kg/day)</b>	10.6	10.6	10.3	9.5	0.107	0.490
<b>average daily gain (kg)</b>	1.4	1.3	1.3	1.2	0.344	0.091
<b>feed conversion</b>	8.4	8.9	8.3	8.3	0.599	0.568

Data provided by Dr. Renata Nassu.

Carcass characteristics (Table 2) did not differ between the different levels of mate extract in the animal feed ( $p > 0.05$ ). The mean values for hot carcass weight (261.9 kg)

were similar to reported values for castrated Nellore steers finished in feedlot with the same age. The average result found for carcass yield were 54.7% and are in the range of variation considered adequate (55.7 to 58.7%) for Nellore steers<sup>135</sup>. No significant variations for rib eye area and back-fat thickness were observed for animals supplemented with different levels of mate extract, Table 2.

**Table 2.** Carcass characteristics for animals fed different levels mate extract.

Carcass trait	mate extract supplementation (%)				p-value	SEM
	none	0.5	1.0	1.5		
HCW (kg)	292	289	292	283	0.804	10.25
CY (%)	55.8	56.1	56.2	56.6	0.624	0.571
REA (cm <sup>2</sup> )	56.3	55.7	56.2	56.8	0.825	1.142
BFT (mm)	10.8	13.3	9.0	10.2	0.155	1.902

HCW = hot carcass weight; CY = overall carcass yield; REA = rib eye area; BFT= back fat thickness.

Data provided by Dr. Renata Nassu.

#### 4.1.2. Mate extract characterization and analysis of polyphenols in beef

Following the UPLC–ESI–HRMS characterization of the mate extract, over forty phenolic compounds could be identified in the mate extract by their exact mass and fragmentation pattern. From the identified phenolic compounds, 11 compounds of significant peak area were quantified by UPLC–ESI–HRMS and the result of analysis is collected in Table 3. Among the identified phenolic compounds, chlorogenic acid and 1,5-dicaffeoylquinic acids were the most abundant phenolic compounds in the mate extract with a concentration of  $12.3 \pm 0.01$  and  $6.0 \pm 0.01$  mg g<sup>-1</sup>extract, representing 58.2% and 28.4% of the total phenols quantified by UPLC–ESI–HRMS, respectively. In order to verifying the bioavailability and uptake of these phenolic compounds by the animals, we have performed the analysis of these compounds in meat extracts, however, none of the compounds identified in the mate extract or their known bacterial metabolites<sup>136</sup> like ferulic acid, coumaric acid, phenylpropionic and benzoic acid could be detected in meat at a detection limit of 200 nmol L<sup>-1</sup>, which clearly suggest that the site of action of the phenolic compounds is the rumen.

**Table 3.** Concentration of the major phenolic compounds identified in the mate extract as determined by UPLC–ESI–HRMS (n = 3, mg·g<sup>-1</sup> extract).

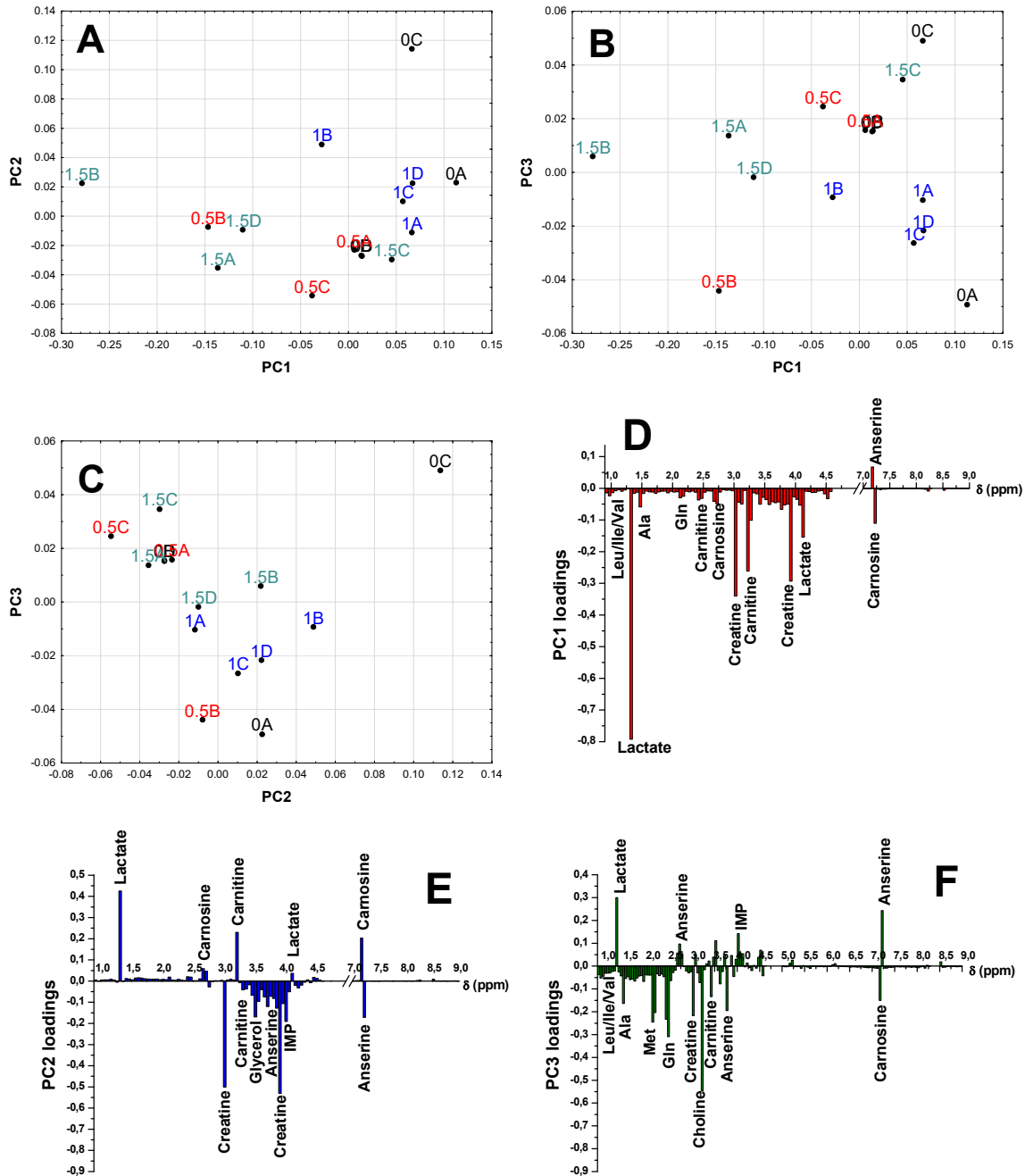
Phenolic compounds	Concentration (mg g <sup>-1</sup> extract)
chlorogenic acid	12.3 ± 0.01
1,5- dicaffeoylquinic acid	6.0 ± 0.01
1,3-dicaffeoylquinic acid	9.1 ± 0.43 10 <sup>-2</sup>
caffeic acid	8.1 ± 0.02 10 <sup>-1</sup>
p-coumaric acid	6.3 ± 1.80 10 <sup>-3</sup>
ferulic acid	5.5 ± 0.08 10 <sup>-2</sup>
galic acid	1.8 ± 0.43 10 <sup>-2</sup>
quinic acid	8.8 ± 0.06 10 <sup>-1</sup>
shikimic acid	1.2 ± 0.01 10 <sup>-2</sup>
quercetin	1.1 ± 0.04 10 <sup>-1</sup>
rutin	8.6 ± 0.02 10 <sup>-1</sup>
<b>Total phenolic content</b>	<b>21.15 ± 0.04</b>

Data provided by Leandro O. Arrivetti.

#### 4.1.3. <sup>1</sup>H-NMR metabolite untargeted sample screening: Principal components analyses (PCA) of full <sup>1</sup>H NMR spectra

In order to find the most suitable clustering representation of the <sup>1</sup>H NMR spectra of beef extracts from animals fed different levels of mate extract, we have performed standard PCA on the complete data set. We have identified three significant PC's in our data set, which together explain 96% of the total variance (PC1 85%, PC2 7%, and PC3 4%). Figure 22 (A, B and C) at supporting information shows the clustering and trends of beef extracts from animals fed different levels of mate extract.

**Figure 22.** Principal component score plots A) PC1xPC2, B) PC1xPC3, and C) PC2xPC3 and variable loading plots D) PC1, E) PC2, and C) PC3 for the full <sup>1</sup>H NMR spectra recorded for meat extracts from animals fed different levels of mate extract (none, 0.5%, 1.0%, and 1.5%).



The samples of beef extracts from animal feed without mate extract show a higher variability for PCA results; however, these samples trend to stay in the positive-value region of both PC1 (Figures 22A and B) and PC2 (Figure 22C). The loadings plot (Figure 22D and E) suggests that the signals of anserine, carnosine, lactate, and carnitine provided a high variability for these samples.

The samples of beef extracts from cattle fed with mate extract show trends towards small clusters. The samples with 1.0% of mate extract added to feed formed a small tight cluster in the positive-values region of the PC1 and PC2, and negative-values of the PC3 (almost in the midpoint of the PCA model). The signals of anserine, carnitine, carnosine, lactate, creatine, glycerol, and IMP were identified for loadings plot (Figures 22D, E, and F) as responsible for this small tight cluster. Unlike samples from beef from feeding with 1.0% of mate extract, the samples from feeding with 0.5% and 1.5% of mate extract demonstrated a higher variability over the scores plot in Figures 22A and B. However, the samples from meat from feeding with 1.5% of mate extract grouped more loosely in the positive-values region of PC3 almost in the center of PCA model (Figure 22C). The signals for the metabolites creatine, carnitine, lactate, carnosine, glycerol, anserine, and IMP were responsible for the main information of the samples into the both groups (0.5% and 1.5% of mate extract). Thus, following analysis of the information from  $^1\text{H}$  NMR spectra as an initial data screening, we performed a quantification of the individual metabolites for each beef sample.

#### 4.1.4. Quantitative $^1\text{H}$ NMR and High-resolution Accurate Mass Spectrometry

Based on  $^1\text{H}$  NMR spectra for meat extracts as the spectrum shown in Figure 23 for the 0.5% mate extract-feeding group, 19 metabolites could be quantified using quantitative  $^1\text{H}$  NMR analysis. The compounds are listed in Table 4 together with the median concentration in all four-treatment groups for cattle feeding. The concentrations were estimated for meat extracts and corrected to the concentrations in the meat as presented in Table 4 by the method previously described.<sup>137–139</sup>

Considering that overlapping peak regions in the NMR spectrum gave high variance values for concentration of some compounds, only nineteen metabolites were quantified by the Chenomx NMR suite 7.7 software library. Moreover, peaks in the aromatic region had variations of chemical shift due to slightly differences in pH and ionic strength complicating quantification<sup>61</sup>. In this case, assignments were based on signal shape and multiplicity assuming a chemical shift variation allowed by Chenomx library and, also, by comparison with other data base sources and references<sup>54,61</sup> and by 2D homonuclear and heteronuclear experiments ( $^1\text{H}$ - $^1\text{H}$  TOCSY and 2D  $^1\text{H}$ - $^{13}\text{C}$  HSQC). For some of these compounds, high-resolution accurate mass spectrometry was used for quantification and the results are shown in Table 4.

**Figure 23.** Typical 600 MHz  $^1\text{H}$ -RMN spectra for the methanol/water meat extract. Assignments: Ace (acetate); Ado (adenosine); Ala (alanine); Ans (anserine); Bet (betaine); Car (carnosine); Cho (choline); Crn (carnitine); Cre (creatine) Gln (glutamine); Gly (glycine); GLY (glycerol); Glc (glucose); Ile (isoleucine); Lac (lactate); Leu (leucine); Met (methionine); Val (valine).

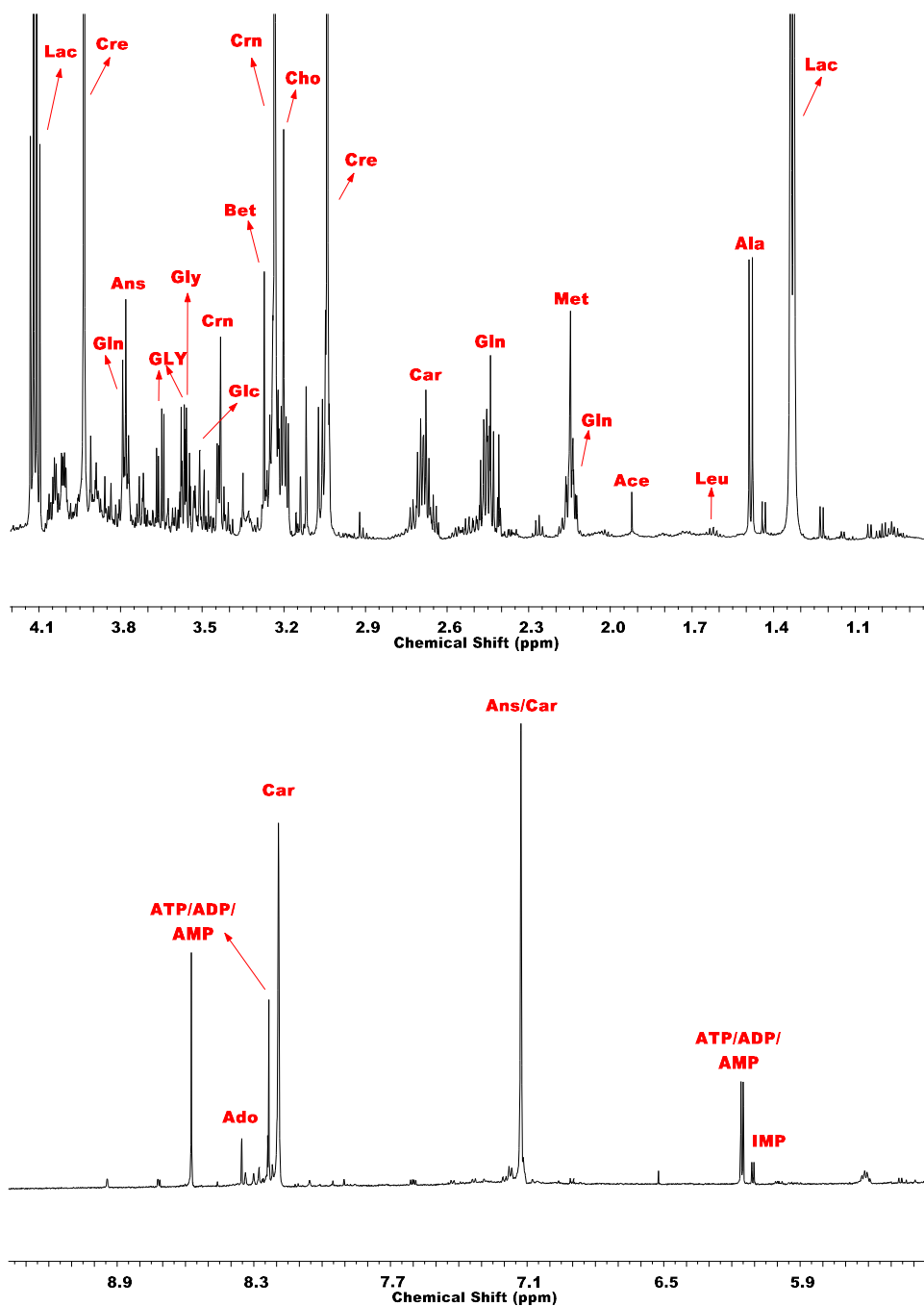


**Table 4.** Mean concentration of the polar metabolites (n = 3 per feeding treatment,  $\mu\text{mol}\cdot\text{g}^{-1}$  meat) as obtained by quantitative  $^1\text{H-NMR}$  of the methanol/water extract of meat from animals fed different levels mate extract.

	mate extract supplementation (%)				p-value
	none	0.5	1.0	1.5	
<b>leucine</b>	0.183±0.032	0.197±0.006	0.230±0.010	0.233±0.01	0.109
<b>isoleucine</b>	0.118±0.003	0.128±0.002	0.166±0.011	0.143±0.01	0.002
<b>valine</b>	0.166±0.030	0.184±0.006	0.201±0.024	0.133±0.01	0.085
<b>lactate</b>	36.9±3.2	40.2±3.5	52.4±2.3	49.2±1.6	0.071
<b>β-alanine</b>	0.217±0.04	0.231±0.05	0.209±0.14	0.298±0.05	0.251
<b>alanine</b>	1.52±0.35	1.93±0.06	2.37±0.12	2.14±0.17	0.034
<b>methionine</b>	0.66±0.16	0.68±0.12	0.91±0.045	0.90±0.20	0.283
<b>creatine</b>	5.70±1.4	8.48±0.4	20.3±1.98	10.2±0.3	2.9 10 <sup>-5</sup>
<b>glycerol</b>	1.74±0.42	2.11±0.22	2.47±0.47	2.36±0.07	0.452
<b>glycine</b>	0.666±0.037	0.688±0.076	0.794±0.085	0.941±0.09	0.047
<b>carnosine</b>	5.82±0.56	7.99±0.57	9.06±1.00	9.08±0.83	0.013
<b>carnitine</b>	2.80±0.09	2.65±0.25	2.19±0.39	3.57±0.21	0.007
<b>betaine</b>	0.51±0.051	0.57±0.089	0.51±0.021	0.70±0.08	0.078
<b>anserine</b>	0.626±0.061	0.89±0.074	0.772±0.141	0.879±0.04	0.113
<b>glucose-6-phosphate</b>	1.58±0.97	2.39±0.26	2.76±0.63	2.50±0.46	0.417
<b>NADH</b>	0.25±0.073	0.071±0.011	0.52±0.025	0.49±0.050	0.002
<b>adenosine</b>	0.411±0.091	0.288±0.035	0.326±0.018	0.367±0.03	0.236
<b>IMP</b>	1.29±0.13	1.87±0.30	2.03±0.36	2.30±0.14	0.041
<b>ATP/ADP/AMP</b>	0.335±0.067	1.56±0.11	0.921±0.105	1.84±0.41	0.001

Table 5 displays the mean concentration of polar metabolites found in meat extract as determined by ESI-HRMS analysis. More than 30 metabolites could be identified using high-resolution accurate mass spectrometry targeted analysis with electrospray ionization (ESI) or with atmospheric pressure chemical ionization (APCI).

**Table 5.** Mean concentration of the polar metabolites (n = 12 per feed treatment,  $\mu\text{mol}\cdot\text{g}^{-1}$  meat) as obtained by ESI-HRMS of the methanol/water extract of meat from animals fed different levels of extract.

	mate extract supplementation (%)				p-value
	none	0.5	1.0	1.5	
<b>proline</b>	0.033±0.003	0.032±0.002	0.031±0.003	0.030±0.003	0.078
<b>succinate</b>	0.075±0.005	0.110±0.008	0.152±0.006	0.117±0.005	3.9 10 <sup>-4</sup>
<b>aspartate</b>	0.012±0.002	0.010±0.001	0.007±0.002	0.009±0.002	0.559
<b>glutamine</b>	0.965±0.014	1.125±0.018	0.818±0.019	0.894±0.011	0.012
<b>glutamate</b>	0.084±0.006	0.096±0.006	0.084±0.003	0.101±0.007	0.844
<b>creatinine</b>	0.146±0.002	0.144±0.001	0.146±0.002	0.155±0.002	4.2 10 <sup>-4</sup>
<b>choline</b>	0.094±0.002	0.084±0.001	0.070±0.001	0.073±0.001	0.457
<b>serine</b>	0.161±0.009	0.176±0.008	0.159±0.004	0.170±0.003	0.136
<b>lysine</b>	0.046±0.001	0.045±0.004	0.037±0.002	0.039±0.001	0.016
<b>inosine</b>	0.973±0.014	0.912±0.018	0.942±0.013	0.982±0.012	0.276
<b>arginine</b>	0.053±0.001	0.059±0.001	0.045±0.001	0.050±0.001	0.022
<b>citrate</b>	0.047±0.003	0.050±0.005	0.028±0.003	0.046±0.003	0.507
<b>glutathione</b>	0.624±0.015	0.660±0.017	0.578±0.011	0.595±0.015	0.939
<b>phenylalanine</b>	0.036±0.005	0.038±0.005	0.030±0.004	0.036±0.005	0.703
<b>hypoxanthine</b>	0.210±0.003	0.198±0.003	0.189±0.002	0.197±0.002	0.918

Data provided by Leandro O. Arrivetti.

Notably, Table 5 lists only the metabolites not detected by <sup>1</sup>H NMR or which had high variance of the concentration values based on replicate <sup>1</sup>H NMR analysis. From the 15 polar metabolites identified and quantified by MS, only succinate, glutamine, creatinine, lysine, and arginine show significant variation (p<0.05) for extracts of meat from control animals and animals fed with mate extracts. The metabolites proline, aspartate, glutamate, choline, serine, inosine, citrate, glutathione, phenylalanine, and hypoxanthine shows standard deviations for feeding group greater than the variability of the variable values among meat extract from animals fed different diets.

Despite the fact that no significant changes were observed in the <sup>1</sup>H NMR qualitative spectral profiling of samples from animals fed different diets, important differences in the metabolite concentrations among the animal treatments are noted. Among the 19 polar metabolites quantified by <sup>1</sup>H NMR, Table 4, only the concentrations of

isoleucine, alanine, creatine, glycine, carnosine, carnitine, NADH, IMP and ATP/ADP/AMP differ significantly ( $p < 0.05$ ) between different animals fed different diets and all increased with increasing mate extract supplementation. The highest metabolite levels were in most cases achieved for the supplementation with 1.0% or 1.5% of mate extract in the feed. Clearly supplementation with mate extracts to the feed changes the animal metabolism as probed by quantitative MS and  $^1\text{H}$  NMR data.

Notably, concentration of carnosine and NADH, both endogenous antioxidants, was higher in the samples from animals fed with 1.5% of mate extract compared to other treatments. Increased variations in the concentration of these two metabolites could be related to  $\beta$ -alanine metabolism<sup>140</sup>. However, as shown in Table 3, dietary supplementation with mate extract seems not to alter significantly the concentration of  $\beta$ -alanine in meat extracts of meat from animals supplement with different levels of mate extract.

The diet with 1.5% of mate extract also enhanced the production of L-carnitine and IMP in the muscle. All of these compounds have a wide range of functions in the organism<sup>6,27,141</sup> and have been in focus as attractive meat-based bioactive compounds as also have anserine, carnosine, creatine, and leucine in muscle tissue manipulated by animal diet<sup>6</sup>.

The metabolites L-carnitine and betaine are involved in the fatty acid metabolism related to energy production in the muscle<sup>26,27,142</sup>. High levels of L-carnitine together with a significantly increased level of glycerol for animals supplemented with mate extract in comparison with control fed suggest an increasing lipolysis and triglyceride oxidation to provide energy for biosynthetic pathways like protein synthesis<sup>54,142-145</sup>. Concomitantly, a higher concentration of the branched-chain amino acid leucine was found for animals supplement with mate extract, Table 4. Leucine has a fundamental role for the initiation of anabolic processes in the muscle including myofibrillar protein synthesis<sup>146</sup>. Myofibrillar proteins have been recognized to be involved in protection of muscles against oxidation<sup>16</sup> and are related to meat tenderness<sup>3,4,91</sup>. Mate extract addition to feed may, accordingly, induce a reduction in the intramuscular fat content and an increase in the protein synthesis leading to the production of more lean beef.

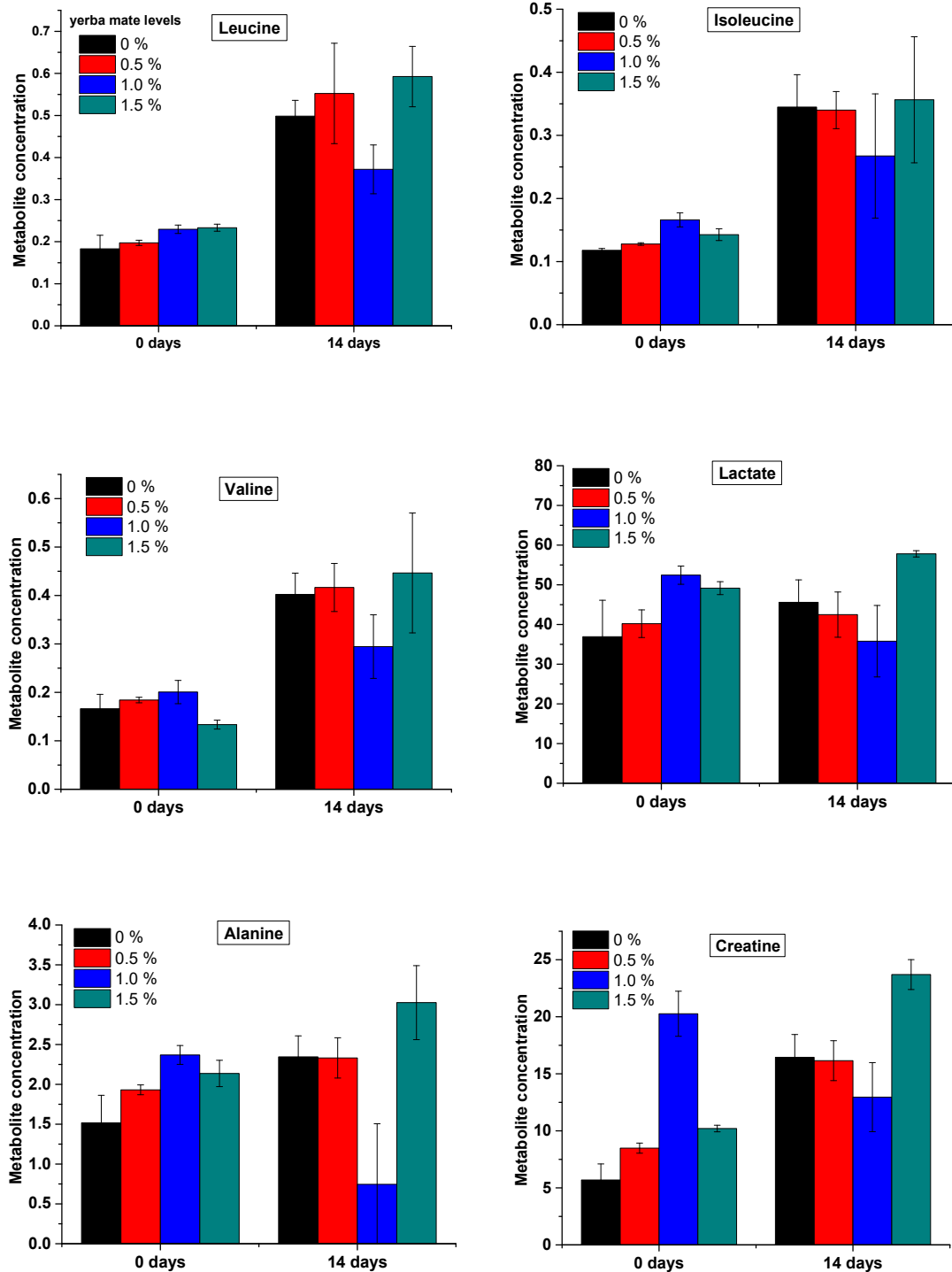
High levels of IMP for meat extract from animals fed with the highest levels of mate extract suggest a slow post mortem metabolism and may infer that these animals were less stressed<sup>54</sup>. An improvement of meat quality may be achieved by decreasing the formation of inosine through dephosphorylating of IMP, since this process has been shown to be associated with a high susceptibility to stress<sup>54</sup>. Furthermore, IMP is well known as a non-

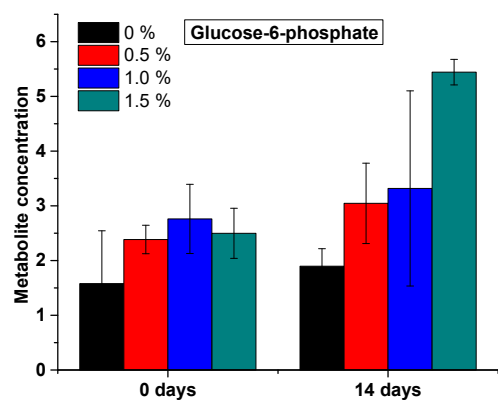
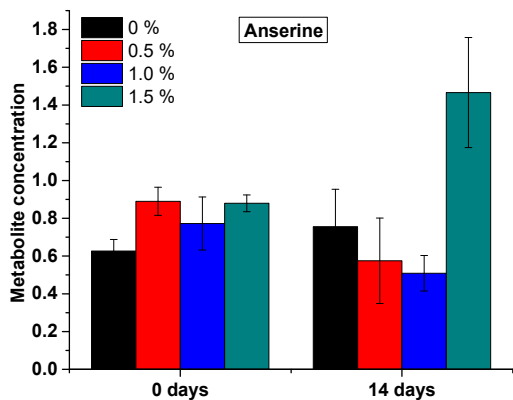
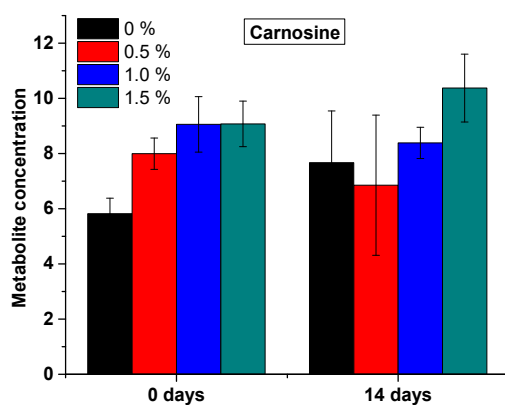
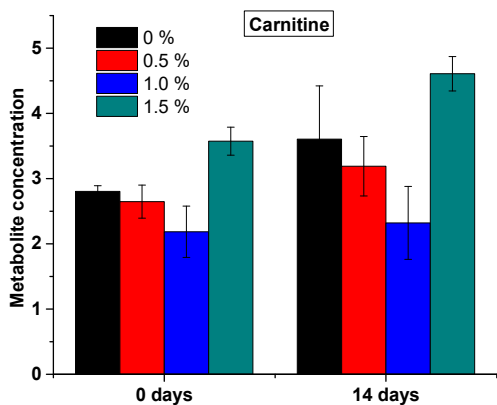
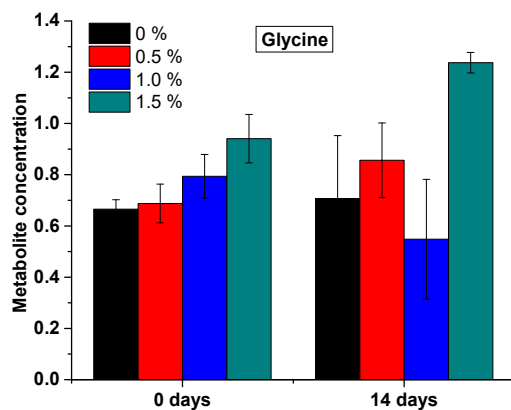
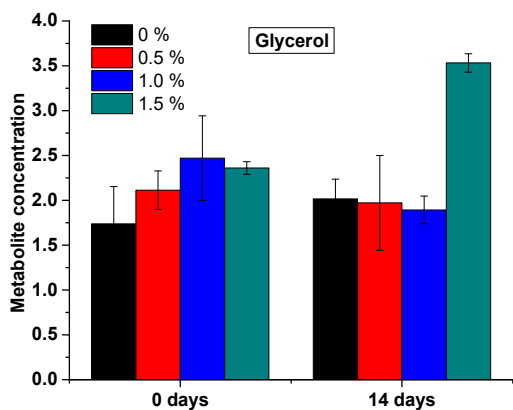
volatile flavour enhancer in meat and it is desirable to keep its concentration high by preventing its degradation during meat processing<sup>56,58</sup>.

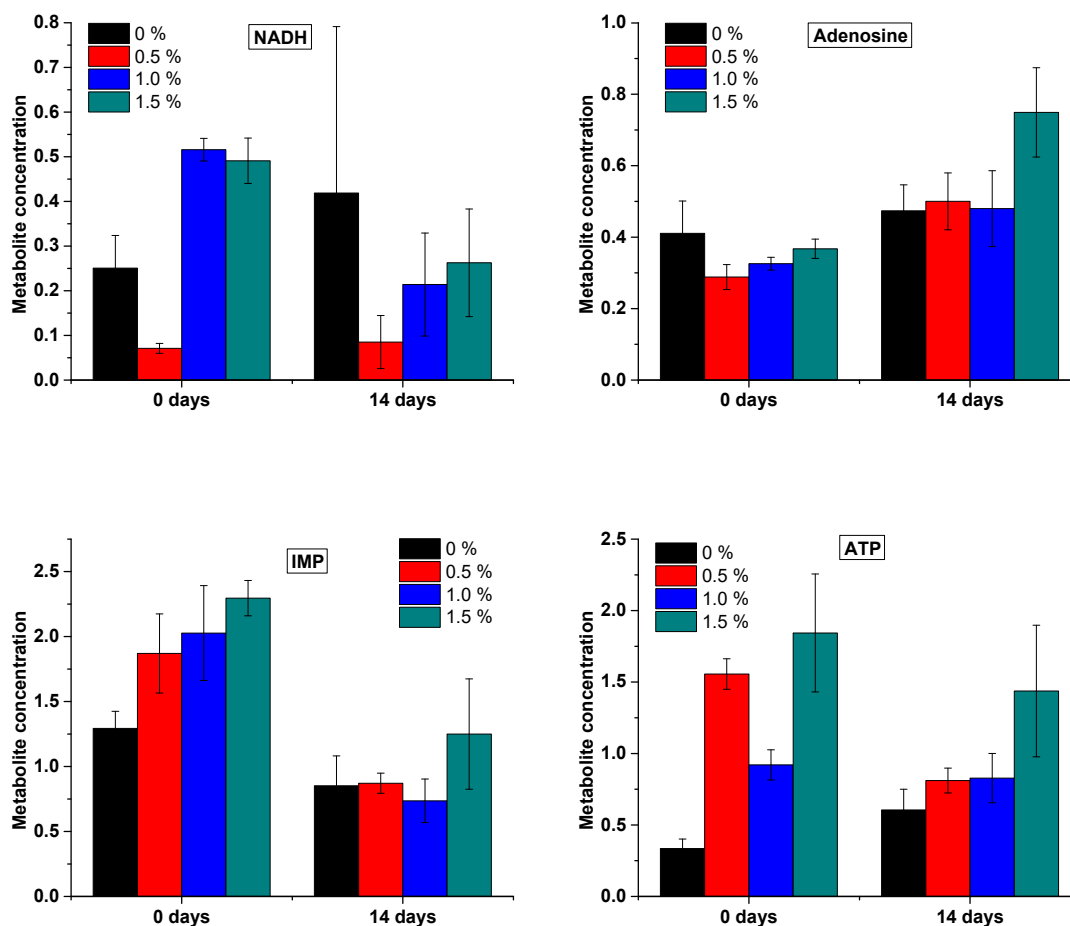
In order to follow the development of eating quality of meat, <sup>1</sup>H NMR was used to follow the metabolites considered most important during meat aging with special focus on proteolysis. Several chemical, physical and biological changes take place in ageing and influence most of the components of meat. For example, structural proteins of muscle fibers are degraded to smaller peptides or amino acids by proteolytic enzymes<sup>40,53,61,138</sup>. Animal metabolism prior to slaughtering also affects the development of *post mortem* changes. Thus, the metabolic changes processed after 14 days of ageing were investigated in order to determine the effect of diet in the post mortem metabolism (Figure 24—metabolite concentration changes after 14 days of storage at 4 °C). As expected an increase in the level of amino acid and amino acids derivatives after 14 days of ageing was observed. This proteolysis is most advanced in the samples representing the group fed 1.5% of mate extract and aged for 14 days as seen by the highest concentration of amino acids. For these group, also important metabolites as carnosine, carnitine, creatine and glycerol had shown to increase in concentrations after ageing of meat.

For all of the feeding-treatments, the levels of NADH, IMP and ATP/ADP/AMP seem to deplete during the ageing period. Concerning the nucleotide metabolites, several degradation pathways have been found to be enhanced during post mortem changes. IMP could during such ageing be converted to inosine and hypoxanthine leading to undesirable development of bitter taste<sup>54,57,147,148</sup>. Depletion of ATP/ADP/AMP after 14 days of ageing has been shown to occur to maintain the enzymatic functionality of the muscle under anaerobic conditions<sup>61,137</sup>. The observed decrease in NADH concentration is expected, since other antioxidants may be protecting the muscle against oxidation instead of participating in regeneration of NADH through redox cycling.

**Figure 24.**  $^1\text{H}$  NMR metabolite concentration ( $\mu\text{mol g}^{-1}_{\text{meat}}$ ) changes during meat ageing at  $5^\circ\text{C}$  (0 and 14 days).



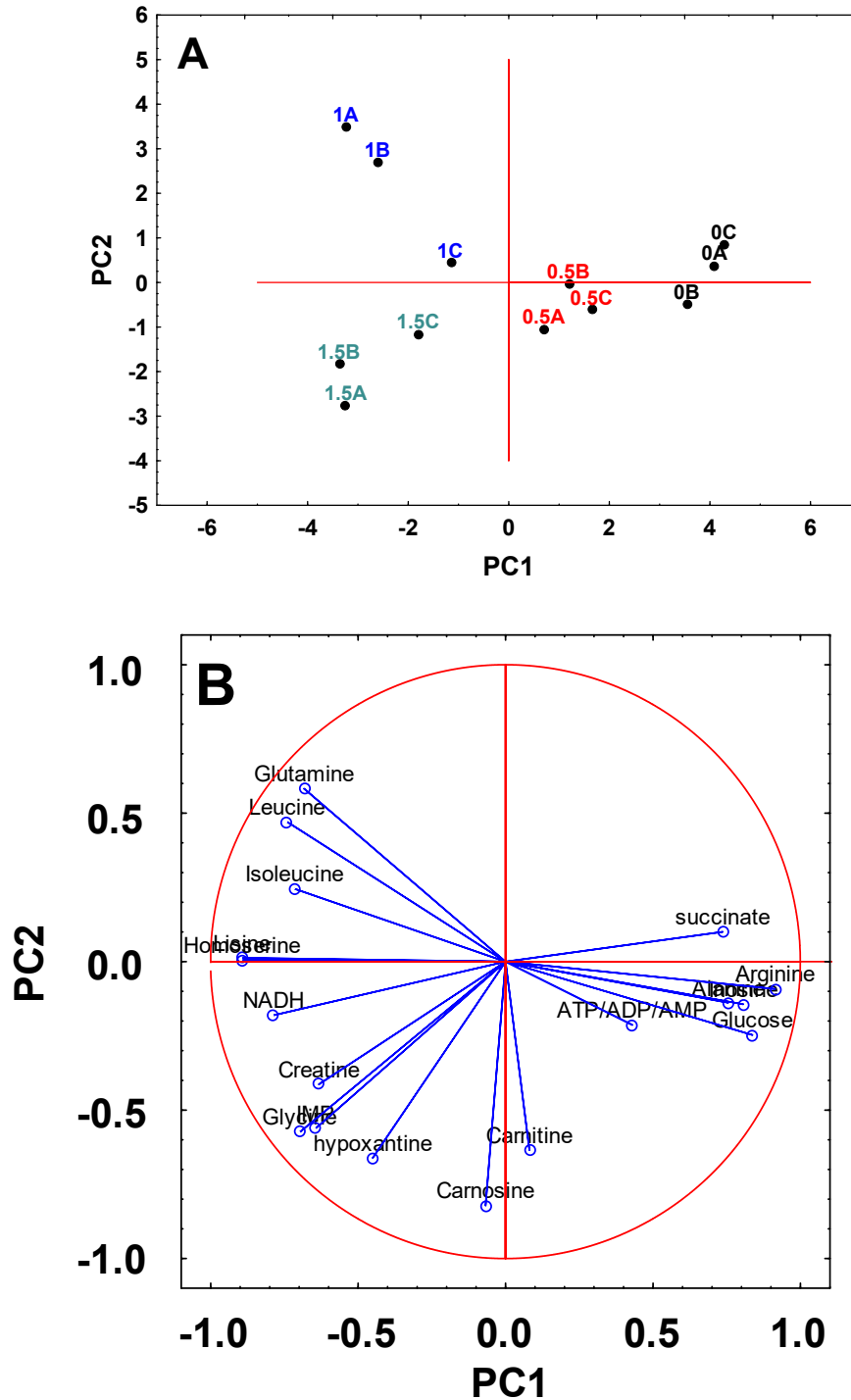




#### 4.1.5. Principal component analysis of targeted profiling metabolomics

In order to observe patterns in the development of metabolites for the four feeding groups, principal component analysis (PCA) was performed for the quantitative  $^1\text{H}$  NMR and ESI-MS polar metabolite profile of beef from animals fed different levels of mate extract. Variables were pre-selected based on the variability of the metabolites mean values among sample groups (ANOVA,  $p = 0.05$ ). PCA scores plot and loading plots (PC1xPC2) for the beef extracts using targeted profiling are represented in Figure 25. The variance between sample groups was explained 48.8% by principal component one (PC1) and 17.5% by principal component two (PC2) providing a good discrimination among the different feeding treatments. The polar metabolites accounting for the discrimination among animal feeding treatment in each principal component are described in Figure 1B. PC1 further differentiates between animals fed higher levels of mate extract (1.0% and 1.5%) from control animals and animals fed with the lowest level of mate extract (0.5%).

**Figure 25.** Principal Component Analysis (PCA) of the quantitative metabolite profile for animals fed with different levels of mate extract. A color-coded number according to mate extract level in the diet represents each meat sample and a letter was used to differentiate animals with the same treatment. Metabolite concentrations determined by <sup>1</sup>H-NMR and ESI-HRMS were selected as variables. A: Two-dimensional plot of samples using the principal components one and two (PC1xPC2) capturing most of the variance in the original dataset (total variance 66.07%). B: Loading plots for PC-variables correlations.



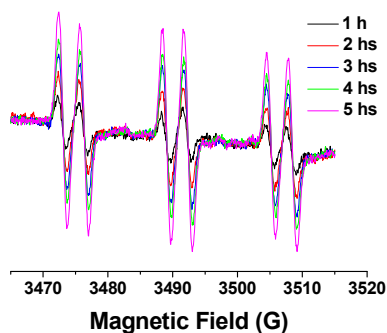
Meat from animals fed with higher levels of mate extract was associated with high levels of glutamine, leucine, isoleucine, homoserine, lysine, NADH, creatine, glycine,

IMP, hypoxanthine, and carnosine. PC2 slightly distinguished the samples from animals fed 1.0 % and 1.5% of mate extract. Animals fed with 1.0% of mate extract characterized by higher levels of glutamine, leucine, and isoleucine and animals fed with 1.5% of mate extract by higher levels of NADH, creatine, glycine, IMP, hypoxanthine, carnosine, and carnitine. Samples from animals fed control feed 0.5% and 1.0% of mate extract were closely clustered in the scores plot along the positive part of PC1-axis that is characterized by a high content of succinate, arginine, alanine, inosine, glucose, and ATP/ADP/AMP in comparison to samples from animals fed 1.0 and 1.5% of mate extract.

#### 4.1.6. EPR spin-trapping and oxidative stability of beef

Formation of radicals is an early event in oxidative degradation of proteins and lipids in muscle and in meat, and the tendency of radical formation may be used to predict oxidative stability of meat products. The oxidative stability of beef was accordingly determined using the spin trapping technique by monitoring the development of radicals in meat slurries subjected to incubation at 65 °C in the presence of PBN as spin trap. PBN adduct radicals are formed, when short-lived reactive radicals from the components of beef like lipid radicals or protein radicals produced during heating or by metal catalysis are adding to spin trap double bonds like in PBN to produce a more stable adduct radical.<sup>149</sup> The X-band EPR spectra of meat slurries displayed the characteristic six-line pattern of PBN-adduct radicals (Figure 26) and the signal was double integrated in order to obtain the area referred to as EPR intensity, which is proportional to radical concentration.

**Figure 26.** Typical EPR spectra of meat slurry added of PBN (400 mmol L<sup>-1</sup>) recorded for different period of incubation at 65 °C.

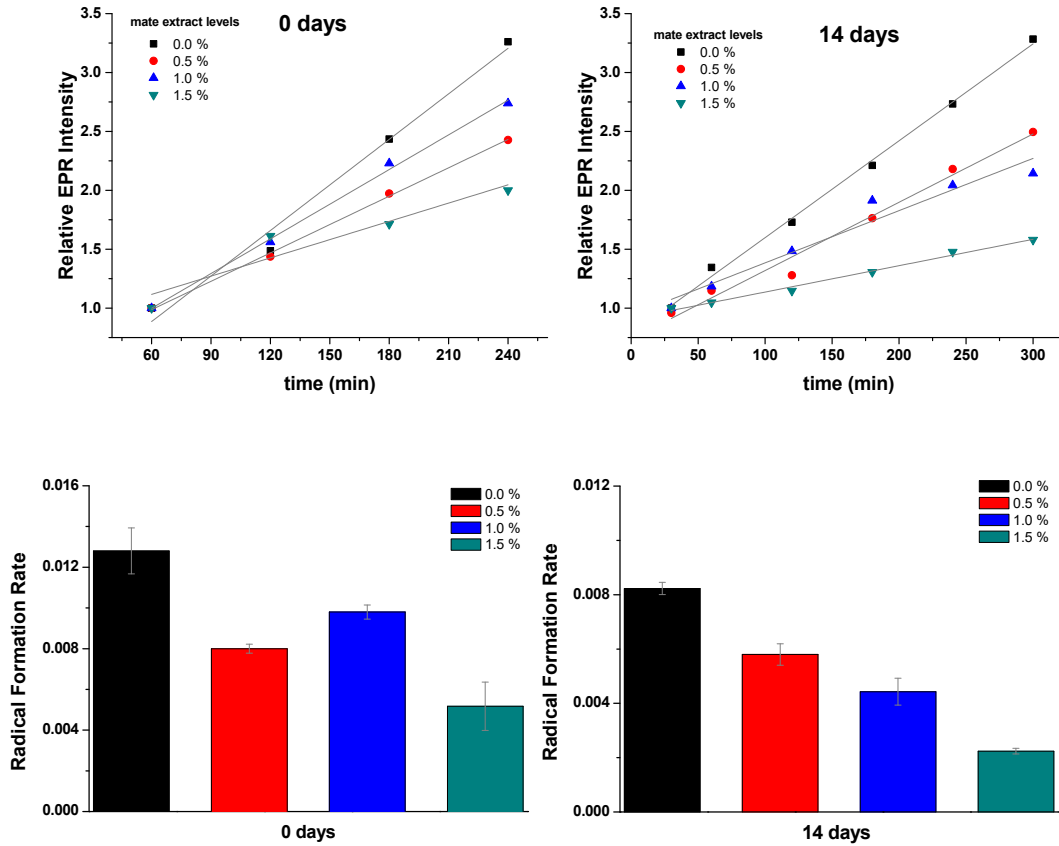


The kinetics of the formation of radicals in beef from different animal feeding treatment was accordingly based on the EPR intensity. Figure 27 shows the development of

PBN radical adducts in meat slurries during 4–5 hours of incubation at 65 °C. For fresh meat and for 14-days aged meat, the radical formation could be described as a zero order reaction. Linear regression of relative EPR intensity as function of incubation time was used to determine the rate of radical formation. For fresh meat samples, the formation of radicals in meat slurries was faster than for meat aged for 14 days. For fresh meat an induction period or so-called lag phase of 60 min was seen prior to the development of radicals at a constant rate during the thermal incubation. For 14 days aged meat, the lag phase was shorter and approximately of 40 min. After approximately 4 hours of incubation, for aged meat and after approximately 5 hours for fresh meat, the level of radicals became constant, which may be described as a steady state, where radical consumption reactions exactly balance the reactions forming radicals. The period with constant rate of radical formation between the end of the induction period and the steady state period was used to characterized the oxidative stability of meat (Figure 27).<sup>2,16,146</sup>

During the incubation at 65 °C, iron is released from the heme porphyrin enhancing the oxidation and initiating the formation of radicals.<sup>150,151</sup> However, some metabolites like peptides and proteins may slow down or prevent the radical formation since they as antioxidants promptly scavenge radicals.<sup>152,153</sup> The high concentration detected for several metabolites capable of radical scavenging in meat when using 1.5% of mate extract supplementation in the feed may explain the improved redox stability as compared to the other treatments. The histidine dipeptide carnosine, which were found to increase in the meat from animals supplemented with mate extract have thus previously been found effective as radical scavengers and inhibitor of oxidation processes.<sup>69,141,152</sup> Besides the reducing power and radical scavenging ability of these two metabolites<sup>154</sup>, their chelating ability toward metal ions may also contribute to the protection against oxidation.<sup>69</sup> Carnosine may thus act as antioxidant both through scavenging radicals and by metal binding, and we suggest that this metabolite gave a major contribution to the oxidative stability of beef from animals supplemented with mate extract.<sup>69</sup>

**Figure 27.** Radical formation as measured by the relative intensity of PBN radical adduct by electron paramagnetic resonance (EPR) in slurry incubated at 65°C made from fresh meat and in meat stored at 5°C for 14 days, PBN concentration of 400 mM. A: EPR intensity was calculated by double integration of EPR signal and expressed as the ratio  $\text{Area}_{T=X_{\text{min}}}/\text{Area}_{T=0}$ . Rates for radical formation were determined by linear regression of relative EPR intensity plots and shown in B for each set of condition.



Ageing of beef seems to increase the peptide and amino acid content through protein hydrolysis. The lowest radical formation rate for 14-days of maturation was found for the meat samples from animals fed with the highest content of mate extract in agreement with higher concentration of radical scavenging metabolites in these samples including the histidine derived peptides and redox active amino acids.

#### 4.1.7. Intramuscular and CLA content

The relative intramuscular fat content (IMF) for fresh meat from animals fed with different levels of mate extract in the diet has been determined by low-field NMR using a continuous wave-free precession sequence (CWFP). Obtained IMF values (given by the  $M_c/M_o$  ratio) were  $0.04 \pm 0.02$ ,  $0.04 \pm 0.01$ ,  $0.05 \pm 0.02$ , and  $0.02 \pm 0.01$  for the feed supplementation with 0, 0.5, 1.0, and 1.5% (w/w) of mate extract, respectively. The  $M_c/M_o$  values were reported to show a positive correlation with the intramuscular fat content and

capable of estimate IMF with a precision of 0.5%.<sup>131</sup> From the  $M_c/M_o$  values found for beef samples from animals fed with different levels of mate extract in the finishing diet, a large variance of the data is found, as expected, for the IMF of beef from animals in the same feeding regime ( $n = 12$ , analysis in triplicate). Interestingly, beef samples from animals supplemented with the highest content of mate extract in the diet show a significant decrease in the IMF compared to the other treatments, which is in good agreement with the elevated levels of betaine, L-carnitine, and leucine in beef from animals supplemented with 1.5% of mate extract supporting an increase in the fatty acid metabolism to generate energy for protein synthesis leading to lean meat.

Conjugated linoleic acid (CLA), a bioconverted fatty acid found in ruminant products, has received considerable attention from nutritionists due to its health benefits associated with a decrease in animal body fatty and its anticarcinogenic, antioxidant, and anticholesteremic properties.<sup>155–157</sup> CLA is known to be formed during ruminal biohydrogenation especially by *Butyviriospp.* bacteria and deposited in the animal tissues.<sup>30</sup> Tannins and phenolic compounds are suggested to modulate rumen biohydrogenation by selective inhibition of some bacteria such as *Fusocillus spp.* and *Clostridium proteoclasticum* that transforms vaccenic acid into stearic acid, thus providing more vaccenic acid to be converted to CLA in the animal tissue.<sup>30</sup> In this view, a quantitative analysis of total CLA in chloroform extract of meat from animals fed different levels of mate extract have been performed using atmospheric pressure chemical ionization with high resolution mass spectrometry (APCI-HRMS). The increase in the mate extract concentration in the animal feed led to an increase in the CLA concentration. For animals that did not receive the supplementation (control), CLA concentration in meat was of  $0.073 \pm 0.007 \mu\text{mol}\cdot\text{g}^{-1}$  and in the range of values found in the literature. For animals fed with 0.5, 1.0, and 1.5% mate extract, obtained CLA concentration were  $0.08 \pm 0.01$ ,  $0.09 \pm 0.01$ , and  $0.12 \pm 0.01 \mu\text{mol}\cdot\text{g}^{-1}$ , respectively (CLA concentration obtained by the analysis of meat from 12 animals of each feed treatment with triplicate injection into the LC-MS system). From the quantitative analysis for CLA in fresh meat, it is clear that addition of mate extract as a supplement to the animal feed modulates the production of CLA and vaccenic acid in the rumen and lead to a CLA enriched beef production for animals fed with mate extract in comparison to control feeding. For beef from animals supplemented with 1.5% of mate extract an increase of about 60% in the intramuscular CLA content is observed, despite a reduced IMF compared to animals fed without mate extract.

#### 4.1.8. Meat quality parameters

Significant differences among diets and ageing time as isolated effects were found for meat quality parameters ( $p < 0.05$ ). There were no interactions between these two factors. Different treatments affected luminosity ( $L^*$ ), meat pH, cooking loss, and shear force as shown in Table 6.

**Table 6.** Meat quality for meat from animals fed different levels of mate extract.

	mate extract supplementation (%)				SEM	<i>p</i> -value
	none	0.5	1.0	1.5		
<b>L*</b>	40.8 <sup>a</sup>	41.1 <sup>a</sup>	41.7 <sup>b</sup>	41.0 <sup>a</sup>	0.65	0.008
<b>a*</b>	17.8	17.9	17.9	18.1	0.49	0.512
<b>b*</b>	15.8	16.1	16.2	16.0	0.42	0.127
<b>pH</b>	5.4 <sup>b</sup>	5.3 <sup>a</sup>	5.4 <sup>a, b</sup>	5.3 <sup>a, b</sup>	0.03	0.026
<b>WHC (%)</b>	73.4	73.5	73.1	73.4	1.02	0.87
<b>cooking loss (%)</b>	27.4 <sup>a, b</sup>	26.4 <sup>a</sup>	28.1 <sup>b</sup>	27.3 <sup>a, b</sup>	1.16	0.017
<b>shear force</b>	4.4 <sup>b</sup>	3.9 <sup>a</sup>	4.1 <sup>a, b</sup>	4.2 <sup>a, b</sup>	0.37	0.024

$L^*$ ,  $a^*$ , and  $b^*$  are three stimulus color parameters

WHC = water holding capacity

<sup>a and b</sup> Means in the same row with different superscripts are significantly different ( $p < 0.05$ )

Data provided by Dr. Renata Nassu.

Animals fed with 1% w/w of mate extract had the higher luminosity ( $L^*$ ) compared to the other samples. Values for this parameter ranged from 33.2 to 41.0, which are in agreement with average values found for beef.<sup>158</sup> Animals used were castrated and the meat is expected to show higher brightness compared to non-castrated animals due to a higher amount of intramuscular fat.<sup>159</sup> Although pH values present significant differences, the overall variation was very small. Higher values for cooking loss were observed in animals fed with 1% of mate extract, while lower cooking loss values were observed for meat from animals fed with 0.5% mate extract. However, all cooking loss values are close to the values found in literature for Nellore beef cattle.<sup>159</sup> Meat from animals fed with the control diet showed higher values for shear force as a measurement of tenderness, and meat from animal supplemented with mate extract may be considered very tender due to the observed values

lower than 4.5 kgf for shear force. Animals fed with 0.5% extract of mate showed the lowest shear force values compared to animals fed with higher levels of mate extract. In summary, the addition of mate extract to animal feed affected the meat characteristics of luminosity, cooking loss and shear force and meat from animals fed with 0.5% of mate extract exhibits better overall quality.

#### **4.1.9. Sensory descriptive analysis and acceptance**

Results from sensory descriptive analysis are shown in Table 7. Characteristic beef aroma and tenderness attributes were clearly affected by the animal diet. The control sample showed the highest value ( $p < 0.05$ ) of characteristic beef aroma, but no difference in the characteristic beef flavor nor strange aroma and flavor attributes were found. Even though it was expected that mate extract would affect beef aroma and flavor, the sensory analysis shown that for a significance level of  $p > 0.05$ , no differences were found. The addition of mate extract to the animal diet is thus concluded to affect the beef tenderness positively, with the control sample being less tender, especially compared to the beef from animals fed with mate extract at 0.5% in the diet.

Table 8 contains the sensory acceptance results. Flavor acceptance was not affected by animal feeding with mate extract. However, in relation to texture (tenderness) and overall acceptance, the beef from animals supplemented with mate extract was found more accepted probably due to its better tenderness. The use of mate extract as an antioxidant in meat has been shown to limit lipid and protein oxidation. Protein oxidation as the cross-linking of myofibrillar proteins may affect tenderness<sup>3,160</sup> and bioactive compounds from mate extract or their ruminal metabolites may change the metabolic profile of the muscle tissue improving its redox status and preventing protein oxidation, in effect increasing the meat tenderness.

Beef from animals fed with diet containing mate extract were more tender and was also more accepted by consumers. Other sensory attributes such, as aroma and flavor were not affected by the addition of mate extract to the cattle feed. Mate extract may accordingly be used in beef cattle diets without affecting the beef sensory properties negatively and providing more tender meat.

**Table 7.** Sensory descriptive analysis of meat from animals fed different levels of mate extract.

Attributes <sup>1</sup>	mate extract supplementation (%)				SEM	p-value
	none	0.5	1.0	1.5		
<b>characteristic beef aroma</b>	6.5 <sup>b</sup>	6.0 <sup>ab</sup>	6.0 <sup>ab</sup>	5.9 <sup>a</sup>	0.26	0.049
<b>strange aroma</b>	8.0	7.8	7.9	7.8	0.29	0.913
<b>characteristic beef</b>	6.1	5.9	5.8	5.5	0.26	0.146
<b>strange flavor (off-flavor)</b>	7.6	7.6	7.7	7.6	0.31	0.959
<b>tenderness</b>	4.0 <sup>a</sup>	5.0 <sup>b</sup>	4.4 <sup>ab</sup>	4.6 <sup>ab</sup>	0.31	0.020
<b>juiciness</b>	5.0	5.2	5.4	5.1	0.27	0.365

<sup>1</sup> beef characteristic aroma/flavor (1 = extremely bland; 9 = extremely intense), strange aroma/flavor (1 = extremely intense; 9 = none), tenderness (1 = extremely tough; 9 = extremely tender) and juiciness (1 = extremely dry; 9 = extremely juicy)

<sup>a,b</sup> Mean values in the same row with different superscripts are significantly different ( $p < 0.05$ ; s.e.m., standard error for the mean value).

Data provided by Dr. Renata Nassu.

**Table 8.** Sensory acceptance of meat from animals fed 1.5% mate extract as compared to meat from no supplementation. Non-trained panels of 100 panelists were used.

Acceptance Attributes	mate extract supplementation (%)		SEM	p-value
	none	1.5		
<b>flavor</b>	7.1	7.3	0.22	0.275
<b>texture</b>	6.0 <sup>a</sup>	6.8 <sup>b</sup>	0.26	0.002
<b>overall acceptance</b>	6.6 <sup>a</sup>	7.2 <sup>b</sup>	0.22	0.018

<sup>a and b</sup> Mean values in the same row with different superscripts are significantly different ( $p < 0.05$ ) s.e.m., standard error for the mean value.

Data provided by Dr. Renata Nassu.

## 4.2. Hops $\beta$ -acids as feed additive for improvement of meat from broiler and pigs

### 3.1.1. $^1\text{H-NMR}$ metabolic profile of meat extracts of broilers and pigs fed with different levels of lupulones in the diet

Meat extracts containing the polar metabolites of meat from broilers and pigs were analyzed by NMR. Significant changes were observed in the  $^1\text{H-NMR}$  spectral profile of broilers fed with the highest levels of lupulones when compared to the animals fed with no lupulones (Figure 28). From the visual comparison between the  $^1\text{H-NMR}$  spectra related to the chicken samples from T1 and T4, the major signals at  $\delta$  6.0 ppm –  $\delta$  9.0 ppm were found to promote such variations. Considering the meat extracts from pigs, the addition of lupulones to the diet has not shown to induce changes in the metabolic profile of meat as determined by  $^1\text{H-NMR}$  (Figure 29). However, in both chicken and pig meat extracts, the averaged concentration of polar metabolites demonstrated to change according to the animal diet, as can be observed in Tables 9 and 10.

**Figure 28.**  $^1\text{H-NMR}$  spectra of methanol/water meat extracts containing the polar metabolites of meat from broilers fed with no supplements (black) and from broilers fed with 240 ppm of lupulones (red). Major peak assignments: (A) leucine/isoleucine/valine; (B) lactate; (C) alanine; (D) carnosine; (E) creatine; (F) anserine; (G) ATP/ADP/AMP; (H) carnosine; (I) adenine/hypoxanthine; (J) adenosine/ inosine/carnosine; (K) phosphoglycerate; (L) carnitine.

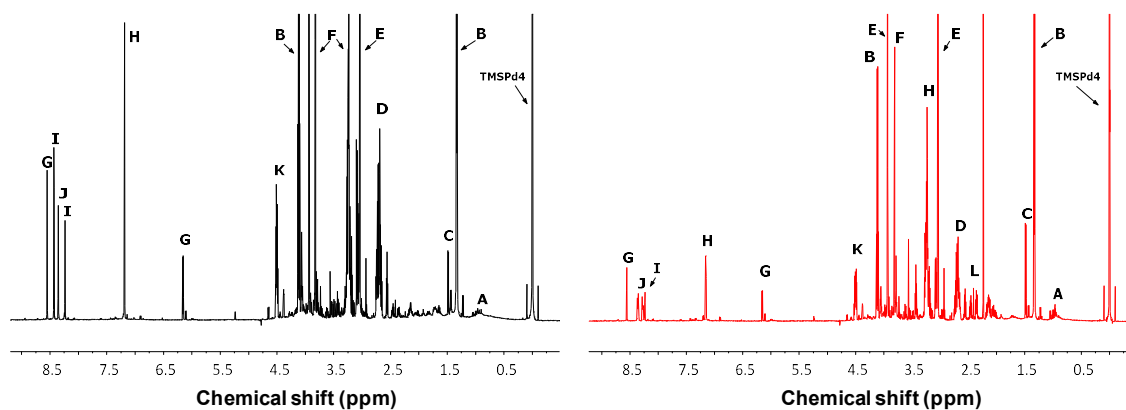


**Figure 29.**  $^1\text{H}$ -RMN spectra of metanol/water meat extracts containing the polar metabolites of meat from pigs fed with no supplements (black) and from broilers fed with 360 ppm of lupulones (red). Major peak assignments: (A) leucine/isoleucine/valine; (B) lactate; (C) alanine; (D) carnosine; (E) creatine; (F) anserine; (G) ATP/ADP/AMP; (H) carnosine; (I) adenine/hypoxanthine; (J) adenosine/ inosine/carnosine; (K) phosphoglycerate; (L) carnitine; (M) sugar region.

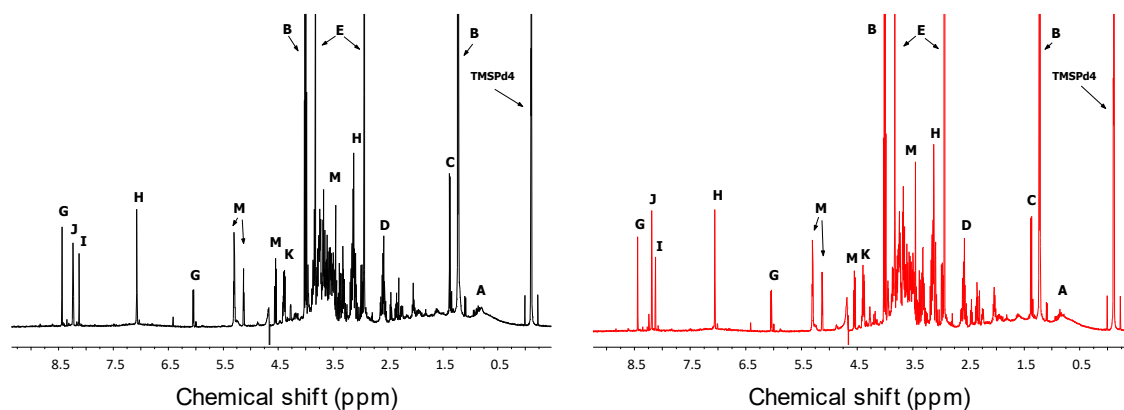


**Table 9.** Mean concentration of the polar metabolites ( $n = 3$  per feeding treatment,  $\mu\text{mol}\cdot\text{g}^{-1}$  meat) as obtained by quantitative  $^1\text{H}$ -NMR of the methanol/water extract of meat from broilers fed different levels hops  $\beta$ -acids.

$\mu\text{mol}\cdot\text{g}^{-1}$ meat $\cdot 10^{-1}$	Hops $\beta$ -acids supplementation				p-value
	T1 <sup>0ppm</sup>	T2 <sup>30ppm</sup>	T3 <sup>60ppm</sup>	T4 <sup>240ppm</sup>	
leucine	0.32±0.04	0.32±0.01	0.28±0.01	0.45±0.01	0.164
isoleucine	0.11±0.02	0.11±0.01	0.11±0.01	0.23±0.01	0.049
valine	0.26±0.03	0.31±0.01	0.31±0.01	0.47±0.02	0.114
lactate	191.7±79.8	228.5±62.2	227.7±52.1	105.5±5.2	0.158
$\beta$ -alanine	5.03±0.53	5.91±0.75	2.41±1.33	3.55±0.52	0.044
alanine	5.66±1.10	6.67±1.80	4.65±2.80	5.07±0.15	0.843
glutamine	4.40±0.37	5.33±0.38	4.93±0.26	4.45±0.20	0.043
creatine	65.79±2.22	74.00±17.4	73.6±14.76	41.99±3.43	0.208
glycerol	0.47±0.20	0.53±0.04	0.68±0.01	0.40±0.01	0.515
glycine	3.50±0.82	1.90±0.06	2.99±0.12	3.60±0.28	0.399
carnosine	44.15±6.53	59.28±1.90	45.37±8.33	11.06±1.40	0.041
carnitine	4.21±0.97	2.65±0.25	0.81±0.10	0.44±0.11	0.002
Adenine/ hypoxanthine	9.44±0.63	13.73±3.36	14.78±4.54	5.74±1.28	0.048
anserine	1.93±0.23	2.51±0.09	1.76±0.24	1.83±0.11	0.199

<b>glucose</b>	5.56±0.54	6.50±1.50	5.54±1.48	2.64±0.36	0.050
<b>NADH</b>	0.20±0.01	0.32±0.01	0.24±0.03	0.13±0.01	0.050
<b>succinate</b>	0.55±0.11	0.85±0.01	0.60±0.01	0.83±0.01	0.017
<b>IMP</b>	24.43±3.55	12.61±3.90	11.45±2.37	5.88±0.60	0.160
<b>ATP/ADP /AMP</b>	2.43±0.35	1.79±0.68	2.23±0.08	5.67±0.56	0.011

**Table 10.** Average concentration of polar metabolites (n=3,  $\mu\text{mol} \cdot \text{g}^{-1}$  of meat) as determined by  $^1\text{H-NMR}$  in meat from pigs fed with different levels of  $\beta$ -acids.

$\mu\text{mol} \cdot \text{g}^{-1}$ meat	Hops $\beta$ -acids supplementation (%)				p- value
	T1 <sup>0ppm</sup>	T2 <sup>120ppm</sup>	T3 <sup>240ppm</sup>	T4 <sup>360ppm</sup>	
<b>leucine</b>	0.20±0.04	0.10±0.01	0.08±0.01	0.10±0.01	0.081
<b>isoleucine</b>	0.16±0.02	0.08±0.01	0.20±0.01	0.11±0.01	0.049
<b>valine</b>	0.18±0.03	0.08±0.01	0.07±0.01	0.11±0.02	0.003
<b>lactate</b>	57.9±-.8	49.7±62.2	41.7±52.1	71.9±5.2	0.001
<b>alanine</b>	2.09±0.53	1.67±1.80	1.57±2.80	2.09±0.15	0.370
<b>creatine</b>	16.29±2.22	16.41±17.4	21.49±14.76	25.75±3.43	0.094
<b>glycerol</b>	0.47±0.20	0.44±0.04	0.66±0.01	1.07±0.01	0.018
<b>glycine</b>	1.86±0.82	1.37±0.06	2.17±0.12	2.18±0.28	0.544
<b>carnosine</b>	6.44±6.53	5.73±1.90	7.18±8.33	10.25±1.40	0.009
<b>carnitine</b>	0.27±0.97	0.28±0.25	0.22±0.10	0.36±0.11	0.322
<b>anserine</b>	2.29±0.23	1.80±0.09	0.71±0.24	0.80±0.11	0.381
<b>glucose</b>	2.24±0.54	3.22±1.50	3.12±1.48	5.57±0.36	0.001
<b>NADH</b>	0.21±0.01	0.12±0.01	0.13±0.03	0.19±0.01	0.050
<b>succinate</b>	0.19±0.11	0.18±0.01	0.30±0.01	0.22±0.01	0.100
<b>IMP</b>	0.48±3.55	0.20±3.90	0.27±2.37	0.39±0.60	0.430
<b>ATP/ADP /AMP</b>	0.25±0.35	0.11±0.68	0.28±0.08	0.55±0.56	0.002

The use of hops  $\beta$ -acids in the animal diet was concluded to promote alterations in the levels of metabolites that are relevant for meat quality, including amino acids, sugars, nucleotides and peptides. Such changes were more pronounced in the concentration of the polar metabolites valine, lactate,  $\beta$ -alanine, creatine, carnosine, carnitine, NADH, succinate, IMP and ATP/ADP/AMP. The addition of lupulones in the diet of broilers was found to increase the concentration of valine, glutamine, adenine/hypoxanthine and succinate when compared to the animals fed with no supplement. Broilers fed with 30 ppm of  $\beta$ -acids showed high concentrations of lactate,  $\beta$ -alanine, glutamine, creatine, carnosine, anserine, glucose, NADH and succinate. Increasing levels of lupulones demonstrated to decrease the concentration of carnitine and IMP in chicken meat. Broilers fed the highest level of lupulones (T4) presented the highest concentrations of the amino acids leucine, isoleucine, valine and glycine and of the nucleotides ATP/ADP/AMP. Such high ATP levels indicate significant alterations in the energetic metabolism of broilers of T4 compared to the other treatments. Contrary to what we expected, the main variation in the metabolite concentrations in chicken meat does not seem to follow trends associated to the level of dietary supplement. Notably, the major metabolic differences between T1 (control group) and broilers fed different levels of  $\beta$ -acids were achieved using 30 ppm of supplement.

Despite the fact that no significant changes were observed in the metabolic profile of the pork samples, animals fed without lupulones shown the highest concentrations of leucine and anserine and, the animals fed with the highest level of  $\beta$ -acids shown high concentration of lactate, creatine, carnosine.

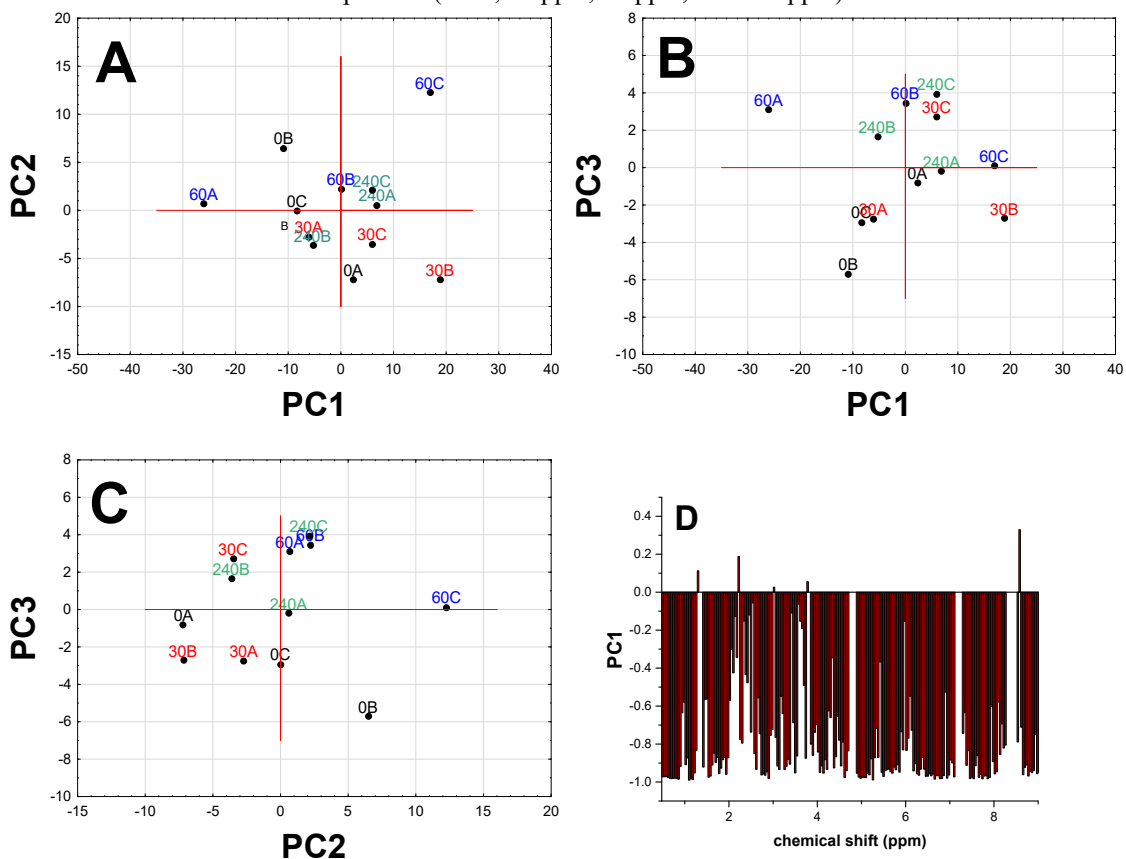
### **3.1.2. $^1\text{H}$ -NMR metabolite untargeted of meat from broilers and pigs fed $\beta$ -acids: Principal components analyses (PCA) of full $^1\text{H}$ NMR spectra**

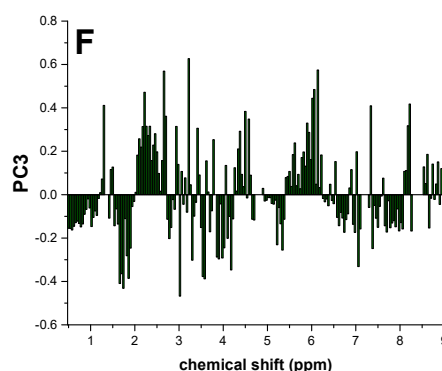
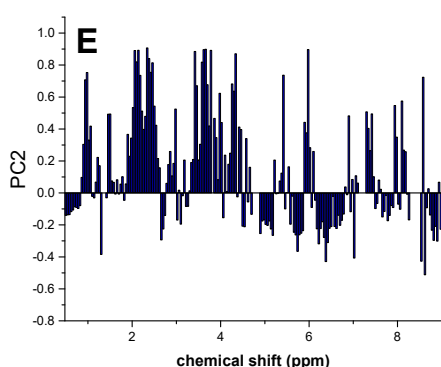
Standard PCA was performed on the complete data set of the  $^1\text{H}$  NMR spectra of meat extracts from animals fed different levels lupulones in order to find possible clustering representations of the samples. Full  $^1\text{H}$  NMR spectra of meat extracts of broilers and pigs were obtained by the use of AMIX and CRAFT platforms, respectively.

Three significant PC's were identified in the data sets of the broiler samples. Together, these PC's explain 88% of the total variance (PC1 70%, PC2 14%, and PC3 4%), and the clustering and trends are presented in Figure 30 (A, B and C). The samples of meat extracts from broilers fed without  $\beta$ -acids and with 30 ppm of  $\beta$ -acids show a higher

variability for PCA results. However, these samples trend to stay together when compared to the animals fed with 60 ppm and 240 ppm of lupulones (except sample 30C). The samples of meat extracts from broilers feed without  $\beta$ -acids trend to stay in the negative-value region of both PC1 (Figures 30A and B) and PC3 (Figure 30C). The loadings plots do not provide significant information on the signals that contribute to cluster the samples, considering the higher variability for these samples. The samples from animals fed with 60 ppm of  $\beta$ -acids trend to stay in the negative-value region of both PC2 and PC3.

**Figure 30.** Principal component score plots A) PC1xPC2, B) PC1xPC3, and C) PC2xPC3 and variable loading plots D) PC1, E) PC2, and C) PC3 for the full  $^1\text{H}$  NMR spectra recorded for meat extracts from broilers fed different levels of lupulones (none, 30 ppm, 60 ppm, and 240 ppm).





The samples from broilers fed with 60 ppm of lupulones also demonstrated a higher variability over the scores plot in Figure 30. These samples trend to stay in positive-value regions of both PC2 and PC3.

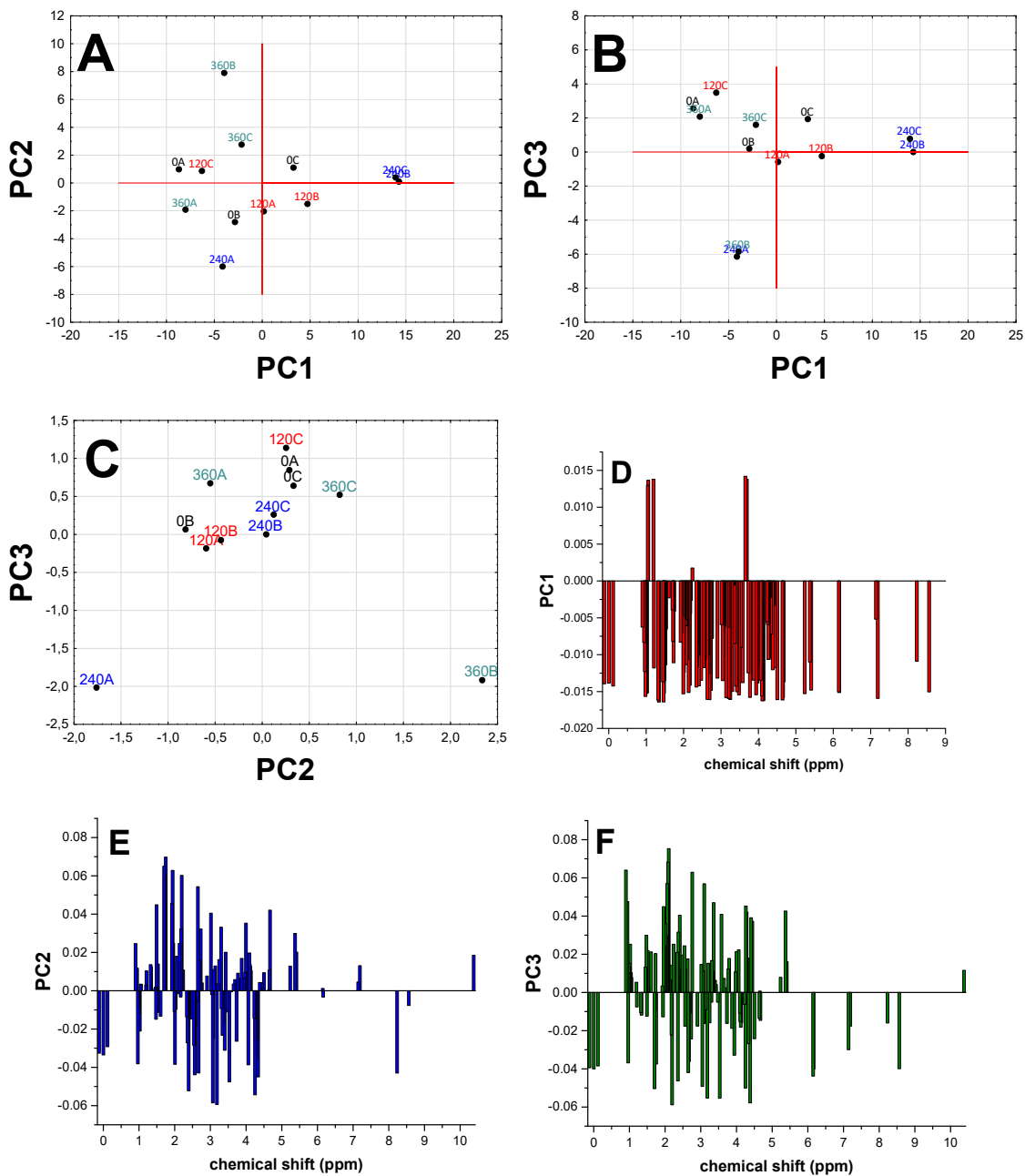
Unlike samples from broilers from the other feeding treatments, samples from broilers fed with 240 ppm of lupulones have not demonstrated a higher variability over the scores plot in Figure 30. These samples formed a tight cluster in the positive-values region of the PC3, and almost in the midpoint of the PCA model considering the positive-values of the PC1 and PC2. The signals responsible for this tight cluster could not be identified.

Considering the samples from broilers fed different levels of lupulones, untargeted metabolomics demonstrated to provide preliminary information on the clustering of the samples according to the diet. PCA results performed on the full NMR spectra allowed to observe that samples fed with no lupulones or with the lowest level of lupulones can be differentiated from the samples from broilers fed the highest levels of lupulones. However, complementary statistical analysis is necessary to evidence that  $\beta$ -acids can promote changes in the metabolic profile of broilers.

For the samples from pigs fed with different levels of hops  $\beta$ -acids, the three PC's together explain 71% of total variance (PC1 53%, PC2 10% and PC3 8%) and the trends and clustering are shown in Figure 31 (A, B and C). All samples of meat extracts from pigs fed with different levels of hops  $\beta$ -acids show a higher variability for PCA results. Meat extracts from pigs fed with 360 ppm of lupulones were the only samples that presented a trend to stay together in the negative-value region of PC1. However, these samples are poorly clustered considering PC2 and PC3. Therefore, the initial data screening of the full  $^1\text{H}$  NMR spectra does not provide information on the suitable

clustering of the samples according to the diet. The quantification of the individual metabolites for each meat sample as well as the attribute selection is necessary to obtain further information from statistical analysis.

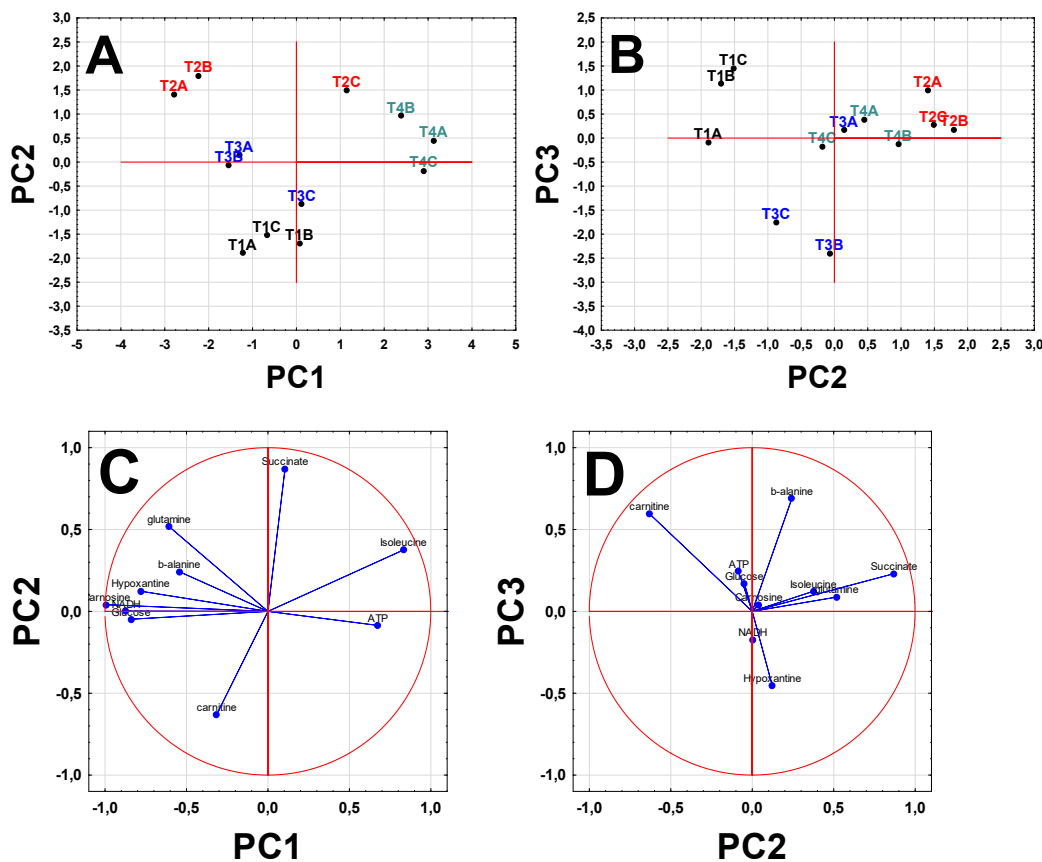
**Figure 31.** Principal component score plots A) PC1xPC2, B) PC1xPC3, and C) PC2xPC3 and variable loading plots D) PC1, E) PC2, and C) PC3 for the full  $^1\text{H}$  NMR spectra recorded for meat extracts from pigs fed different levels of lupulones (none, 120 ppm, 240 ppm, and 360 ppm).



### 3.1.3. <sup>1</sup>H-NMR targeted metabolomics of meat from broilers and pigs fed $\beta$ -acids: Principal components analyses (PCA)

Further investigation of variations between metabolic profiles required the use of statistical methods on the quantitative profile of meat. Samples from broilers fed different levels of hops  $\beta$ -acids showed high variability considering all the metabolites that were quantified by NMR. Thus, one-way ANOVA was used to select which metabolites were effective to discriminate between different feeding regimes. PCA was applied to the metabolomic data as determined from the <sup>1</sup>H-NMR quantitative approach using the variables selected by ANOVA ( $p < 0.05$ ) in order to represent possible clustering of the chicken samples. PCA score plot for the data derived from the metabolic quantitative profile of meat extracts from broilers is shown in Figures 32A and 32B. Loading plots were examined to determine the main metabolites responsible for the separation in the PCA maps (Figure 32C and 32D).

**Figure 32.** Principal component score plots A) PC1xPC2, B) PC2xPC3, and variable loading plots associated to C) PC1xPC2 and D) PC2xPC3 for the quantitative metabolite profile for meat extracts from broilers fed different levels of lupulones (none, 30 ppm, 60 ppm, and 240 ppm).



Three significant PC's were identified in the data sets of the broiler samples. Together, these PC's explain 78% of the total variance (PC1 46%, PC2 18%, and PC3 14%). Samples from animals fed with no supplement trend to be separated from the animals fed different levels of lupulones considering three principal components PC1, PC2 and PC3. The samples of meat extracts from broilers feed without  $\beta$ -acids also trend to form a small tight cluster in the negative-value region of both PC1 (Figure 2A) and PC2 and in the positive-value region of PC3 (Figure 2B). Loadings plot indicated carnitine as the main metabolite that contributes for the clustering of T1 samples (Figures 2C and 2D).

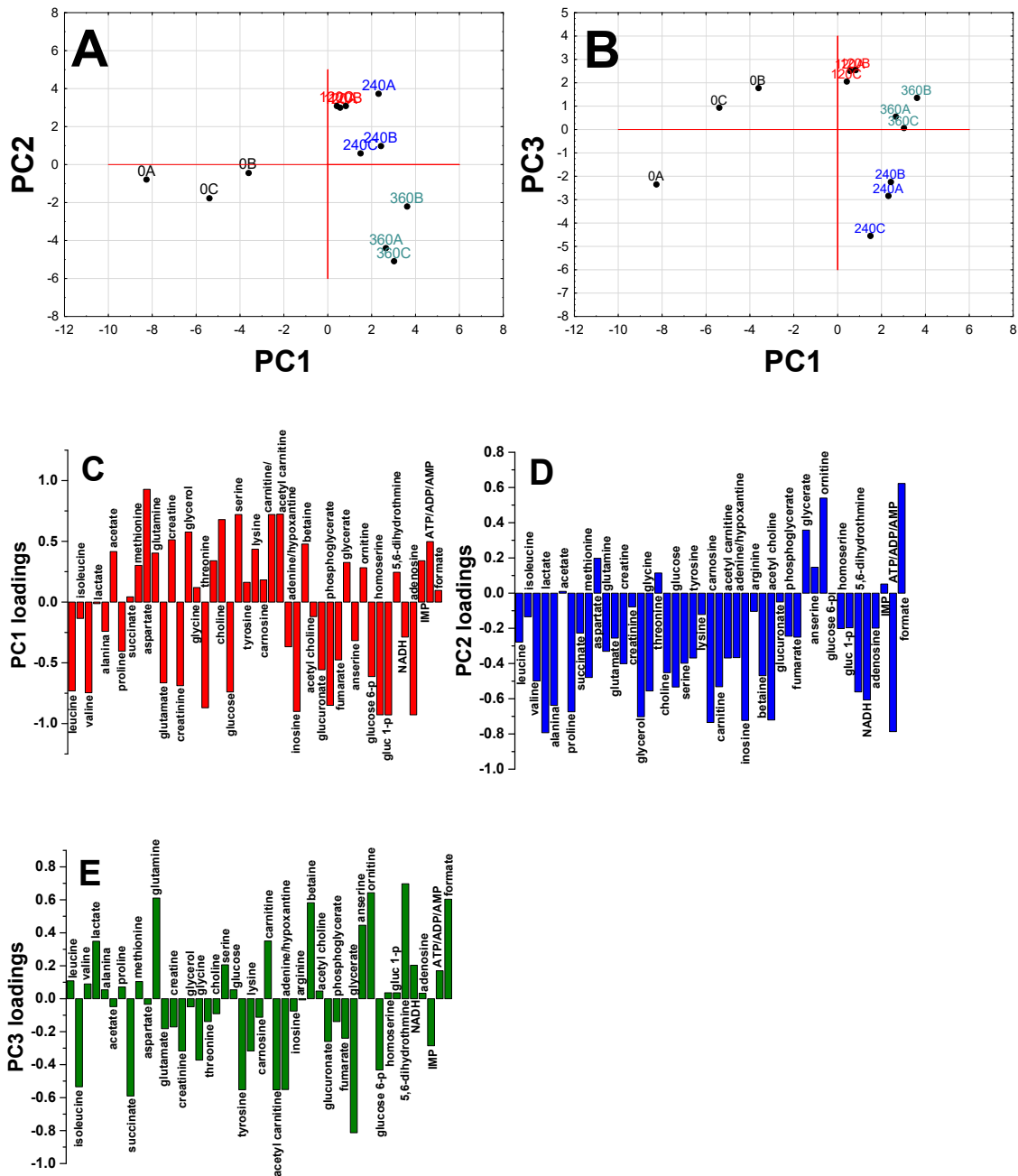
The samples of meat extracts from broilers fed with 30 ppm (T2) and 60 ppm (T3) of  $\beta$ -acids showed a considerable variability for PCA results. Samples from T2 seem to be related to high levels of glutamine, isoleucine, glutamine, carnosine, NADH, hypoxantine, glucose and succinate. Considering the higher variability for samples from broilers fed 60 ppm of lupulones, the loadings plots do not provide significant information on the signals that contribute to separate the samples of T3 from other treatments.

Unlike samples from broilers submitted to other feeding regimes with  $\beta$ -acids, samples from broilers fed with 240 ppm of lupulones have not demonstrated a higher variability over the scores plot of Figure 2. These samples trend to stay together in the positive-values region of the PC1 and PC2, and almost in the midpoint of the PCA model considering the positive-values of the PC2 and PC3. The metabolites responsible for this small tight cluster were identified as isoleucine, ATP and glutamine.

PCA was also performed on the quantitative metabolite profile of meat from pigs fed  $\beta$ -acids. For pork, however, one-way ANOVA was not used for variable selection. Three PC's were found to respond for 64% of total variance (PC1 31 %, PC2 20% and PC3 13%) and the trends and clustering are shown in Figure 33 A and B. Loading plots are present in Figure 33C, D and E. Despite the fact that meat extracts from pigs fed without supplements presented high variability when compared to the other treatments, these samples trended to be separated from the animals feed with  $\beta$ -acids. PC1 was found to give the highest contribution for such separation in two main groups: animals fed without supplements trend to stay in the negative-values region of PC1 while all the samples from animals fed with lupulones trend to form small tight clusters in the positive-values region of PC1. Samples from pork fed without supplements showed high concentrations of leucine, isoleucine, valine, alanine, proline, glutamate, creatinine, glucose, inosine,

acetylcholine, glucuronate, phosphoglycerate, fumarate, glucose-1-phosphate, NADH and adenosine.

**Figure 33.** Principal component score plots A) PC1xPC2, B) PC2xPC3, and variable loading plots associated to C) PC1xPC2 and D) PC2xPC3 for the quantitative metabolite profile for meat extracts from pigs fed different levels of lupulones (none, 120 ppm, 240 ppm, and 360 ppm).



Inside the group related to animals fed with dietary hops  $\beta$ -acids, three other small groups can be observed in the PCA maps of Figure 33. Notably, small tight clusters were found in the samples from animals fed the lowest level of supplement (120 ppm)

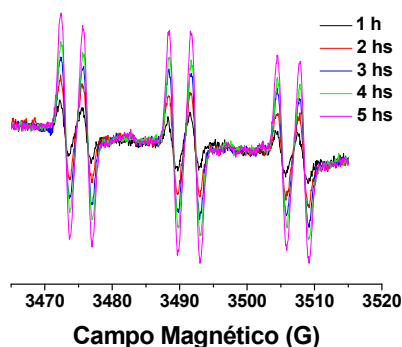
when compared to the other treatments. These samples trend to stay together in both positive-values region of PC2 and PC3 and nearly to the 0-value of PC1. Loading plots indicated that the metabolites aspartate, lactate, glycerate, IMP and formate were responsible for the clustering in T2 pork samples.

Samples from pigs fed with 240 ppm of lupulones presented higher variability when compared to all the samples from animals fed with dietary supplement. T3 samples trend to stay in the positive-values region of both PC1 and PC2 and in the negative-values region of PC3 which was found to separate this treatment from the T2 and T4. Isoleucine, succinate, glutamate, creatine, glycerol, glycine, tyrosine, lysine, carnosine, acetyl carnitine, glycerate and IMP were identified as the metabolites responsible for the clustering of T3 samples. Samples from T4 (360 ppm of dietary lupulones) trended to stay together in the positive-values region of both PC1 and PC3 and in the negative-values region of PC2. Animals fed 360 ppm presented high levels of methionine, succinate, glutamine, creatine, glycerol, choline, serine, lysine, carnitine, acetyl carnitine, betaine, 5,6-dihydrothimine and ATP/ADP/AMP.

#### **3.1.4. Redox stability of meat from animals fed with different levels of hops $\beta$ -acids as determined by EPR**

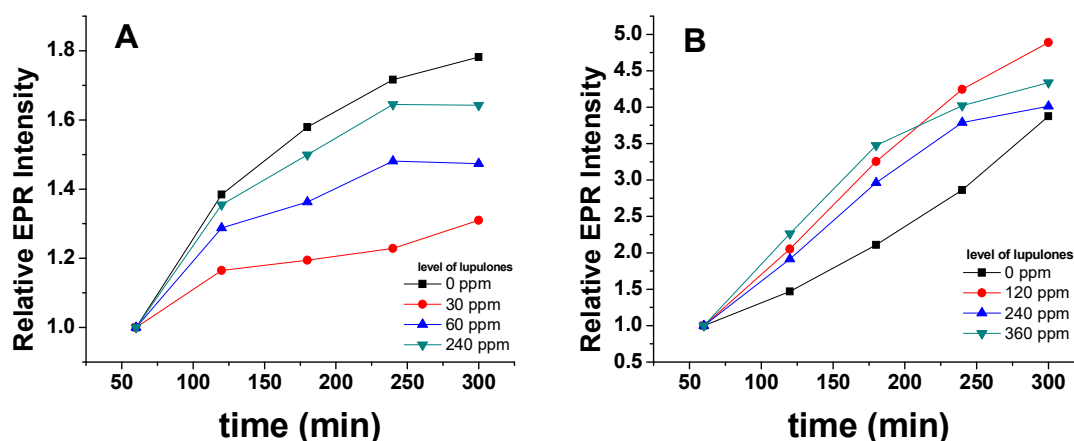
EPR spectra of meat slurries from animals fed with different levels of  $\beta$ -acids were presented in Figure 34. Reactive short-lived free radicals can be thermally produced in meat slurries incubated at 65 °C because some meat components, such as lipids and proteins, are easily oxidizable. In the presence of PBN, these reactive free radicals are added to the double bond of the spin trap PBN yielding a more stable radical adduct which has a suitable lifetime for EPR monitoring.<sup>149</sup> The 6-line spectral profile that can be observed in Figure 34 is characteristic of PBN adduct radicals.<sup>130,149</sup> As the intensity of the EPR signal is proportional to the PBN adduct radical concentration, the development of radicals in meat slurries can be accordingly used to deduce the radical formation rate in the system. The intensity of the signals has shown to be dependent on the period of thermal incubation that the meat slurries have been subjected to.

**Figure 34.** Typical EPR spectrum for the PBN radical adduct produced during incubation of chicken meat slurries at 65 °C.



The relative EPR intensities related to the PBN radical adduct were calculated during the total period of thermal incubation, as shown in Figure 35. Significant changes were verified in the redox status of meat from broilers fed with different diets. The lowest radical formation rate was ascribed to the samples referring to the animals fed 30 ppm of lupulones. The increased redox stability in these samples can be related to the highest level of endogenous antioxidants, especially anserine and carnosine. For the meat slurries from broilers fed different levels of hops  $\beta$ -acids, the redox stability has shown a positive correlation with the concentration of anserine.

**Figure 35.** Radical formation as measured by the relative intensity of PBN radical adduct in meat slurry incubated at 65° C during different time intervals. (A) Broilers and (B) pigs. EPR intensity was calculated by double integration of EPR signal and the ratio  $\text{Area}_{T=X_{\text{min}}}/\text{Area}_{T=0}$ .



The samples from pigs fed different levels of lupulones have not shown significant differences in their radical formation rate in agreement with the data taken from the PCA result which shown that there are no significant differences between pork samples. For this system, the radical formation rate has shown to be higher while compared

to the samples from broilers, indicating that the oxidation is more pronounced in pork. This result is in agreement with the data taken from the NMR which shown lower concentrations of antioxidants in pork.

### **3.1.5. Investigation of myofibrillar protein oxidation in chicken meat through immuno spin-trapping**

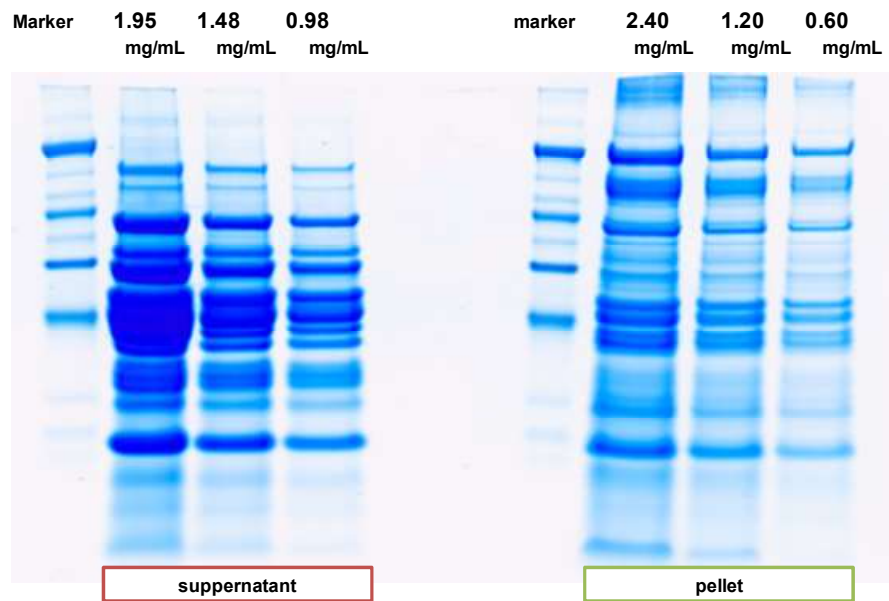
Protein oxidation reactions can lead to reversible and irreversible modifications on the amino acid chains of the protein structure. Considering that the protein structure is associated to its biological function, several biological pathways may be affected by protein oxidation, damaging the organism. Hence, the study of the protein oxidation processes is of importance to develop techniques that allow identifying such modifications<sup>161</sup> and to use antioxidants to prevent these processes.

The combination of SDS-Page and immunoblotting techniques was used to investigate the possible effect of hops  $\beta$ -acids on preventing the oxidation of myofibrillar proteins from broilers.

#### ***3.1.5.1.SDS-Page for the characterization of myofibrillar proteins from broilers***

Myofibrillar (MP) and sarcoplasmic (SP) proteins were separated and characterized by SDS-Page, as shown in Figure 36. The electrophoretic profile of MP showed to be different from the profile of sarcoplasmic proteins and this result is in agreement with the literature.<sup>132</sup> Myosin (220 KDa), actin (45 KDa), thropomyosin (35 KDa) and throponine (35 KDa) were identified in the fraction corresponding to the myofibrillar proteins.<sup>162</sup>

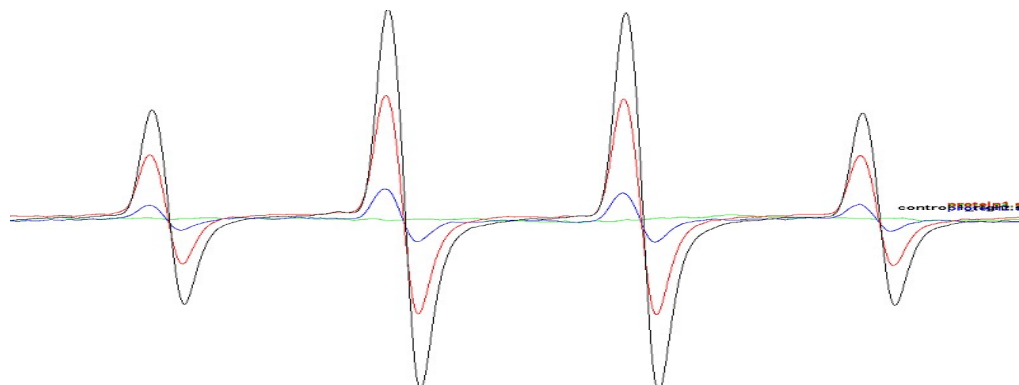
**Figure 36.** Characterization of the sarcoplasmic proteins (SC) and myofibrillar protein (MP) by SDS-Page in gel NuPAGE® Novex® 10% Bis-Tris. Protein concentration was determined spectrophotometrically using a NanoDrop system.



### 3.1.5.2. Investigating the oxidation of myofibrillar proteins from broilers by Electron Paramagnetic Resonance

In the present study, the formation of radicals in the presence of different concentrations of MP was monitored by EPR spin-trapping technique (Figure 37). Oxidative conditions were imposed to the system by the use of  $\text{Fe}^{2+}$  and hydrogen peroxide and the behaviour of MP toward DMPO was evaluated.

**Figure 37.** EPR spectra of hydroxyl-DMPO radicals produced under different levels of myofibrillar proteins. Reactions were carried out in 50 mM phosphate buffer pH 6.8 at room temperature. Conditions: DMPO (5.0 mM),  $\text{FeSO}_4 \cdot 7\text{H}_2\text{O}$  (1.0 mM),  $\text{H}_2\text{O}_2$  (1.0 mM), control (no protein [black]) and MP (8.0 mM [red], 32.0 mM [blue] and 64.0 mM [green]).



A negative control composed by DMPO and  $\text{Fe}^{2+}/\text{H}_2\text{O}_2$  was prepared in order to identify the spin adduct that can be produced in the system. The EPR spectrum represented as a black line (control) in Figure 37 shown the hyperfine coupling pattern with four lines in the proportion 1:2:2:1 and  $g_{\text{iso}} = 2,005$  with  $a_{\text{N}} = 15$  G and may be assigned to the radical adduct hydroxyl-DMPO [DMPO-OH] $\cdot$ . [DMPO-OH] $\cdot$  radical adducts may be produced in the presence of  $\text{Fe}^{2+}$  and hydrogen peroxide by the Fenton reaction.<sup>163</sup> The signal intensity of [DMPO-OH] $\cdot$  has shown to decrease when increasing concentrations of MP were added to the spin-trap solution, suggesting that other radicals can be produced in the system competing for hydroxyl-DMPO radicals or some myofibrillar protein components may reduce [DMPO-OH] $\cdot$  species.

Myofibrillar proteins have shown to produce radicals in their structure under oxidative conditions<sup>3,22</sup> and may react competing with [DMPO-OH] $\cdot$  radicals yielding EPR silent end products. These results indicate that the system can be potentially investigated by the immuno-spin trapping technique using DMPO in order to find the myofibrillar proteins that are more susceptible to the oxidation.

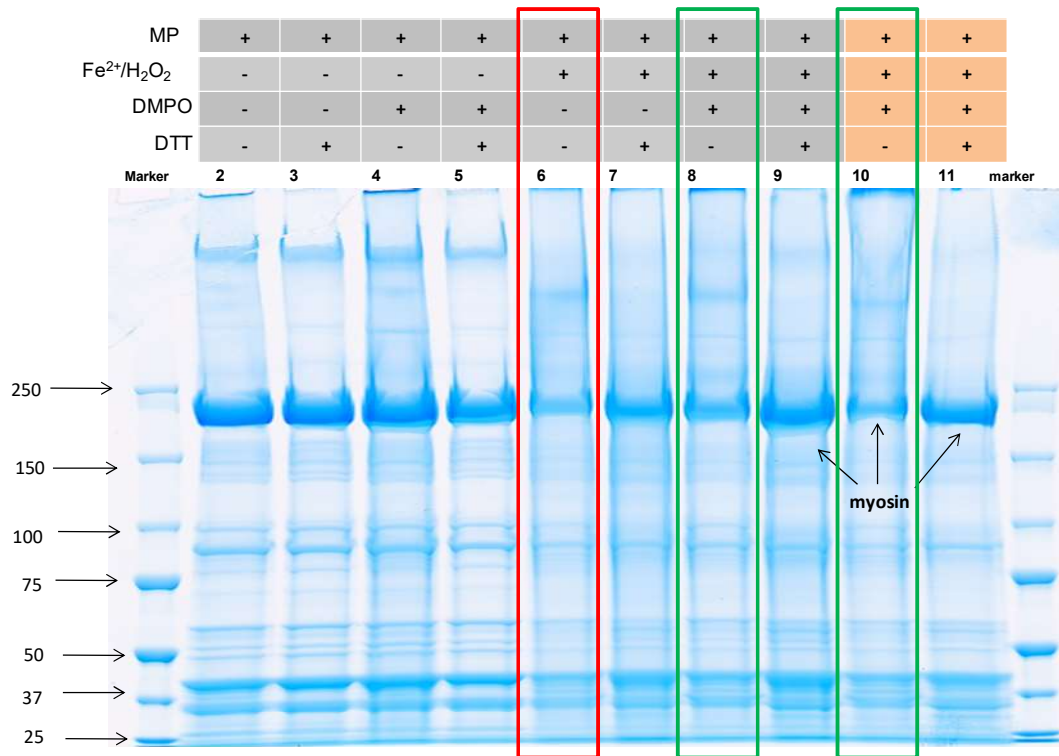
### ***3.1.5.3. Investigation of protein oxidation and cross-linking by SDS-Page and Western Blot***

Samples containing myofibrillar proteins and DMPO were subjected to oxidative conditions and SDS-Page was used to investigate the formation of protein cross-linking and other oxidative modifications in the protein structure (Figure 38).

The presence of prooxidant agents have shown to not change the electrophoretic profile of the MP fraction. However, the intensity of some bands decreased when compared to the bands related to the samples without oxidants. Since the intensity of the electrophoretic bands is proportional to the protein concentration, the myofibrillar proteins that have shown decrease in the band intensity may be taking part in oxidation reactions to yield higher-molecular-mass material through intermolecular cross-linking. The formation of lower-molecular-mass material via protein fragmentation has not shown to occur. The band assigned to myosin presented the higher decrease in intensity when compared to other proteins and this decrease shown to be greater in non-reducing gels than in the reducing gels (with DTT), indicating that reducible and non-reducible cross-links can be produced. These results are in agreement with the study of Lund et al.,

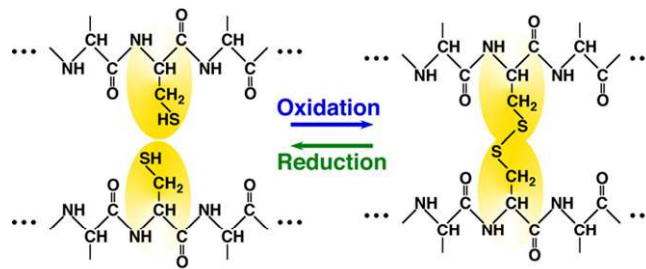
that demonstrated that myosin–myosin species can be produced under oxidative conditions provided by H<sub>2</sub>O<sub>2</sub>-activated myoglobin.<sup>22</sup>

**Figure 38.** Effect of oxidation on the structural integrity of myofibrillar proteins incubated in the presence of: (i) Fe<sup>2+</sup>/H<sub>2</sub>O<sub>2</sub>; (ii) Fe<sup>2+</sup>/H<sub>2</sub>O<sub>2</sub> and DMPO; (iii) Fe<sup>2+</sup>/H<sub>2</sub>O<sub>2</sub> and DTT; (iv) Fe<sup>2+</sup>/H<sub>2</sub>O<sub>2</sub> and DTT and DMPO). The table presents the components that are present (+) and absent (-) in the samples. Two concentrations of DMPO were used: 2.5 mM (grey) and 25.0 mM (salmon).



Myosin, as a thiol-rich protein (RSH), is easily oxidizable (Figure 37) and the oxidation of its cysteine residues yields disulfides (RSSR).<sup>22,164</sup> The band with a molecular weight of 220 kDa corresponding to myosin has shown to decrease in the samples that contain Fe<sup>2+</sup>/H<sub>2</sub>O<sub>2</sub> at the same time that a band with a molecular weight of approximately 440 kDa is present in the non-reducing gels. This higher-molecular-mass band may be assigned to myosin-myosin dimers. The intensity of the myosin bands showed to be regenerated by the presence of 0.1 M DTT corroborating that the formation of cross-link in myosin occur via thiol oxidation since DTT is a specific reducing agent for disulfide bonds that can regenerate the oxidized thiols.

**Figure 39.** Formation of cross-link in protein via oxidation of cysteine residues.

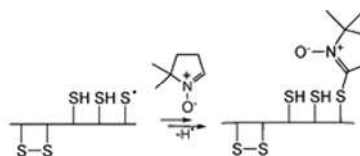


Source: Figure elaborated by the author.

Despite the fact that DMPO has not shown to change the electrophoretical profile of the MP, samples that contain simultaneously DMPO and DTT shown a more pronounced regeneration of the band assigned to myosin (Figure 36, wells 8,9, 10 and 11) under oxidative conditions, suggesting that DMPO may contribute to the reduction of the protein or may prevent myosin oxidation. These DMPO potential properties have been described by Kezler et al.<sup>165</sup> Moreover, the samples that were incubated under oxidative conditions, in the presence of DMPO and in the absence of DTT keep the intensity of the myosin band, indicating that the spin trap may inhibit the oxidation of this protein.

The formation of disulfides through the cross-linking of myosin may occur via a radicalar mechanism as described by Lund et al.<sup>21</sup> Thyl radicals ( $RS^{\bullet}$ ) produced by the oxidation of cysteine residues may be trapped by DMPO yielding a product that can be detected by immunoblotting (Figure 40).

**Figure 40.** DMPO trapping thyl radicals.

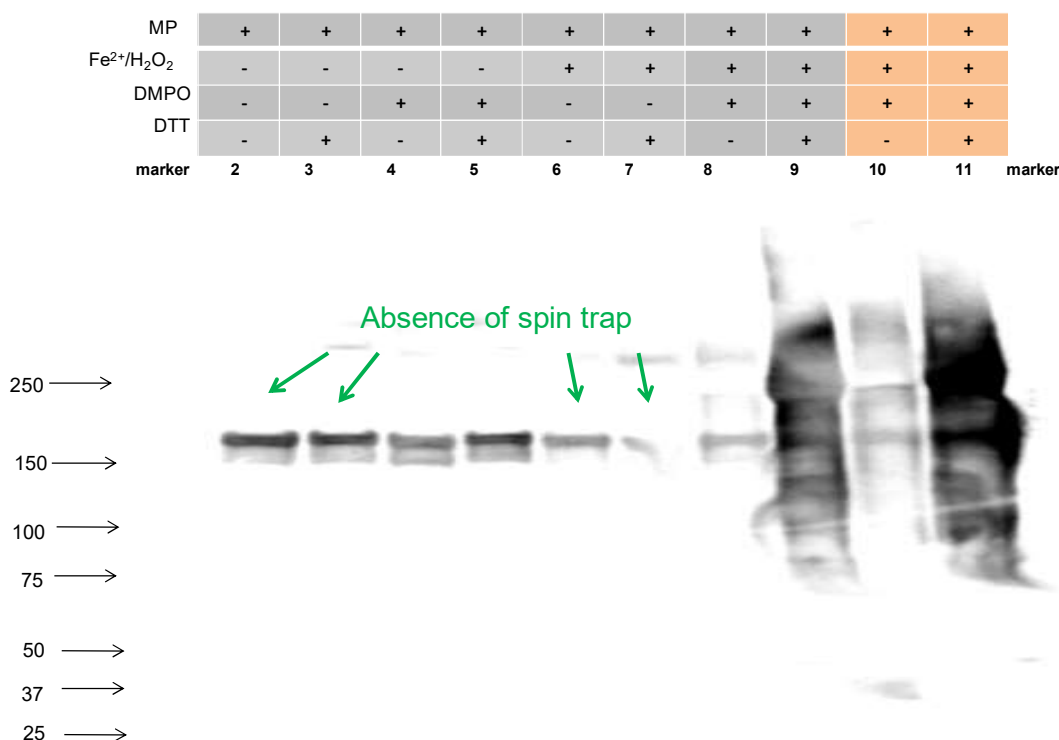


Source: Figure elaborated by the author.

In this context, the viability in the use of the immuno-spin trapping technique to detect the presence of DMPO–nitroxide associated with myofibrillar proteins was evaluated. In order to investigate the presence of radicals in myofibrillar proteins, a second gel identical to the gel of the Figure 38 was used to perform Western Blot and the results are presented in Figure 41. A greater number of bands was immunologically detected by Western Blot in the samples with higher concentrations of DMPO. Upon incubation of MP with both DTT and DMPO, larger bands were detected along the well in which the related

sample was loaded. The reduction of oxidized MP by DTT may result in the generation of immunologically detectable DMPO adduct which responds to the observable blurry bands related to the wells 9, 10 and 11 of Figure 41. Furthermore, a band was detected at approximately 100 kDa in all the samples, including the samples whose DMPO was absent and the samples without oxidants, suggesting that the proteins at 100 kDa interfere in the assay. These proteins may possibly have affinity for the antibodies that were used to incubate the membrane not necessarily producing radicals. Hence, immuno-spin trapping technique has not shown to be effective to investigate the oxidation of myofibrillar proteins.

**Figure 41.** Immunoblotting assay of myofibrillar protein radicals. Protein extract incubated with (i)  $\text{Fe}^{2+}/\text{H}_2\text{O}_2$ ; (ii)  $\text{Fe}^{2+}/\text{H}_2\text{O}_2$  and DMPO; (iii)  $\text{Fe}^{2+}/\text{H}_2\text{O}_2$  and DTT; (iv)  $\text{Fe}^{2+}/\text{H}_2\text{O}_2$  and DTT and DMPO. The table on the top presents the components that are present (+) and absent (-) in the samples. Two concentrations of DMPO were used: 2.5 mM (grey) and 25.0 mM (salmon).

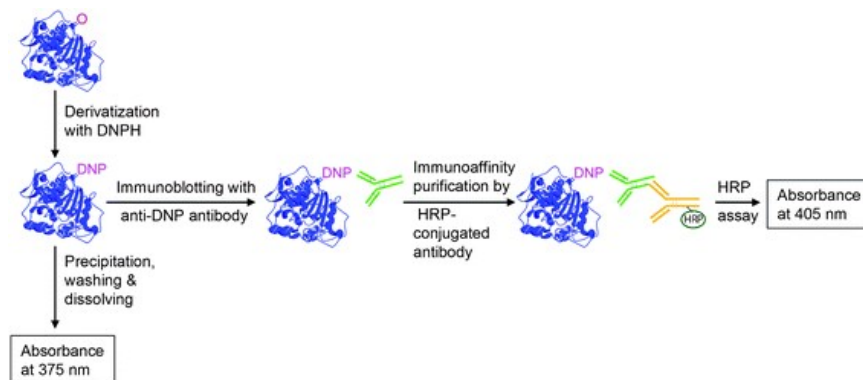


#### 3.1.5.4. Investigating the formation of carbonyl groups in the SDS-Page e Oxyblot: *investigação da formação de grupos carbonila na cadeia lateral de aminoácidos de proteínas*

Metal-catalyzed modifications in proteins include the formation of radicals and cross-links and, also, the formation of carbonyl groups. The detection of all of these modifications has been taking into account to determine the level of oxidative damage in proteins.<sup>127</sup>

Considering that myofibrillar proteins have demonstrated to be susceptible to oxidation in the previous sections, the Oxyblot technique was used to determine if carbonyl groups can be produced by  $\beta$ -fragmentation of the amino acid side chain.<sup>127</sup> The Oxyblot principle is illustrated in Figure 42.

**Figure 42.** Principle for the detection of protein carbonyls by spectrophotometric and immunoblotting methods derivatized with 2,4-dinitrophenylhydrazine (DNPH). Reproduced with permission from Törnvall, 2010.<sup>161</sup>

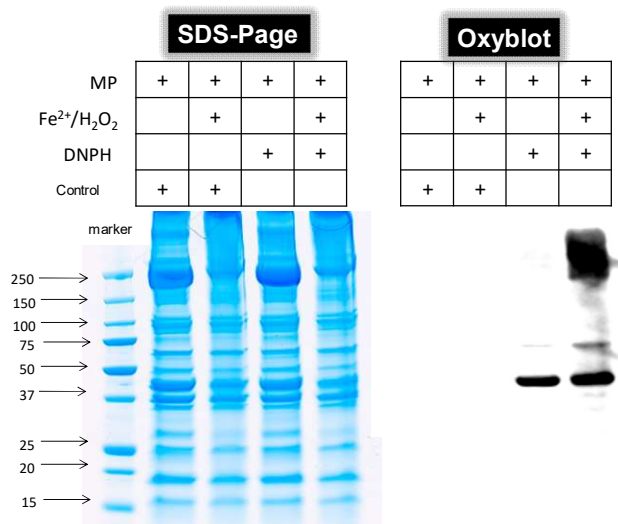


Source: TÖRNVALL, U. *Anal. Methods*, 2010,2, 1638-1650.

Initially, some assays for method validation were carried out using a control sample of MP extracted from chicken meat. MP samples were incubated with  $\text{Fe}^{2+}/\text{H}_2\text{O}_2$ , DNPH and a control solution provided by the Oxyblot kit assay (Figure 43). The presence of prooxidant agents, DNPH and the control solution have shown to not change the electrophoretic profile of the MP fraction (data not shown). Bands assigned to higher-molecular-weight proteins were immunologically detected by Oxyblot in the samples incubated with DNPH under oxidative conditions, indicating that the formation of carbonyl groups occurs specially in myosin and its cross-linked dimers produced via oxidation. A band at 45 kDa was detected even in the absence of the oxidants  $\text{Fe}^{2+}/\text{H}_2\text{O}_2$ . This band is possibly assigned to actin and may negatively interfere in the assay since it interacts with the antibodies and/or other components of the Oxyblot kit assay. Other hypothesis to explain the detection of carbonyl groups in actin even without the presence of oxidants is related to the increased accessibility of oxidation sites in actin due to structural properties. Such hypothesis is in agreement with Dalle-Donne et al. who found that purified actin is strongly susceptible to oxidation.<sup>166</sup> Carbonylated actin and myosin were detected in myofibrillar proteins extracted from lambs by Santé-Lhoutellier et al.<sup>167</sup> In this study, authors found that diet and storage period affect protein oxidation as determined by

Oxyblot and from the carbonyl content in myofibrillar proteins exposed to oxidative conditions.

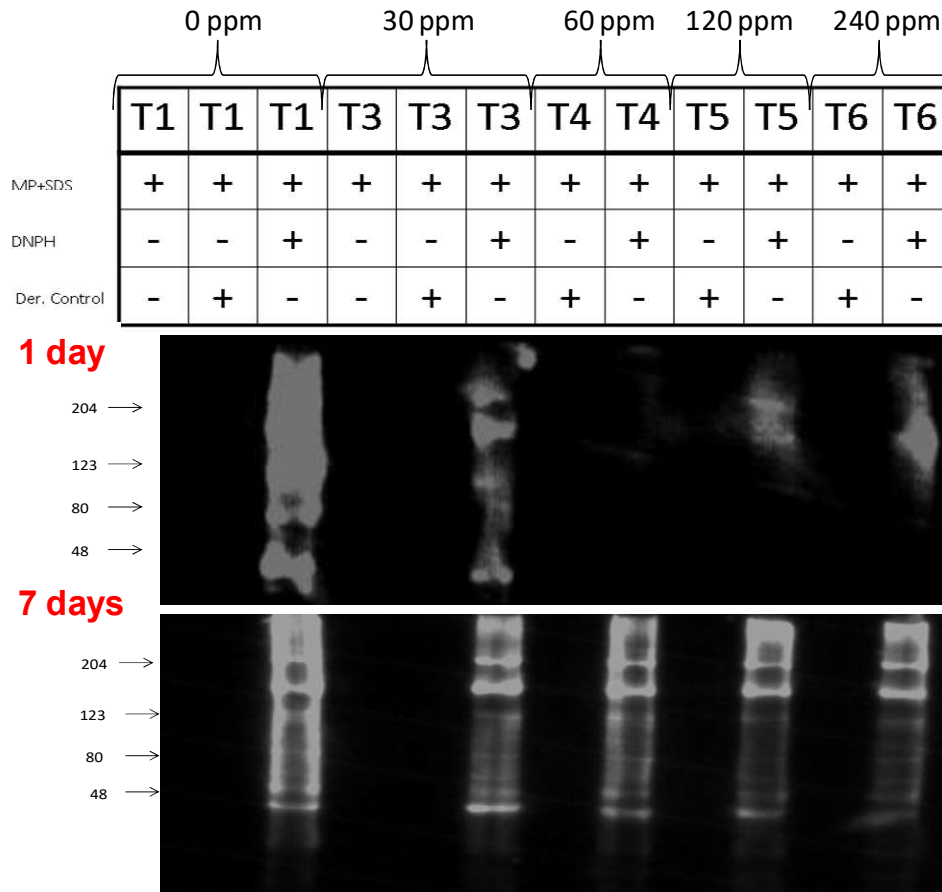
**Figure 43.** SDS-Page gel electrophoresis and Oxyblot results for myofibrillar proteins extracted from chicken meat and incubated with  $\text{Fe}^{2+}/\text{H}_2\text{O}_2$ , DNPH and control solution. MP were incubated at 4 °C with (i)  $\text{Fe}^{2+}/\text{H}_2\text{O}_2$ ; (ii)  $\text{Fe}^{2+}/\text{H}_2\text{O}_2$  and DNPH; (iii)  $\text{Fe}^{2+}/\text{H}_2\text{O}_2$  and solution control. The table on the top presents the components that are present (+) and absent (-) in the samples.



The Oxyblot technique was concluded to be useful for the investigation of the redox stability of meat from animals fed with different diets by considering the extension of oxidative modifications in proteins. Hence, animals fed with different levels of  $\beta$ -acids were analyzed by Oxyblot to evaluate if the diet has effect on the prevention of oxidative reactions in muscle tissues. Also, the effect of the storage on the protein oxidation was examined by Oxyblot. Chicken samples were stored for 1 and 7 days and after the extraction of MP, Oxyblot was performed being the results present in Figure 44.

The formation of carbonyl groups were observed in all the MP samples. However, the MP samples from animals fed with no lupulones showed higher intensity bands associated to carbonyl groups. The increase in the storage period demonstrated to intensify oxidative reactions since the the formation of carbonyl groups is more pronounced in the samples stored for 7 days while compared to the samples stored for 1 day. The oxidation of MP produced carbonyl groups mostly in the proteins with high molecular weigh, such as myosin, and in actin. Myosin and actin remained the main targets of oxidation after 7 days of storage. Although, other myofibrillar proteins seem to be affected by oxidation producing carbonyl groups considering 7-day storage.

**Figure 44.** Effect of the storage on the formation of carbonyl groups in myofibrillar proteins extracted from broilers fed with different levels of hops  $\beta$ -acids. MP were incubated at 4 °C with (i)  $\text{Fe}^{2+}/\text{H}_2\text{O}_2$ ; (ii)  $\text{Fe}^{2+}/\text{H}_2\text{O}_2$  and DNPH; (iii)  $\text{Fe}^{2+}/\text{H}_2\text{O}_2$  and solution control. The table on the top presents the components that are present (+) and absent (-) in the samples.



Considering the impact of the diet in preventing the formation of carbonyl groups in myofibrillar proteins, the samples from animals fed with higher levels of hops  $\beta$ -acids showed to be less susceptible to oxidation as demonstrated by the decreased intensity of the bands immunologically detected in these samples. Following 7 days of storage, the content of carbonyl groups slightly increased in the samples from broilers fed  $\beta$ -acids, although, this content was considerable lower when compared to the control group. This result indicates that the addition of lupulones to the animal feed has a positive effect on the redox stability of the meat myofibrillar proteins and may prevent tenderness loss and quality deterioration.

## 5. CONCLUSION

Production of red meat has been receiving increasing public attention due to environmental concerns related to especially cattle farming and due to epidemiological indications of increasing health risks following high intake of red meat. The major findings of the current research where cattle feed was manipulated may be seen in relation to both of these aspects. The addition of mate extract, at varying levels from 0.5 to 1.5% w/w, in the diet of feedlot cattle did not affect animal performance, carcass characteristics, and commercial meat cut weights for the feedlot-finished Nellore steers. Beef produced from cattle finished on a feed supplemented with extracts of mate as a locally abundant plant in one of the most important regions for beef production worldwide, was shown to have increased oxidative stability, which may result in longer shelf-life, and at the same time to get better sensory evaluation and consumer acceptance. The beef from cattle fed a feed with mate extract added should accordingly result in less wasted food with a possible effect on environment. Beef produced from cattle finished on feed added mate extract also had a significant increase in the content of conjugated linoleic acid (CLA) and creatine, which will increase the nutritive value of the beef. It may further be speculated, that the beef with increased oxidative stability also will have a lower tendency of inducing iron-catalyzed radical formation in the gastrointestinal tract during digestion following meat consumption, in effect lowering the risk of colorectal cancer.

Based on the comparison between the effect of added mate extract to the cattle feed on the oxidative stability of the beef and to the effect on the content of CLA, creatine and the peptide carnosine, it is clear that the high level of addition of 1.5% mate extract gives most significant improvements. However, even the lower supplementation level of mate extract in the cattle feed resulted in significant effects and in full effects for improvement of tenderness, and beef from cattle fed the low level of 0.5% mate extract have the best overall acceptance by a sensory panel. For practical application in beef production these conclusions should, however, be considered together with production costs related to the change in feed by adding mate extract to increase oxidative stability and to improve the sensory quality of beef.

Considering the health concern in replacing red meat for healthier protein sources, chicken meat and pork can offer good alternatives for consumers. However, protein and lipid oxidation have been also evidenced in chicken meat and pork, responding for meat quality deterioration. Diet manipulation of broilers and pork has demonstrated to be a potential strategy for enhancing meat quality. In the present study, the impact of the

use of hops  $\beta$ -acids as supplement for broilers and pork has been evaluated and indicates that the supplement has different effects depending on the animal species. Significant changes were verified in the redox status and in the metabolic quantitative profile of broilers fed with different diets. Pork fed with dietary hops showed slight changes in the meat metabolism when compared to animals control while the redox stability of pork has not shown to be significantly affected by the diet. The concentration of dietary supplement was found to be of relevance for the improvement of the meat composition and the redox stability as demonstrated by the lowest rate of radical formation rate that was ascribed to the meat samples from chickens fed with 30 ppm of lupulones (lowest level of supplement). The redox stability was concluded to be proportional to the levels of endogenous antioxidants, especially anserine, carnosine and NADH. Such compounds may be responsible for the antioxidant activity of the meat polar metabolites.

Furthermore, the use of hops  $\beta$ -acids in the animal diet showed a positive effect on the prevention of myofibrillar protein oxidation since broilers fed with lupulones presented lower protein carbonyl content when compared to the animals fed without supplement. Myosin and actin were recognized as the main targets of oxidation considering myofibrillar proteins. However, protein oxidation does not seem to follow the redox stability behavior that was obtained from the spin-trapping assay neither the concentration of antioxidants. It suggests that protein oxidation can provide evidences of the redox status, although meat proteins are not the main factor involved in the maintenance of the total redox stability, which results from the combination of all the meat components.

# CHAPTER II: Reduction of ferrylmyoglobin by uric acid

Parts of this chapter have been published in: A. Zawadzki; D. R. Cardoso; L.H. Skibsted. (2017). Proton-coupled electron transfer promotes the reduction of ferrylmyoglobin by uric acid under physiological conditions. *RSC Advances*, 7(29), 17824-17831. DOI: 10.1039/C6RA28314D

## 1. Introduction

Uric acid is the final metabolite of purine bases in humans.<sup>168,169</sup> Uric acid is an acid with a  $pK_{a1}$  value of 5.75 and a  $pK_{a2}$  of 9.8. Uric acid in plasma is mainly present as the urate monoanion<sup>168,170-172</sup> and is considered to be the major antioxidant in human plasma. However, the low aqueous solubility of both uric acid and sodium urate carries a risk of precipitation of crystals of uric acid or sodium urate in tissue and joints.<sup>168,169,173-175</sup> Hyperuricemia may lead to gout and other diseases and is often related to dietary habits and lifestyle.<sup>175-178</sup>

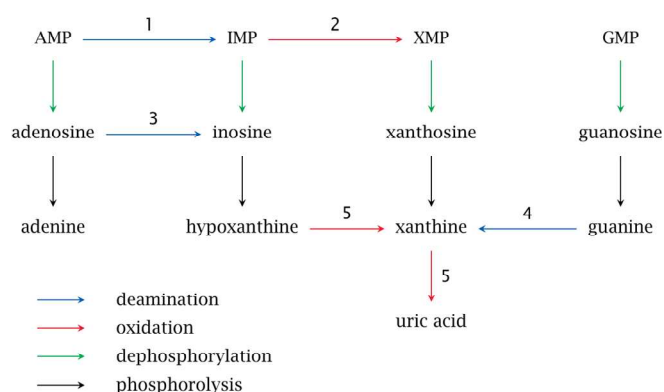
A high intake of red meat is frequently related to oxidative stress and radical damage in the gastrointestinal tract leading to pathological disorders.<sup>15,20,37-39,179,180</sup> The oxidative damage seems to arise from the formation of the hypervalent meat pigments perferrylmyoglobin ( $\bullet\text{MbFe(IV)=O}$ ) and ferryl myoglobin ( $\text{MbFe(IV)=O}$ ).<sup>179,180</sup> This activation of metmyoglobin ( $\text{MbFe(III)}$ ) by  $\text{H}_2\text{O}_2$  and/or organic hydroperoxides as present in foods initiates a pseudoperoxidase catalytic cycle of myoglobin.<sup>15,19,20,179,180</sup> Activation of  $\text{MbFe(III)}$  thus yields the very short lived compound I ( $\bullet\text{MbFe(IV)=O}$ ) which subsequently decays to the long-lived compound II ( $\text{MbFe(IV)=O}$ ).<sup>181,182</sup> Both  $\bullet\text{MbFe(IV)=O}$  and  $\text{MbFe(IV)=O}$  are strong oxidants known to initiate lipid and protein oxidation in muscle tissues and in meat products during storage and digestion.<sup>15,19,20</sup> Knowledge of the reaction kinetics and mechanisms by which toxic effects of hypervalent myoglobin species can be prevented or at least diminished by diet components such as natural antioxidants, are of relevance to improve human health through dietary recommendations.<sup>179</sup>

Uric acid is generated in the gastrointestinal tract through the breakdown of purine bases from the diet.<sup>169,170,174,183</sup> Both serum and gastrointestinal levels of uric acid may thus be modulated by dietary factors and a high intake of red meat is traditionally considered a risk factor for hyperuricemia and diseases resulting from this condition.<sup>174-177,184,185</sup> A higher level of uric acid formed in the digestive tract during food digestion could, however, also have positive health effects, since uric acid could be important as a reductant of hypervalent meat pigments.<sup>186</sup> The capability of uric acid and urate to deactivate hypervalent myoglobin through the formation of iron(III) or iron(II) states in effect protecting the gastrointestinal tract and muscles against radical damage has, however, not been studied.

### 1.1. Uric acid and oxidative stress

As consequence of mutational events responsible for silencing of the uricase gene along the primate evolution, uric acid became the last product of the enzymatic degradation of purine nucleosides and free bases in humans (Figure 45). Unlike humans, other mammals are able to enzymatically oxidize uric acid to allantoin while lower vertebrates can further degrade allantoin to urea. The evolutionary implication of the loss in the urate oxidase (uricase) activity is an increased blood level of uric acid in humans (200 – 400  $\mu\text{M}$ ) when compared to other vertebrates.<sup>169,183</sup>

**Figure 45.** Pathways of purine catabolism in humans.<sup>187</sup>



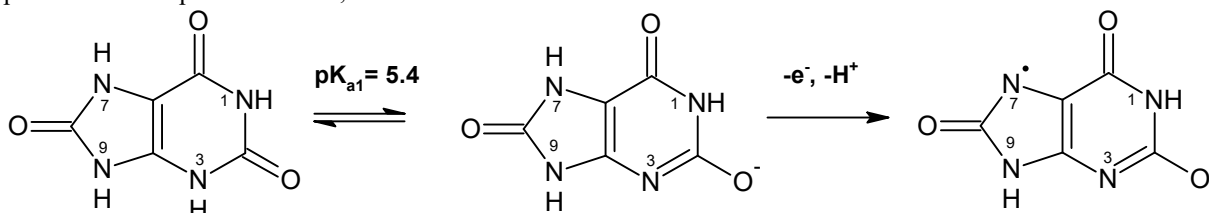
Source: <http://watcut.uwaterloo.ca/webnotes/Metabolism/Nucleotides.html#sec-nucleotidesPurineDegradationSalvage>

Several studies have demonstrated the antioxidant activity of uric acid as a powerful scavenger of singlet oxygen, peroxy and hydroxyl radicals ( $\text{RO}_2^\bullet$  and  $^\bullet\text{OH}$ ) and

to prevent the cellular damage arising from the oxidative stress. Based on these findings, Ames et al. proposed that higher blood levels of uric acid enhanced defense mechanisms against oxygen radicals during primate evolution, preventing aging and cancer and, consequently, allowed the lengthening of human life span.<sup>183</sup> Taking into account that the blood levels of urate are higher than the levels of ascorbate, uric acid has been recognized as the major antioxidant in human plasma.<sup>168–170,183</sup>

Uric acid is present in biological conditions as urate anion.<sup>170,171</sup> Although different  $pK_a$  values are reported for uric acid, the most cited values are 5.4 and 5.75.<sup>170,171,188–190</sup> Experimental and theoretical studies have demonstrated that the deprotonation of uric acid occur primarily at N3–H position (Figure 46).<sup>170,188</sup> The one-electron redox potential of urate in fluids ( $E^0(\text{urate}^\bullet/\text{urate})=0.56\text{V}$ ) is appropriated to scavenge radicals preventing chain reaction propagation.<sup>170,191</sup> The radical resulting from the one-electron oxidation of uric acid, urate radical ( $\text{urate}^\bullet$ ), is a resonance-stabilized radical since its unpaired electron is highly delocalized.<sup>170,171</sup> This oxidation formally represents a hydrogen abstraction at N7–H (Figure 46).<sup>188</sup>

**Figure 46.** Acid/base equilibrium between uric acid/urate and one-electron oxidation of urate coupled to proton loss. Adapted from Telo, 2003.<sup>188</sup>



Uric acid and its anions can reduce oxidant species and radicals through proton loss coupled to electron transfer mechanisms.<sup>170,171</sup> Double two sequential  $1H^+/1e^-$  hydrogen atom transfer (HAT), double electron transfer followed by proton transfer (ET–PT) and double sequential proton loss electron transfer (SPLET) were proposed as the possible mechanisms using water as a solvent. The preferential mechanism depends on the electronic properties of the radical and/or the oxidant.<sup>171</sup>

Although the antioxidant evolutionary advantage, the higher levels of uric acid in humans have been associated with the epidemiologic evidence of gout, hyperuricemia and cardiovascular diseases. Hyperuricemia is responsible for excessive levels of uric acid and occur due to disorders of the purine metabolism or due to the inefficient excretion of uric acid by the kidneys. As result of this excess, uric acid crystals

accumulate in the joints causing a type of inflammatory arthritis known as gout. Besides that, several studies have shown the role of the increased level of uric acid in the development of hypertension, obesity, cardiovascular diseases, kidney diseases, diabetes type II and insulin resistance. The oxidant effect of uric acid on the adipose tissue demonstrated to be the link for the association between hyperuricemia and obesity. The combination between genetics, diet and lifestyle has been considered determinant factors for the predisposition to hyperuricemia. High protein and purine diets, sedentary lifestyle and high alcohol consumption have been associated with an increase risk for hyperuricemia as well as for many diseases related to inflammatory processes, cancer and cardiovascular disorders.<sup>169,173,174,176-178</sup>

Under oxidative stress conditions, uric acid may act as pro-oxidant and pro-inflammatory factor implicating in the propagation of chain reactions and cellular damage. The pro-oxidant action of uric acid has shown to occur mainly in the hydrophobic environment where produces radicals targeting low density lipids and membranes, increasing the risk for cardiovascular diseases. Moreover, uric acid can react with strong oxidants, such as peroxyxynitrite, yielding other free radicals or cytotoxic products.<sup>168,169,174,177</sup> Hence, considering that uric acid acts either as antioxidant and pro-oxidant, Sautin et al. hypothesised the urate oxidant-antioxidant paradox aiming to explain the behaviour of uric acid in different compartments of the human organism (plasma or cell) and under different physicochemical circumstances.<sup>169</sup>

## 1.2. Pseudo peroxidase activity and redox mechanisms of heme proteins

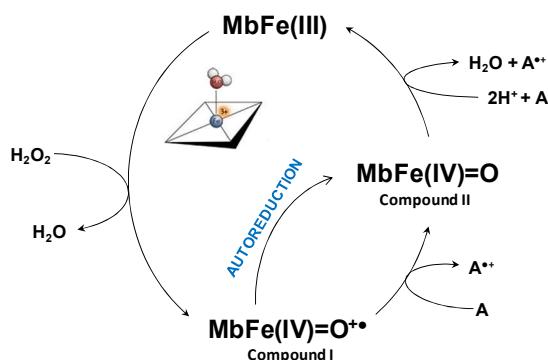
As described in the sections 1.1.3 and 1.1.5 of Chapter I, the peroxidase activity of hypervalent iron compounds derived from heme proteins has been further reported in the literature and is commonly associated with oxidative stress and the risk of colorectal cancer. However, under oxidative stress, the biological system provides defense mechanisms to deactivate these strongly oxidizing heme-Fe(IV)=O species. Certain biological antioxidants, such as ascorbate<sup>192,193</sup>, chlorogenate<sup>193</sup>, NADH<sup>194</sup>, cysteine<sup>195</sup>, H<sub>2</sub>S<sup>21</sup>, carotenoids<sup>196</sup>, polyunsaturated fatty acids<sup>101</sup> and thiol-rich proteins<sup>22</sup>, have shown to be involved in the reductive deactivation of ferryl heme species.

Hypervalent iron species are produced through the activation of myoglobin and haemoglobin by hydrogen peroxide (Scheme 2). The first oxidation equivalent of the heme-Fe(III) center of MbFe(III) and HbFe(III) by H<sub>2</sub>O<sub>2</sub> yields Compound II (ferryl

myoglobin and ferryl haemoglobin, respectively) which has iron in an oxidation state 4+ with an oxygen atom bonded to the iron (Fe(IV)=O). The second oxidation equivalent of the heme-Fe(III) species by peroxide leads to the formation of a transient protein radical which is called Compound I or perferryl myoglobin ( $\bullet\text{MbFe(IV)=O}$ ) or perferryl haemoglobin ( $\bullet\text{MbHe(IV)=O}$ ).<sup>194,196</sup> Perferryl Mb compounds also have the Fe(IV)=O center and comprise very short-lived radicals ( $\bullet\text{MbFe(IV)=O}$ ,  $\tau = 200 \mu\text{s}$ ) localized on a tyrosine residue of the globin that are detectable by EPR spectroscopy.<sup>182</sup> As an unstable radical, perferryl myoglobin can be converted to ferryl myoglobin through an autoreduction mechanism that was described by Mikkelsen & Skibsted.<sup>194</sup> Although perferryl species are stronger oxidants than ferryl species, both hypervalent compounds have shown to be pseudo-peroxidases able to damage important cellular structures.

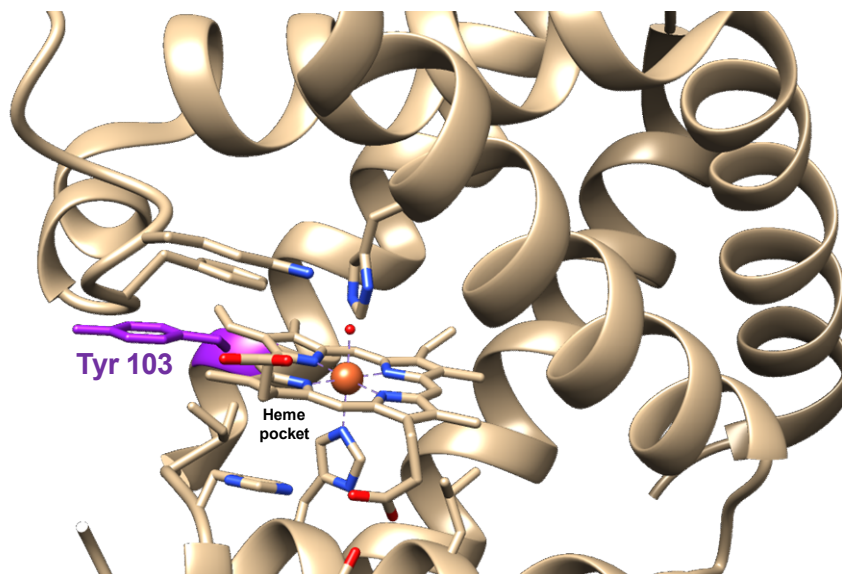
The pseudo-peroxidase activity of myoglobin involves a two-electron transfer from heme-Fe(III) with the subsequent regeneration of the heme-Fe(III) by the acceptance of one electron from each two electron donors (Scheme 2). The iron-oxygen bond formally arises from the heme-iron species through two-electron transfers when an oxygen atom from  $\text{H}_2\text{O}_2$  binds to the heme iron: (i) one electron comes from Fe(III) undergoing to Fe(IV) and, (ii) one electron comes from the porphyrin ring producing a radical cation which immediately oxidizes an amino acid residue of the surrounding peptide chain, yielding a protein radical. The overall effect of the catalytic cycle depends on the nature of the electron donor. Proteins, lipids and peroxides trend to initiate and propagate oxidative reactions through the pseudo-peroxidase cycle of myoglobin while antioxidants trend to remove peroxide and produce non-reactive radicals. Having the same reactions of the peroxidase cycle of the classical peroxidases, myoglobin, however, has shown oxidative modifications in its peptide chains due to repeated peroxidase cycling. Hence, the cycle presented in Scheme 2 is described as a pseudo-peroxidase mechanism.<sup>23</sup>

**Scheme 2.** Pseudoperoxidase cycle of myoglobin and production of the hypervalent species ferryl myoglobin ( $\text{MbFe(IV)=O}$ , Compound II) and perferryl myoglobin ( $^{\bullet}\text{MbFe(IV)=O}$ , Compound I).



The reduction of ferryl and perferryl myoglobin to the less toxic ferric form (Fe(III)) deactivates the metal centre and the protein radical, preventing the oxidative damage arising from these hypervalent species. Electron-transfer has been described as the mechanism responsible for changes in the redox state of myoglobin. Two independent reductant binding sites are recognized as centers for electron-transfer to the heme iron and to the protein radical in globins.<sup>197</sup> The first redox-active center is located in the heme pocket of the globin domain and gives access to the heme iron. According to its structural properties, size and charge, a reductant can reach the heme pocket to transfer directly one electron to the ferryl heme iron producing the ferric protein. A second route for electron transfer to heme iron is known as a “through-protein” pathway and comprises a radicalar mechanism involving a tyrosine residue. In horse heart myoglobin this residue is tyr103, which is located close to both heme iron and the protein surface (Figure 47). In general, the characteristics of the reductant play a crucial role to determine the preferential site of electron transfer.<sup>197,198</sup> The heme pocket has been shown to be a low affinity site for organic reductants and preferably, a long-range electron transfer has been shown to occur via the surface-exposed tyrosine, tyr103.<sup>197,198</sup> At low reductant concentrations, the “through-protein” electron transfer has shown to be faster compared to the pathway of direct transfer to the heme pocket. However, some organic reductants, such as ascorbate, were reported for reducing ferrylmyoglobin using both pathways. The rate constants for the reduction of ferrylmyoglobin by ascorbate through direct electron transfer to the heme edge presented high pH dependence while tyrosine site did not shown to be pH dependent.<sup>197</sup>

**Figure 47.** Heme pocket and Tyr 103 as redox-active centres for electron transfer in ferryl myoglobin. Drawing was prepared with UCSF Chimera software from PDB 5d5r.



The electron transfers from both redox-active centers of myoglobin can also involve proton transfers through a process known as proton-coupled electron transfer (PCET). Such process is described in eqn (16) and is responsible for the formation of tyrosyl radicals in the tyrosine residues of myoglobin.



PCET processes correspond to a simultaneous transfer of protons and electrons and can be denoted by  $\text{H}^{+}/e^{-}$ . Although considered a new concept for redox processes, PCET reactions have been widely investigated in biochemical processes and biological catalysis. A thermochemistry approach has been used to understand the mechanisms behind proton-couple electron transfer processes.<sup>197–199</sup>

In this context, the investigation of the kinetics and the thermodynamic of reduction of hypervalent iron species by potential reductants are of importance to comprehend the protection mechanisms of the biological system against iron-mediated oxidation.

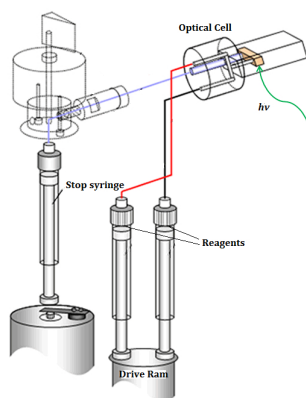
### **1.3. Kinetics investigation of the redox reactions involving myoglobin by stopped-flow spectroscopy**

Kinetics of reduction of hypervalent heme iron may follow different mechanisms although the deactivation occurs at high rates requiring the use of fast kinetic

methods. Stopped-flow spectroscopy uses UV-vis detection methods, such as absorbance and fluorescence, to investigate fast kinetic changes in solutions. These changes can be monitored on the millisecond to second time scale.

Stopped-flow technique rapidly mixes two solutions and the flow is “stopped” in an optical cell that is illuminated. Photodiode array detector measures the emitted light as function of the time to give the spectral changes occurring in the full absorption spectra. A schematic representation of a single mixing Applied Photophysics SX20 sequential stopped-flow system is shown in Figure 48.

**Figure 48.** Single mixing SX20 stopped-flow spectrometer.<sup>200</sup>



Source: <https://www.photophysics.com/lab/stopped-flow-spectroscopy-beginners-guide>

Stopped-flow spectroscopy has been widely used in biomolecular research to investigate enzyme kinetics, reaction mechanisms, protein structure elucidation, and interactions between proteins and biological species including nucleic acids, drugs, other proteins, and peptides.

## 2. Goals

Chapter II of the present PhD thesis aims to contribute to a better knowledge of the antioxidant role of uric acid and urate in biological system. The reactivity of uric acid toward the hypervalent meat pigment ferryl myoglobin under various pH and temperature conditions was investigated by fast kinetic absorption spectroscopy. Specifically, the present research aims to:

- Determine the second-order rate constants for the reduction of ferryl myoglobin by uric acid at different pH and different temperature;
- Determine the activation parameters from the second-order rate constants;
- Investigate the mechanism by which ferryl myoglobin is reduced by uric acid through a kinetic and thermodynamic approach.

## 3. Materials and Methods

### 3.1. Chemicals

Appropriate pH buffer solutions were prepared from  $K_2HPO_4/KH_2PO_4$  (J. T. Baker, Phillipsburg, NJ, USA) and from  $CH_3COONa/CH_3COOH$  (Sigma-Aldrich, Steinheim, Germany) with deionized Milli-Q water (Merck Millipore Corporation, Darmstadt, Germany). Sodium chloride (Sigma-Aldrich) was used to keep the ionic strength constant at  $0.067 \text{ mol L}^{-1}$  for all pH investigated. Ethylenediaminetetraacetic acid disodium salt (EDTA), uric acid sodium salt, catalase from bovine liver and metmyoglobin, MbFe(III), (from horse heart; purity >90%), were from Sigma-Aldrich (Steinheim, Germany). Catalase was used without purification. Myoglobin was chromatographically purified on a pD10 column (GE Healthcare Life Sciences, Chicago, USA) and eluted with Milli-Q water, using  $\epsilon_{525\text{nm}} = 7,700 \text{ M}^{-1} \text{ cm}^{-1}$  for spectrophotometric standardization of MbFe(III) solution.<sup>194</sup> Hydrogen peroxide (30% v/v) was obtained from Sigma-Aldrich (Steinheim, Germany) and used without further treatment. Ferrylmyoglobin was prepared from metmyoglobin and hydrogen peroxide as previously described using catalase to remove the excess of hydrogen peroxide.<sup>193</sup> Uric acid stock solutions were prepared in phosphate or acetate buffers and were diluted in the suitable buffer to get a final concentration of  $2 \times 10^{-3} \text{ mol L}^{-1}$ . The final pH and uric acid concentration were adjusted by dilution to the required value for the kinetic studies.

### 3.2. Kinetic experiments

Optical absorption spectra were recorded at  $25.0 \pm 0.1 \text{ }^\circ\text{C}$  on a Varian Cary 100 Bio UV-visible Spectrophotometer (Agilent Technologies, Palo Alto, CA, USA) using quartz cuvettes of 1 cm x 1 cm (Hellma Analytics, Müllheim, Germany).

The reduction of ferrylmyoglobin by uric acid was studied by stopped flow absorption spectroscopy under pseudo-first order conditions with an excess of uric acid. Kinetic studies were carried out in an Applied Photophysics SX20 sequential stopped-flow system coupled to a photodiode array detector (Applied Photophysics, Leatherhead, United Kingdom), which is located at Faculty of Life Science – University of Copenhagen (Denmark). Fresh solutions of ferrylmyoglobin and buffered uric acid were placed in two different syringes of the equipment and a regular mixing mode was used. The initial concentration was  $15 \times 10^{-6} \text{ mol L}^{-1} \text{ MbFe(IV)=O}$ , and for uric acid concentrations in the range of  $150 - 750 \times 10^{-6} \text{ mol L}^{-1}$  were used. The pH-jump technique was used as previously described in order to prevent protein denaturation during a long exposure of MbFe(IV)=O to acidic conditions.<sup>21,195</sup> Absorption spectra were recorded from 200 to 800 nm at different time intervals depending on the reaction rate. Kinetic traces were taken from single wavelength to calculate each observed rate constant by non-linear regression for each set of conditions.

In order to investigate the influence of temperature and pH on the rate constant for the reduction of ferrylmyoglobin by uric acid and urate, reactions were carried out at 25 °C, 30 °C, 35 °C and 40 °C using buffered uric acid solutions with varying pH at each temperature. All the solutions and the mixing chamber were thermostated using a circulating water bath system. For the pH range of 4.7 – 5.7, reactions were carried out in acetate buffer, while at higher pH values, phosphate buffer was preferred. Final pH of the mixture was measured at the end of the reactions at the respective temperatures.

### 3.3. Kinetic Calculations

The OriginPro 2015 (OriginLab Corporation, Northampton, MA, USA) software package was used to process the experimental datasets. Pseudo-first order rate constants  $k_{\text{obs}}$  were determined by single exponential parameter fitting. From the slope of the linear fit of  $k_{\text{obs}}$  plotted against total uric acid concentration, values for second-order rate constants were obtained for the reactions at specific pH and temperature. From the pH-dependence of the second-order rate constants,  $k'$  specific rate constants for the four possible reaction path identified were derived using non-linear regression analysis, see Results and Discussion section.

The activation parameters were determined from the specific rate constants at varying temperature through the use of the Eyring equation<sup>201,202</sup>:

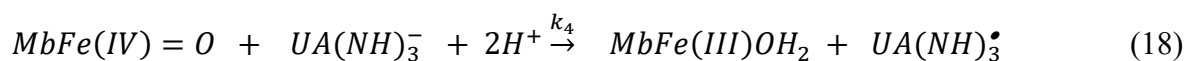
$$k' = \frac{k_B T}{h} \times e^{\frac{\Delta S^\ddagger}{R}} \times e^{\frac{-\Delta H^\ddagger}{RT}} \quad (17)$$

where  $k_B$  is the Boltzmann constant,  $h$  is Planck's constant and  $R$  is the gas constant.

Plotting  $\ln(k'/T)$  versus  $1/T$ , where  $T$  is the temperature in Kelvin and fitting to an linear equation provided  $\Delta H^\ddagger/R$  as the slope and  $\ln(k_B/h) + \Delta S^\ddagger/R$  as intercept for each of the bimolecular reaction.

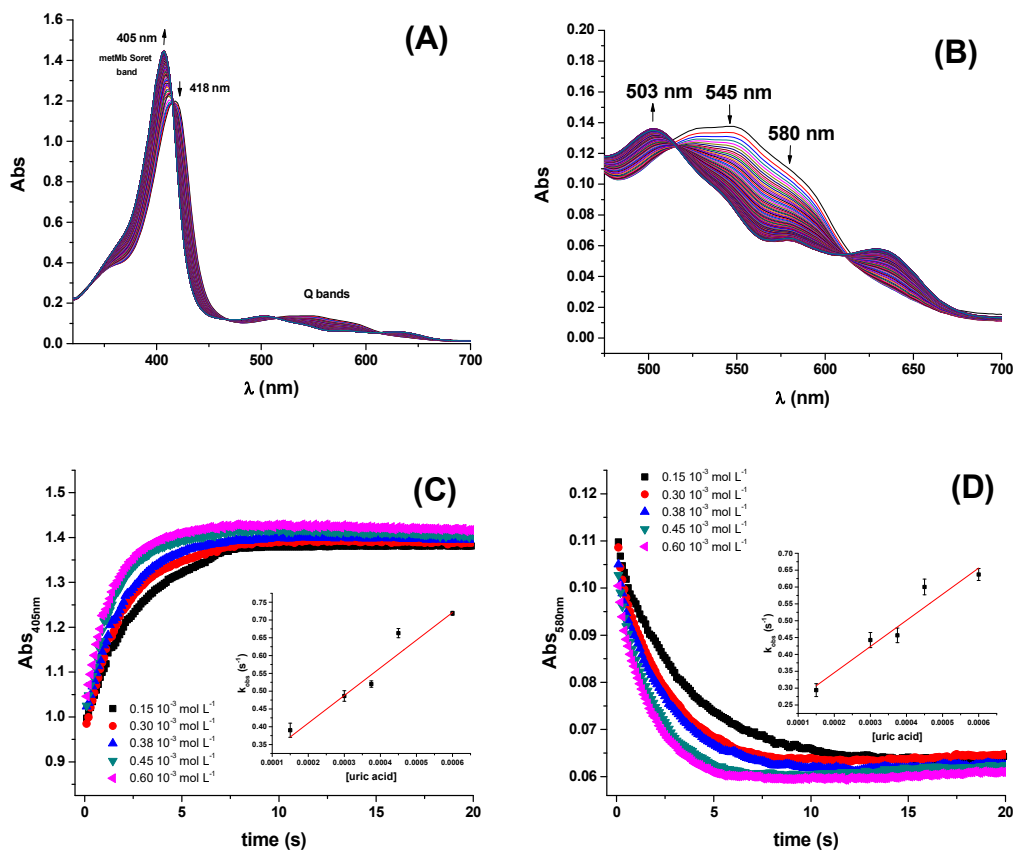
## 4. Results and discussion

Ferrylmyoglobin, MbFe(IV)=O, the hypervalent muscle pigment, was not or only extremely slowly reduced by uric acid at physiological conditions with neutral pH, where uric acid with a  $pK_a = 5.75$  is deprotonated to form the urate anion,  $UA(NH)_3^-$ , despite a negative driving force of  $\Delta G^0 = -29 \text{ kJ mol}^{-1}$  for the reaction:



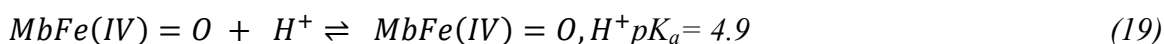
as calculated from the reduction potential  $E^0 = +0.85 \text{ V}$  for the MbFe(IV)=O/MbFe(III) couple and  $E^0 = +0.59 \text{ V}$  for the  $UA(NH)_3^\bullet/UA(NH)_3^-$  couple at pH = 7.<sup>23,170,203</sup>

**Figure 49.** Spectral changes for (A) Soret band and (B) Q bands indicating reduction of MbFe(IV)=O by uric acid. (C) Stopped-flow kinetic traces at 405 nm (Soret Band) for the reduction of ferryl myoglobin by uric acid and dependence of  $k_{\text{obs}}$  on uric acid concentration at 25 °C. Conditions:  $5 \times 10^{-3}$  mol L<sup>-1</sup> acetate buffer pH 4.7 containing  $1 \times 10^{-3}$  mol L<sup>-1</sup> of EDTA;  $[\text{MbFe(IV)=O}]_0 = 15 \times 10^{-6}$  mol L<sup>-1</sup>. Second-order rate constants found by linear regression was  $775 \pm 109$  L mol<sup>-1</sup> s<sup>-1</sup>. (D) Stopped-flow kinetic traces at 580 nm (Q band) for conditions as for (C). Second-order rate constant found by linear regression was  $791 \pm 133$  L mol<sup>-1</sup> s<sup>-1</sup>.



For more acidic conditions the reduction of MbFe(IV)=O by uric acid occurred with increasing rate for decreasing pH. For all conditions investigated the initial reduction product metmyoglobin, MbFe(III)OH<sub>2</sub>, was not reduced further to ferrous myoglobin as was concluded from the UV-visible absorption spectra (Figure 49) in agreement with a potential for the MbFe(III)/MbFe(II) couple of  $E^0 = +0.05$  V.<sup>204,205</sup>

The reactivity of ferrylmyoglobin is known to be affected by pH.<sup>21,94,194</sup> Protonation of ferrylmyoglobin (eqn (19)) and its intermediates has been shown to occur under acidic conditions to form highly reactive species that promptly oxidize relevant biologic reductants.<sup>19,21,194</sup>





nm to 430 nm). Figure 49 shows the spectral changes for the reduction of ferrylmyoglobin at  $25.0 \pm 0.1$  °C and pH 4.7 monitored both at 405 nm and 580 nm. The observed pseudo first-order rate constants  $k_{\text{obs}}$  were found to depend linearly on the total uric acid concentration in agreement with a bimolecular rate-determining step, see inserts in Figure 49C and 49D. Consistent observations of isobestic points, as may be seen in Figure 49, for all the conditions investigated, indicate that no secondary reactions are occurring. The second-order rate constants,  $k'$ , determined for the reduction of ferrylmyoglobin using UV and visible wavelengths regions gave numerical values for two different spectral regions not differing significantly ( $\rho < 0.05$ ). Then, for subsequent analysis, reactions were tracked by measuring the increase in the absorbance of metmyoglobin at 405 nm. The second-order rate constants were obtained at pH range of 4.7 to 7.5 at 25 °C (Appendix A and Figure 50) and the reduction showed pseudo-first-order kinetics behavior in this pH region of physiological relevance for excess of urate/uric acid.

The four potential reactions according to the reactions of Scheme 3 are

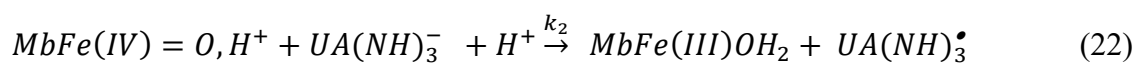
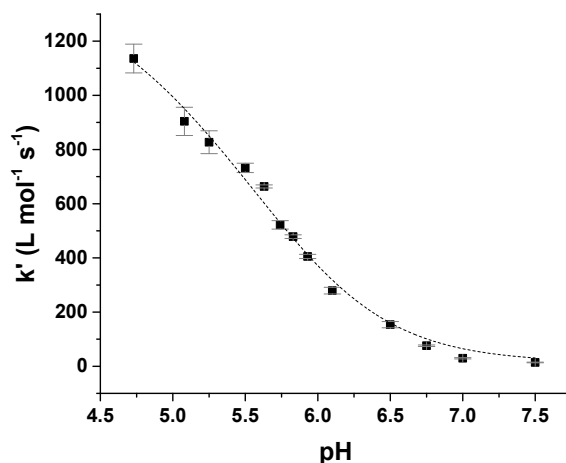


**Figure 50.** Dependence of second-order rate constant,  $k'$ , on pH for the reduction of ferrylmyoglobin by uric acid in aqueous  $0.067 \text{ mol L}^{-1}$  NaCl at  $25.0 \pm 0.1$  °C with full line calculated by non-linear regression according to eqn (26).



On the basis of the possible four reactions between the acid/base forms of the reactants, the second-order rate constant,  $k'$ , as dependent on pH was used to estimate the specific rate constants for these four reactions according to the following rate expression for conditions of excess of uric acid/urate<sup>21,202</sup>:

$$\frac{-d[\text{MbFe(IV)=O}]}{dt} = k' \times [\text{MbFe(IV)=O}] \times [\text{reductan}] + k_{\text{autoreduction}}^{\text{MbFe(IV)=O}} \quad (25)$$

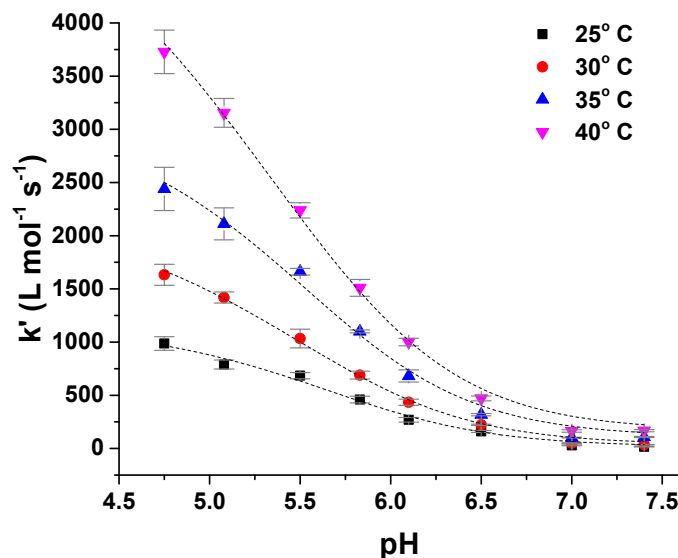
in which,

$$k' = \frac{1}{([\text{H}^+] + K_a^{\text{UA}}) \times ([\text{H}^+] + K_a^{\text{MbFe(IV)=O,H}^+})} \times [k_1 \times [\text{H}^+]^2 + (k_3 \times K_a^{\text{MbFe(IV)=O,H}^+} + k_2 \times K_a^{\text{UA}}) \times [\text{H}^+] + k_4 \times K_a^{\text{UA}} \times K_a^{\text{MbFe(IV)=O,H}^+}] \quad (26)$$

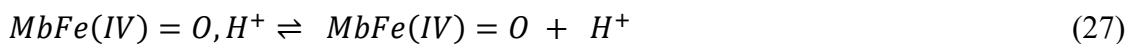
and where  $K_a^{\text{MbFe(IV)=O,H}^+}$  is the acid dissociation constant of MbFe(IV)=O,H<sup>+</sup> and  $K_a^{\text{UA}}$  is the acid dissociation constant of uric acid at 25 °C. The  $k_{\text{autoreduction}}^{\text{MbFe(IV)=O}}$  is known from previous studies and makes a negligible contribution to the overall rate in the actual pH-region.<sup>194</sup>

The rate constants for the two pathways,  $k_1$  and  $k_4$ , were accordingly estimated by nonlinear fitting of  $k'$  as function of pH at 25 °C together with the rate constant for the two reactions of eqn (22) and eqn (23) according to eqn (26). The reactions of eqn (22) and (23) with the rate constants  $k_2$  and  $k_3$ , respectively, notably have a common transition state  $\{\text{MbFe(IV)=O} \cdots \text{H}^+ \cdots \text{urate}\}^\ddagger$ , and due to proton ambiguity the experimental rate constant derived from eqn (26) can not be assigned to one of the two reactions alone based on reaction kinetics.<sup>21,194</sup> The non-linear regression also included estimation of the pK<sub>a</sub>-value for uric acid and the pK<sub>a</sub>-value for ferrylmyoglobin from the experimental data, see Figure 51 for the four temperatures. Notably, the numerical values for the two pK<sub>a</sub> values were in agreement with the literature values, see Table 11.<sup>170,171,189,190</sup> The distribution between acid/base forms of the two reactants as a function of pH in agreement with the determined pK<sub>a</sub>-values are shown in Figure 52 for 25 °C together with the net charge on ferrylmyoglobin.

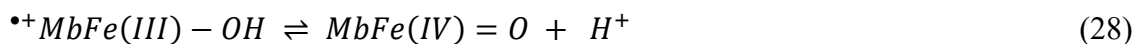
**Figure 51.** Temperature dependence of pH-profile for second-order rate constant,  $k'$ , for reduction of ferryl myoglobin by uric acid in aqueous  $0.067 \text{ mol L}^{-1}$  NaCl at varying temperature.



Based on a number of spectroscopic techniques, the  $\text{pK}_a$ -value of ferrylmyoglobin has been assigned to a value of  $\text{pK}_a \leq 2.7$ , which is significantly lower than the value obtained from analysis of reaction kinetics. The two methods for estimating the  $\text{pK}_a$ -value may be related to two different equilibrium:

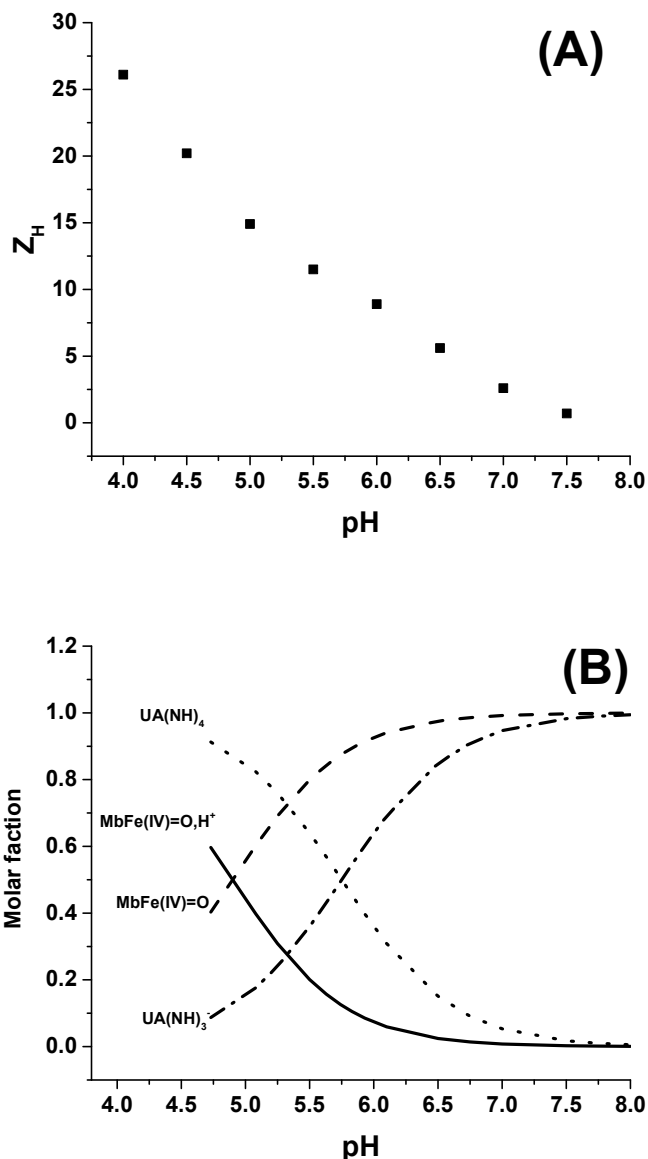


with  $\text{pK}_a^{\text{spec}} = 2.7$ , and



with  $\text{pK}_a^{\text{kin}} = 4.9$ . The difference in the  $\text{pK}_a$ -values is explained by the intramolecular equilibrium of eqn (20) for which  $K_{\text{intra}} = K_a^{\text{kin}}/K_a^{\text{spec}} = 160$  now may be calculated.

**Figure 52.** (A) Total protein charge  $Z_H$  as function of pH for horse heart myoglobin calculated with Protein Calculator v3.4 (<http://protpcalc.sourceforge.net/cgi-bin/protpcalc>), sequences taken from pdb files (P68082.2). (B) Acid/base equilibrium distribution of uric acid and ferryl myoglobin as function of pH.



The rate constant for the reduction of eqn (24) was not significantly different from zero and the reaction of eqn (24) was accordingly concluded not to make any contribution to the reduction of ferrylmyoglobin. The reaction of eqn (21) on the other hand had the value of  $1.1 \pm 0.1 \cdot 10^3 \text{ L mol}^{-1} \text{ s}^{-1}$  at  $25^\circ\text{C}$ , which makes this reaction very fast compared to the autoreduction of ferrylmyoglobin which has a hydrogen ion dependent second-order rate constant of  $7.9 \pm 1.8 \times 10^2 \text{ L mol}^{-1} \text{ s}^{-1}$  at  $25^\circ\text{C}$  for pH 7 with  $0.16 \text{ mol L}^{-1}$  of ionic strength.<sup>194</sup> As for the reaction dominating for intermediate pH, the calculated constant for the reaction on eqn (22) and the calculated rate constant for the reaction of eqn

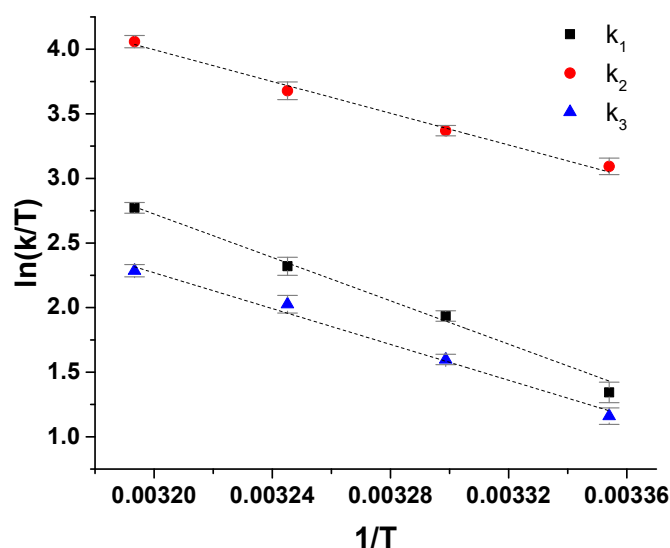
(23) can not be used to resolve the reaction into the individual reactions, since these two reactions has a common transition state.

The reduction of ferrylmyoglobin by uric acid was followed at four temperatures in the same pH-region, see Figure 51, and for these four temperatures, the values for the specific rate constant and  $pK_a$ -values presented in Table 11 were obtained by non-linear regression using eqn (26). The second-order rate constants for each of the three reactions were analyzed according to transition state theory as seen from the Eyring plot of Figure 53, not considering the reaction of eqn (24). The experimental  $pK_a$ -values showed little variation as demonstrated in the temperature-region investigated, see Table 11. The activation parameters calculated by linear regression from the three plots of Figure 53 may be found in Table 11.

**Table 11.** Second-order rate constants, activation enthalpy and activation entropy for possible reaction path of importance for the reduction of MbFe(IV)=O by uric acid/urate in aqueous 0.067 M NaCl as calculated by non-linear regression at each temperature (see Figure 51) together with  $pK_a$  values of protonated ferryl myoglobin and uric acid as estimated from the temperature dependence of the pH-reduction profile.

	$k'$ ( $L mol^{-1} s^{-1}$ )				$\Delta H^\ddagger$ (kJ $mol^{-1}$ )	$\Delta S^\ddagger$ (J $mol^{-1} K^{-1}$ )
	25° C	30° C	35° C	40° C		
$k_1$	1.14±0.09 $10^3$	2.10±0.09 $10^3$	3.13±0.22 $10^3$	5.00±0.21 $10^3$	69.9± 0.1	57.3± 0.2
$k_2$	6.57±0.42 $10^3$	8.81±0.35 $10^3$	12.20±0.08 $10^3$	18.14±0.86 $10^3$	51.1± 0.1	-0.9± 0.1
$k_3$	9.51±0.61 $10^2$	1.50±0.06 $10^3$	2.34±0.16 $10^3$	3.08±0.15 $10^3$	57.6± 0.1	5.8± 0.2
$pK_a$	4.90±0.11	4.92±0.06	4.94±0.12	4.92±0.07		
<b>MbFe(IV)=O, H<sup>+</sup></b>						
$pK_a$ UA(NH) <sub>4</sub>	5.74±0.24	5.70±0.14	5.66±0.25	5.69±0.16		

**Figure 53.** Eyring plots for reduction of ferrylmyoglobin by uric acid/urate for each possible reaction path, see Scheme 1.

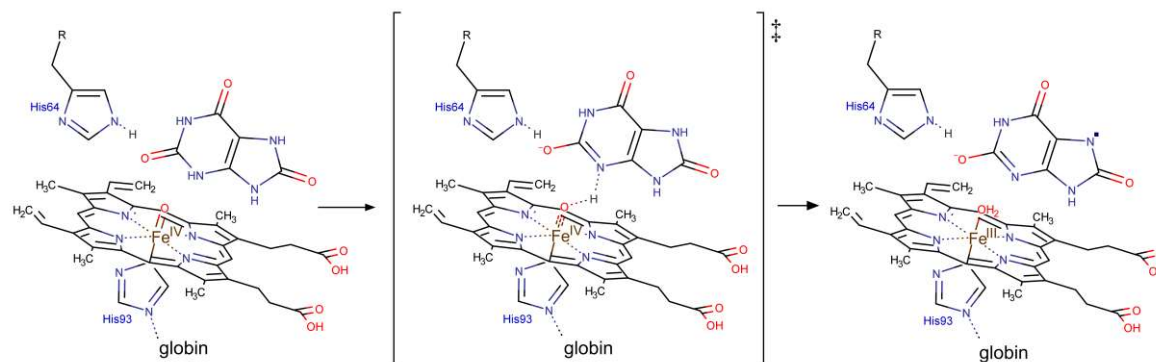


The reaction between the protonated ferrylmyoglobin and uric acid dominating at low pH has a relative large value for the enthalpy of activation, which is larger than the value obtained for reduction by ascorbate and by chlorogenate, as will be discussed below and, notably, is also larger than the value for autoreduction. The activation is largely entropy-controlled for the reduction by uric acid. Autoreduction seems to include an initial intermolecular acid/base equilibrium involving a protein radical cation, see eqn (20), leading to reduction of iron(IV)-oxo to iron(III) and to protein oxidation.

For reduction by uric acid, proton coupled electron transfer may be important for the formation of the radical cation form of ferrylmyoglobin. Proton-coupled electron transfer seems even more important for the reduction of ferrylmyoglobin at intermediate pH. An initial proton-transfer to ferrylmyoglobin by uric acid as depicted in Figure 54 will lead to a protonated ferrylmyoglobin,  $\text{MbFe(IV)=O,H}^+$ , for which electron transfer becomes facilitated. This process involves proton transfer from uric acid followed by electron transfer from urate and corresponds to the reaction of eqn (23). However, a transition state with the same composition arises from the reaction of eqn (22) for which, however, the proton is transferred from protonated ferrylmyoglobin to urate followed by electron transfer in the opposite direction. The proton-coupled electron transfer, i.e. the reaction of eqn (23) seems a more feasible reaction path and activation parameters for this reaction will be used for comparison with reduction of ferrylmyoglobin by other reactants.

The important role of a proton for electron transfer is evident, since the reaction between the non-protonated ferrylmyoglobin and urate becomes non-significant. A suggested mechanism for the proton-coupled electron transfer is shown in Figure 54.

**Figure 54.** A possible mechanism for the proton coupled electron transfer from uric acid to non-protonated ferrylmyoglobin.



Deactivation of ferrylmyoglobin is important in muscles during oxidative stress and decreasing pH as for anaerobic metabolism. Uric acid seems to be important for such conditions rather than for normal pH-conditions. The reduction of ferrylmyoglobin by ascorbate has a similar pH-profile and ascorbate is also faster as a reductant at lower pH, as may be seen from the comparison of rate constants and activation parameters in Table 12. Hydrogen sulfide ( $\text{H}_2\text{S}$ ) seems to have a special role in deactivating hypervalent muscle pigments, since cystein as another sulfur based reductant, is less efficient than hydrogen sulfide as reductant and even less efficient than oxygen-based reductants like ascorbate and chlorogenic acid.<sup>21,193,195</sup> Uric acid is a nitrogen-based reductant and apparently the nitrogen-based anion does not allow transfer of an electron without the assistance of a proton, see Scheme 4. Hydrogen atom transfer from uric acid is kinetically hampered due to a strong hydrogen bonding pattern involving the nitrogen-hydrogen bonds.<sup>208</sup> However, the hydrogen of N–H is slightly acidic corresponding to a  $\text{pK}_a = 5.75$  and may initiate reduction through a proton transfer. Urate is as reductant different from cystein, as the anion of cystein reduces ferrylmyoglobin without the assistance of a proton in contrast to urate.

**Table 12.** Rate constant and activation parameters for reduction of ferrylmyoglobin and protonated ferrylmyoglobin in aqueous solution by physiological relevant reductants at 25 °C.

	<b>k (L mol<sup>-1</sup> s<sup>-1</sup>)</b>	<b>ΔH<sup>‡</sup> (kJ mol<sup>-1</sup>)</b>	<b>ΔS<sup>‡</sup> (J mol<sup>-1</sup> K<sup>-1</sup>)</b>
<b>MbFe(IV)=O,H+</b>			
<b>reduction by</b>			
ascorbate <sup>a</sup>	1.7 10 <sup>3</sup>	62	24
chlorogenate <sup>a</sup>	2.7 10 <sup>3</sup>	59	15
uric acid	1.1 10 <sup>3</sup>	66	35
H <sub>2</sub> S <sup>b</sup>	2.5 10 <sup>6</sup>		
cysteine <sup>c</sup>	5.1		
autoreduction <sup>d</sup>	7.9 10 <sup>2</sup>	59	3
<b>MbFe(IV)=O</b>			
<b>reduction by</b>			
β-lactoglobulin <sup>c</sup>	2.4	45	-93
ascorbate <sup>a</sup>	2.9	51	-63
chlorogenate <sup>a</sup>	2.2 10 <sup>2</sup>	73	41
uric acid	9.5 10 <sup>2</sup>	59	12
urate	0		
H <sub>2</sub> S <sup>b</sup>	4.5 10 <sup>5</sup>		
cysteine thiolate <sup>c</sup>	3.1 10 <sup>-1</sup>		
crocin <sup>f</sup>	1.8 10 <sup>2</sup>	55	-17
autoreduction <sup>d</sup>	1.6 10 <sup>-4</sup>		
<sup>a</sup> from Carlsen et al, 2000 <sup>193</sup> , determined in aqueous solution with ionic strength 0.16 mol L <sup>-1</sup> <sup>b</sup> from Libardi et al, 2013 <sup>21</sup> , apparent values as determined at pH 6.8 <sup>c</sup> from Libardi et al, 2014 <sup>195</sup> , apparent values as determined at pH 6.8 <sup>d</sup> from Mikkelsen et al, 1995 <sup>194</sup> <sup>e</sup> from Østdal et al, 1996 <sup>97</sup> ; apparent values as determined at pH 7.0 <sup>f</sup> from Jørgensen et al, 1997 <sup>196</sup> ; apparent values as determined at pH 7.0.			

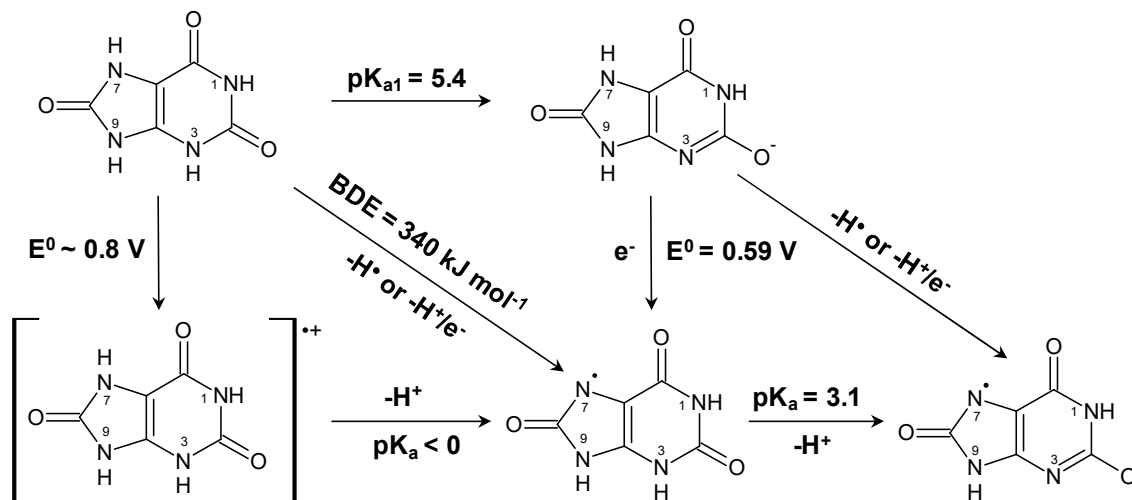
Reduction of ferrylmyoglobin by various physiological relevant reductants has a moderately high enthalpy of activation as may be seen from Table 12, where oxygen and sulfur based reductants are compared with uric acid/urate as a nitrogen-based

reductant. In general, protonization of MbFe(IV)=O to yield MbFe(IV)=O,H<sup>+</sup> accelerates the reduction due to entropy effects as are typically for outer-sphere electron transfer, which has a positive value for entropy of activation. Such outer-sphere electron transfer may occur for a protein radical cation, see eqn (20). For the non-protonated MbFe(IV)=O, entropy of activation is negative or close to zero, in effect counteracting the moderate enthalpy of activation suggesting an inner-sphere electron transfer mechanism. This compensation effect is especially evident for the sulfur-based reductants hydrogen sulfide, cysteine and  $\beta$ -lactoglobulin.<sup>97</sup> For the oxygen-based reductant ascorbate, a similar effect is rather seen, when reduction of the protonated MbFe(IV)=O,H<sup>+</sup> is compared with the non-protonated MbFe(IV)=O.<sup>193</sup> The more negative entropy of activation for the reduction of the non-protonated MbFe(IV)=O by the sulfur-based reductant or by ascorbate may reflect the high organization required in the transition state with a proton partly transferred prior to electron transfer to the iron center of ferrylmyoglobin. For the water-soluble carotenoid crocin, a negative entropy of activation is likewise counteracting the moderate enthalpy of activation and probably relates to direct electron transfer from the conjugated double bond.<sup>196</sup> A similar effect seems evident when reduction of MbFe(IV)=O,H<sup>+</sup> and MbFe(IV)=O by uric acid is compared. For the reduction of non-protonated MbFe(IV)=O by uric acid, the initial proton transfer entails high organization lowering the entropy of activation from 35 J mol<sup>-1</sup> K<sup>-1</sup> to 12 J mol<sup>-1</sup> K<sup>-1</sup> when compared to MbFe(IV)=O,H<sup>+</sup>. For urate as a possible reductant of non-protonated MbFe(IV)=O, a further increase in activation entropy makes this reaction of no importance kinetically when compared to ferrylmyoglobin autoreduction.

Uric acid is accordingly considered to be the active reductant for reaction at acidic conditions and for intermediate pH. For intermediate pH, proton coupled electron transfer is equivalent to donation of a hydrogen atom, as shown in Scheme 4, to MbFe(IV)=O, where the oxidized uric acid is seen subsequently to lose an additional proton from the uric acid neutral radical. The urate ion is concluded not to be a reductant for ferrylmyoglobin.

Sulfur is concluded to be a better electron donor for reduction of ferrylmyoglobin compared to oxygen as evident from lower enthalpies of activation. Uric acid/urate as an N-H purine base reductant is less efficient and comparable to the carotenoid crocin as reductant. For uric acid/urate initial proton transfer from N-H bond becomes of even more importance.

**Scheme 4.** Aqueous thermochemistry of uric acid used to identify the actual reactant for reduction of ferrylmyoglobin.



## 5. Conclusion

The prooxidative activity of hypervalent heme iron as formed during digestion of red meat and meat products is getting increasing attention as one possible explanation of the negative health effect of a high red meat intake.<sup>38,179,180</sup> A balanced diet with plant based antioxidants like polyphenols and carotenoids have been found to protect against radical formation as the primary oxidation step through efficient reduction of perferrylmyoglobin and ferrylmyoglobin under the acidic conditions of the stomach. Endogenous factors in the form of metabolites like carbon monoxide, hydrogen sulfide and nitric oxide may, however, also be important for the protection against toxic effects of hypervalent iron. Uric acid may now be added to the list of small molecules with protective effect against radical formation during digestion of meat and, in muscles, during oxidative stress. The level of uric acid depends on dietary factors. However, an important observation seems to be that urate despite its strong reducing capacity, only becomes active against hypervalent heme iron through proton coupled electron transfer as for the decreasing pH of muscles during anaerobic conditions or under the acidic conditions of the stomach.

## REFERENCES

1. Carlsen CU, Andersen ML, Skibsted LH. Oxidative stability of processed pork. Assay based on ESR-detection of radicals. *Eur Food Res Technol*. 2001 Sep;213(3):170–3.
2. Carlsen CU, Møller JKS, Skibsted LH. Heme-iron in lipid oxidation. *Coord Chem Rev*. 2005 Feb;249(3–4):485–98.
3. Lund MN, Heinonen M, Baron CP, Estévez M. Protein oxidation in muscle foods: A review. *Mol Nutr Food Res*. 2011 Jan;55(1):83–95.
4. Morzel M, Gatellier P, Sayd T, Renerre M, Laville E. Chemical oxidation decreases proteolytic susceptibility of skeletal muscle myofibrillar proteins. *Meat Sci*. 2006 Jul;73(3):536–43.
5. Smet K, Raes K, Huyghebaert G, Haak L, Arnouts S, De Smet S. Lipid and Protein Oxidation of Broiler Meat as Influenced by Dietary Natural Antioxidant Supplementation [Internet]. Vol. 87, *Poultry Science*. 2008. p. 1682–8. Available from:  
<http://www.ncbi.nlm.nih.gov/pubmed/18648067>  
<http://ps.oxfordjournals.org/cgi/doi/10.3382/ps.2007-00384>
6. Arihara K. Strategies for designing novel functional meat products. *Meat Sci*. 2006 Sep;74(1):219–29.
7. FAO - Food and Agriculture Organization of the United Nations. World agriculture towards 2030/2050: the 2012 revision [Internet]. 2013. Available from:  
<<http://www.fao.org>>
8. FAO - Food and Agriculture Organization of the United Nations. *Perspectivas Agrícolas 2015-2024* [Internet]. 2015. Available from:  
<<https://www.fao.org.br/download/PA20142015CB.pdf>>
9. MINISTÉRIO DA AGRICULTURA PECUÁRIA E ABASTECIMENTO. *Animal. Espécies. Aves*. [Internet]. Vol. 2012. Available from:  
<<http://www.agricultura.gov.br/animal/especies/aves>>
10. Racanicci AMC, Menten JFM, Alencar SM, Buissa RS, Skibsted LH. Mate (*Ilex paraguariensis*) as dietary additive for broilers: performance and oxidative stability of meat. *Eur Food Res Technol*. 2011 Jan;232(4):655–61.
11. MEJIA EG DE, SONG YS, Ramirez-Mares MV, Hideka K. Effect of Yerba Mate (*Ilex paraguariensis*) Tea on Topoisomerase Inhibition and Oral Carcinoma Cell

- Proliferation. *J Agric Food Chem.* 2005;53:1966–73.
12. Millis JR, Schendel MJ. Inhibition of food pathogens by hop acids. US5286506 A, 1994.
  13. Maye JP. Hop acids as a replacement for antibiotics in animal feed. US7090873 B2, 2006.
  14. Oostindjer M, Alexander J, Amdam G V., Andersen G, Bryan NS, Chen D, et al. The role of red and processed meat in colorectal cancer development: a perspective. *Meat Sci.* 2014 Aug;97(4):583–96.
  15. Baron CP, Andersen HJ. Myoglobin-induced lipid oxidation. A review. *J Agric Food Chem.* 2002;50(14):3887–97.
  16. Frederiksen AM, Lund MN, Andersen ML, Skibsted LH. Oxidation of Porcine Myosin by Hypervalent Myoglobin: The Role of Thiol Groups. *J Agric Food Chem.* 2008 May;56(9):3297–304.
  17. Suman SP, Joseph P. Myoglobin chemistry and meat color. *Annu Rev Food Sci Technol [Internet].* 2013;4:79–99. Available from: <http://www.ncbi.nlm.nih.gov/pubmed/23190143>
  18. Baron CP, Andersen HJ. Myoglobin-induced lipid oxidation. A review. *J Agric Food Chem [Internet].* 2002 Jul 3;50(14):3887–97. Available from: <http://www.ncbi.nlm.nih.gov/pubmed/21071714>
  19. Reeder BJ, Wilson MT. The effects of pH on the mechanism of hydrogen peroxide and lipid hydroperoxide consumption by myoglobin: A role for the protonated ferryl species. *Free Radic Biol Med.* 2001;30(11):1311–8.
  20. Reeder BJ, Wilson MT. Hemoglobin and myoglobin associated oxidative stress: from molecular mechanisms to disease States. *Curr Med Chem [Internet].* 2005;12(23):2741–51. Available from: <http://www.ncbi.nlm.nih.gov/pubmed/16305469>
  21. Libardi SH, Pindstrup H, Cardoso DR, Skibsted LH. Reduction of ferrylmyoglobin by hydrogen sulfide. Kinetics in relation to meat greening. *J Agric Food Chem.* 2013;61(11):2883–8.
  22. Lund MN, Luxford C, Skibsted LH, Davies MJ. Oxidation of myosin by haem proteins generates myosin radicals and protein cross-links. *Biochem J.* 2008;410(3):565–74.
  23. Carlsen C, Moller J, Skibsted L. Heme-iron in lipid oxidation. *Coord Chem Rev [Internet].* 2005 Feb [cited 2011 Apr 18];249(3–4):485–98. Available from:

- <http://linkinghub.elsevier.com/retrieve/pii/S0010854504002218>
24. Kumar Y, Yadav DN, Ahmad T, Narsaiah K. Recent Trends in the Use of Natural Antioxidants for Meat and Meat Products. *Compr Rev Food Sci Food Saf*. 2015 Nov;14(6):796–812.
  25. Racanicci AMC, Danielsen B, Skibsted LH. Mate (*Ilex paraguariensis*) as a source of water extractable antioxidant for use in chicken meat. *Eur Food Res Technol*. 2007 Jul;227(1):255–60.
  26. Zhan XA, Li JX, Xu ZR, Zhao RQ. Effects of methionine and betaine supplementation on growth performance, carcass composition and metabolism of lipids in male broilers. *Br Poult Sci*. 2006 Oct;47(5):576–80.
  27. Rabie MH, Szilágyi M. Effects of L-carnitine supplementation of diets differing in energy levels on performance, abdominal fat content, and yield and composition of edible meat of broilers. *Br J Nutr*. 1998 Oct;80(4):391–400.
  28. Bortoluzzi C, Menten JFM, Romano GG, Pereira R, Napty GS. Effect of hops  $\beta$ -acids (*Humulus lupulus*) on performance and intestinal health of broiler chickens. 2014;
  29. Butler G. Manipulating dietary PUFA in animal feed: implications for human health. *Proc Nutr Soc*. 2014 Feb;73(1):87–95.
  30. Patra AK, Saxena J. Exploitation of dietary tannins to improve rumen metabolism and ruminant nutrition. *J Sci Food Agric*. 2011 Jan;91(1):24–37.
  31. Heck CI, de Mejia EG. Yerba Mate Tea (*Ilex paraguariensis*): A Comprehensive Review on Chemistry, Health Implications, and Technological Considerations. *J Food Sci*. 2007 Nov;72(9):R138–51.
  32. Ceriello A, Motz E. Is Oxidative Stress the Pathogenic Mechanism Underlying Insulin Resistance, Diabetes, and Cardiovascular Disease? The Common Soil Hypothesis Revisited. *Arterioscler Thromb Vasc Biol*. 2004;24(5):816–23.
  33. Madamanchi NR, Vendrov A, Runge MS. Oxidative stress and vascular disease. *Arterioscler Thromb Vasc Biol*. 2005;25(1):29–38.
  34. Aruoma OI. Free Radicals, Oxidative Stress, and Antioxidants in Human Health and Disease. *Jaocs [Internet]*. 1998;75(2):199–212. Available from: <http://link.springer.com/10.1007/s11746-998-0032-9>
  35. Christen Y. Oxidative stress and Alzheimer disease. *Am J Clin Nutr*. 2000;71(2):621s–629s.
  36. Valko M, Rhodes CJ, Moncol J, Izakovic M, Mazur M. Free radicals, metals and

- antioxidants in oxidative stress-induced cancer. *Chem Biol Interact.* 2006;160(1):1–40.
37. Larsson SC, Rafter J, Holmberg L, Bergkvist L, Wolk A. Red meat consumption and risk of cancers of the proximal colon, distal colon and rectum: The Swedish Mammography Cohort. *Int J Cancer.* 2005;113(5):829–34.
  38. Corpet DE. Red meat and colon cancer: Should we become vegetarians, or can we make meat safer? *Meat Sci.* 2011;89(3):310–6.
  39. Sesink A, Termont DS, Kleibeuker JH, Van Der Meer R. Red meat and colon cancer: dietary haem, but not fat, has cytotoxic and hyperproliferative effects on rat colonic epithelium. *Carcinogenesis* [Internet]. 2000;21(10):1909–15. Available from: <http://carcin.oxfordjournals.org/content/21/10/1909.short>
  40. Paredi G, Raboni S, Bendixen E, de Almeida AM, Mozzarelli A. “Muscle to meat” molecular events and technological transformations: The proteomics insight. *J Proteomics.* 2012 Jul;75(14):4275–89.
  41. Pearson AM. Muscle and meat biochemistry [Internet]. Elsevier; 2012. Available from: [https://books.google.com.br/books?hl=en&lr=&id=ltqvLpKHRWIC&oi=fnd&pg=PP1&dq=proteins+in+meat+sarcoplasmic+myofibrillar+conjunctive+tissue&ots=Sm0pvCrkMj&sig=NtoEfdVfluWs62QCURIZ-2Mr15w#v=onepage&q=proteins in meat sarcoplasmic myofibrillar conjunctive ti](https://books.google.com.br/books?hl=en&lr=&id=ltqvLpKHRWIC&oi=fnd&pg=PP1&dq=proteins+in+meat+sarcoplasmic+myofibrillar+conjunctive+tissue&ots=Sm0pvCrkMj&sig=NtoEfdVfluWs62QCURIZ-2Mr15w#v=onepage&q=proteins+in+meat+sarcoplasmic+myofibrillar+conjunctive+ti)
  42. Kaneko JJ. on the Intramuscular Fatty Pigs and Acid Lipids Birds Composition of Cattle , of Iwao 1 Department of Biochemistry , School of Veterinary Medicine , 2 Dppartment of Clinical Pathology , School of Veterinary Medicine , Currently , concerted efforts are bei. 1991;545–54.
  43. Ruxton CHS, Reed SC, Simpson MJA, Millington KJ. The health benefits of omega-3 polyunsaturated fatty acids: A review of the evidence. *J Hum Nutr Diet.* 2004;17(5):449–59.
  44. Scollan N, Hocquette JF, Nuernberg K, Dannenberger D, Richardson I, Moloney A. Innovations in beef production systems that enhance the nutritional and health value of beef lipids and their relationship with meat quality. *Meat Sci.* 2006;74(1):17–33.
  45. Wood JD, Enser M, Fisher A V., Nute GR, Sheard PR, Richardson RI, et al. Fat deposition, fatty acid composition and meat quality: A review. *Meat Sci.* 2008;78(4):343–58.
  46. Hocquette JF, Botreau R, Picard B, Jacquet A, Pethick DW, Scollan ND.

- Opportunities for predicting and manipulating beef quality. *Meat Sci* [Internet]. 2012;92(3):197–209. Available from:  
<http://dx.doi.org/10.1016/j.meatsci.2012.04.007>
47. Zhang W, Xiao S, Samaraweera H, Lee EJ, Ahn DU. Improving functional value of meat products. *Meat Sci*. 2010;86(1):15–31.
  48. Prema D, Turner TD, Jensen J, Pilfold JL, Church JS, Donkor KK, et al. Rapid determination of total conjugated linoleic acid concentrations in beef by <sup>1</sup>H NMR spectroscopy. *J Food Compos Anal*. 2015 Aug;41:54–7.
  49. Vasta V, Makkar HPS, Mele M, Priolo A. Ruminant biohydrogenation as affected by tannins in vitro. *Br J Nutr*. 2009;102:82–92.
  50. Descalzo AM, Sancho AM. A review of natural antioxidants and their effects on oxidative status, odor and quality of fresh beef produced in Argentina. *Meat Sci*. 2008;79(3):423–36.
  51. Koutsidis G, Elmore JS, Oruna-Concha MJ, Campo MM, Wood JD, Mottram D. Water soluble precursor of beef flavor: I. Effect of diet and breed. *Meat Sci*. 2008;79:124–30.
  52. Tikk M, Tikk K, Tørngren MA, Meinert L, Aaslyng MD, Karlsson AH, et al. Development of Inosine Monophosphate and Its Degradation Products during Aging of Pork of Different Qualities in Relation to Basic Taste and Retronasal Flavor Perception of the Meat. *J Agric Food Chem*. 2006 Oct;54(20):7769–77.
  53. Feidt C, Petit A, Bruas-Reignier F, Brun-Bellut J. Release of free amino-acids during ageing in bovine meat. *Meat Sci*. 1996 Sep;44(1–2):19–25.
  54. Straadt IK, Aaslyng MD, Bertram HC. An NMR-based metabolomics study of pork from different crossbreeds and relation to sensory perception. *Meat Sci*. 2014 Feb;96(2, Part A):719–28.
  55. Chow IS, Jacobson M. Inosine Monophosphate Inosine and Hypoxanthine in Meat from Broilers 5 7 and 9 Weeks of Age. *Poult Sci* [Internet]. 1968;47(2):604-. Available from: <Go to ISI>://WOS:A1968B472400041
  56. Fuke S, Konosu S. Taste-active components in some foods: A review of Japanese research. *Physiol Behav*. 1991 May;49(5):863–8.
  57. Terasaki M, Kajikawa M, Fujita E, Ishii K. Studies on the Flavor of Meats. *Agric Biol Chem*. 1965 Mar;29(3):208–15.
  58. Tikk M, Tikk K, Tørngren MA, Meinert L, Aaslyng MD, Karlsson AH, et al. Development of inosine monophosphate and its degradation products during aging

- of pork of different qualities in relation to basic taste and retronasal flavor perception of the meat. *J Agric Food Chem.* 2006;54(20):7769–77.
59. Benjakul S, Lertittikul W, Bauer F. Antioxidant activity of Maillard reaction products from a porcine plasma protein-sugar model system. *Food Chem.* 2005;93(2):189–96.
  60. Bedinghaus AJ, Ockerman HW. Antioxidative Maillard Reaction Products from Reducing Sugars and Free Amino Acids in Cooked Ground Pork Patties. *J Food Sci* [Internet]. 1995;60(5):992–5. Available from: <http://www3.interscience.wiley.com/journal/119237723/abstract>
  61. Graham SF, Kennedy T, Chevallier O, Gordon A, Farmer L, Elliott C, et al. The application of NMR to study changes in polar metabolite concentrations in beef longissimus dorsi stored for different periods post mortem. *Metabolomics.* 2010 Mar;6(3):395–404.
  62. Wu G. Amino acids: Metabolism, functions, and nutrition. *Amino Acids.* 2009;37(1):1–17.
  63. Lantto R, Puolanne E, Kruus K, Buchert J, Autio K. Tyrosinase-aided protein cross-linking: Effects on gel formation of chicken breast myofibrils and texture and water-holding of chicken breast meat homogenate gels. *J Agric Food Chem.* 2007;55(4):1248–55.
  64. Elias RJ, McClements DJ, Decker EA. Antioxidant activity of cysteine, tryptophan, and methionine residues in continuous phase  $\beta$ -lactoglobulin in oil-in-water emulsions. *J Agric Food Chem.* 2005;53(26):10248–53.
  65. Lafarga T, Hayes M. Bioactive peptides from meat muscle and by-products: Generation, functionality and application as functional ingredients. *Meat Sci.* 2014;98(2):227–39.
  66. Hartmann R, Meisel H. Food-derived peptides with biological activity: from research to food applications. *Curr Opin Biotechnol.* 2007;18(2):163–9.
  67. Erdmann K, Cheung BWY, Schröder H. The possible roles of food-derived bioactive peptides in reducing the risk of cardiovascular disease. *J Nutr Biochem.* 2008;19(10):643–54.
  68. Ryan JT, Ross RP, Bolton D, Fitzgerald GF, Stanton C. Bioactive peptides from muscle sources: Meat and fish. *Nutrients.* 2011;3(9):765–91.
  69. Wu H-C, Shiao C-Y, Chen H-M, Chiou T-K. Antioxidant activities of carnosine, anserine, some free amino acids and their combination. *J Food Drug Anal.*

- 2003;11(2):148–53.
70. Williams P. Nutritional composition of red meat. *Nutr Diet*. 2007;64(SUPPL. 4):5–7.
  71. Arihara K. Strategies for designing novel functional meat products. *Meat Sci*. 2006;74(1):219–29.
  72. Lombardi-Boccia G, Lanzi S, Aguzzi A. Aspects of meat quality: Trace elements and B vitamins in raw and cooked meats. *J Food Compos Anal*. 2005;18(1):39–46.
  73. Leonhardt M, Wenk C. Variability of Selected Vitamins and Trace Elements of Different Meat Cuts. *J Food Compos Anal* [Internet]. 1997;10(3):218–24. Available from: <http://linkinghub.elsevier.com/retrieve/pii/S0889157597905366>
  74. Allen LH. Causes of vitamin B 12 and folate deficiency. 2008;29(2):20–34.
  75. Fenech M. The role of folic acid and Vitamin B12 in genomic stability of human cells. *Mutat Res Mol Mech Mutagen*. 2001;475(1):57–67.
  76. Kernich C a. Vitamin B12 Deficiency and the Nervous System. *Neurologist*. 2006;12(3):169–70.
  77. Cardoso DR, Libardi SH, Skibsted LH. Riboflavin as a photosensitizer. Effects on human health and food quality. *Food Funct*. 2012;3(5):487.
  78. Grippa JM, De Zawadzki A, Grossi AB, Skibsted LH, Cardoso DR. Riboflavin photosensitized oxidation of myoglobin. *J Agric Food Chem*. 2014;62(5):1153–8.
  79. Luciano G, Moloney AP, Priolo A, Röhrle FT, Vasta V, Biondi L, et al. Vitamin E and polyunsaturated fatty acids in bovine muscle and the oxidative stability of beef from cattle receiving grass or concentrate-based rations. *J Anim Sci*. 2011;89(11):3759–68.
  80. Descalzo AM, Insani EM, Biolatto A, Sancho AM, García PT, Pensel NA, et al. Influence of pasture or grain-based diets supplemented with vitamin E on antioxidant/oxidative balance of Argentine beef. *Meat Sci*. 2005;70(1):35–44.
  81. Buckley DJ, Morrissey PA, Gray JI. Influence of Dietary Vitamin-E on the Oxidative Stability and Quality of Pig Meat. *J Anim Sci* [Internet]. 1995;73(10):3122–30. Available from: <Go to ISI>://A1995TA50500034
  82. JUDGE M, ABERLE E, FORREST H. Principles of meat science. Iowa: Kendall Hunt; 1989. 351 p.
  83. FARIA PB. Desempenho e qualidade de carcaça e carne de frangos criados em sistema alternativo. Universidade Federal de Lavras; 2007.
  84. ZARKADAS CG, MARSHALL WD, KHALILI AD, NGUYEN Q, ZARKADAS

- GC, KARATZAS CN, et al. Mineral Composition of Selected Bovine, Porcine and Avian Muscles, and Meat Products. *J Food Sci.* 1987;52(3):520–5.
85. Stadtman ER. Protein oxidation and aging. *Free Radic Res* [Internet]. 2006;40(12):1250–8. Available from:  
<http://www.tandfonline.com/doi/full/10.1080/10715760600918142>
  86. Wood JD, Enser M. Factors influencing fatty acids in meat and the role of antioxidants in improving meat quality. *Br J Nutr.* 1997;78 Suppl 1(1997):S49–60.
  87. Wood JD, Enser M, Fisher A V, Nute GR, Richardson RI, Sheard PR. Animal Nutrition and Metabolism Group Symposium on “Improving meat production for future needs” Manipulating meat quality and composition. *Proc Nutr Soc.* 1999;58(July 1998):363–70.
  88. Picard B, Gagaoua M, Micol D, Cassar-malek I, Terlouw CEM. According to Contractile and Metabolic Properties of the Muscle. 2014;
  89. Ouali A, Gagaoua M, Boudida Y, Becila S, Boudjellal A, Herrera-Mendez CH, et al. Biomarkers of meat tenderness: Present knowledge and perspectives in regards to our current understanding of the mechanisms involved. *Meat Sci* [Internet]. 2013;95(4):854–70. Available from:  
<http://dx.doi.org/10.1016/j.meatsci.2013.05.010>
  90. Polak T, Gašperlin L, Žlender B. Various instrumental and biochemical parameters as ageing indicators of beef Longissimus dorsi muscle and their relation to creatine and creatinine content. *Eur Food Res Technol* [Internet]. 2007;225(5–6):849–55. Available from: <http://link.springer.com/10.1007/s00217-006-0491-x>
  91. Koohmaraie M, Kent MP, Shackelford SD, Veiseth E, Wheeler TL. Meat tenderness and muscle growth: is there any relationship? *Meat Sci.* 2002 Nov;62(3):345–52.
  92. Brown, W.D. and Mebine LB. Autoxidation of oxymyoglobins. *J Biol Chem.* 1969;244(24):6696–701.
  93. Kröger-Ohlsen M V., Carlsen CU, Andersen ML, Skibsted LH. Pseudoperoxidase Activity of Myoglobin: Pigment Catalyzed Formation of Radicals in Meat Systems. In.
  94. Silaghi-Dumitrescu R, Reeder BJ, Nicholls P, Cooper CE, Wilson MT. Ferryl haem protonation gates peroxidatic reactivity in globins. *Biochem J* [Internet]. 2007;403(3):391–5. Available from:  
[http://www.ncbi.nlm.nih.gov/entrez/query.fcgi?cmd=Retrieve&db=PubMed&dopt=Citation&list\\_uids=17214588](http://www.ncbi.nlm.nih.gov/entrez/query.fcgi?cmd=Retrieve&db=PubMed&dopt=Citation&list_uids=17214588)

95. Schieber M, Chandel NS. ROS function in redox signaling and oxidative stress. *Curr Biol* [Internet]. 2014;24(10):R453–62. Available from: <http://dx.doi.org/10.1016/j.cub.2014.03.034>
96. Elstner EF. Oxygen activation and oxygen toxicity. 1982;73–96.
97. Ostdal H, Daneshvar B, Skibsted LH. Reduction of ferrylmyoglobin by beta-lactoglobulin. *Free Radic Res* [Internet]. 1996;24(6):429–38. Available from: [http://www.ncbi.nlm.nih.gov/entrez/query.fcgi?cmd=Retrieve&db=PubMed&dopt=Citation&list\\_uids=8804986](http://www.ncbi.nlm.nih.gov/entrez/query.fcgi?cmd=Retrieve&db=PubMed&dopt=Citation&list_uids=8804986)
98. Rubbo H, Radi R, Trujillo M, Telleri R, Kalyanaraman B, Barnes S, et al. Nitric oxide regulation of superoxide and peroxynitrite-dependent lipid peroxidation. Formation of novel nitrogen-containing oxidized lipid derivatives. *J Biol Chem* [Internet]. 1994 Oct 21;269(42):26066–75. Available from: <http://www.ncbi.nlm.nih.gov/pubmed/7929318>
99. Hogg N, Kalyanaraman B. Nitric oxide and lipid peroxidation. *Biochim Biophys Acta* [Internet]. 1999 May 5;1411(2–3):378–84. Available from: <http://www.ncbi.nlm.nih.gov/pubmed/10320670>
100. Pan M-H, Lai C-. S, Ho C-. T. Anti-inflammatory activity of natural dietary flavonoids. *Food Funct*. 2010;1:15–31.
101. Goupy P, Vulcain E, Caris-Veyrat C, Dangles O. Dietary antioxidants as inhibitors of the heme-induced peroxidation of linoleic acid: Mechanism of action and synergism. *Free Radic Biol Med*. 2007;43(6):933–46.
102. Carrillo JA, He Y, Li Y, Liu J, Erdman RA, Sonstegard TS, et al. Integrated metabolomic and transcriptome analyses reveal finishing forage affects metabolic pathways related to beef quality and animal welfare. *Nature* [Internet]. 2016;6(April):25948. Available from: <http://www.nature.com/articles/srep25948>
103. Neto MG, Pesti GM, Bakalli RI. Influence of Dietary Protein Level on the Broiler Chicken ' s Response to Methionine and Betaine Supplements 1. *Poult Sci*. 2000;79:1478–84.
104. Bremer J. Carnitine in intermediary metabolism: The metabolism of fatty acid esters of carnitine by mitochondria. *J Biol Chem* 237(12), pp3628-3632. 1962;237(12):3628–32.
105. Jongberg S, Torngren MA, Gunvig A, Skibsted LH, Lund MN. Effect of green tea or rosemary extract on protein oxidation in Bologna type sausages prepared from oxidatively stressed pork. *Meat Sci*. 2013;93(3):538–46.

106. Manzoor Ahmad S, Sowriappan John DB, Shabir Ahmad M. Plant extracts as natural antioxidants in meat and meat products [Internet]. Vol. 98, Meat Science. 2014. p. 21–33. Available from: <http://dx.doi.org/10.1016/j.meatsci.2014.03.020>
107. Almeida NEC de, Nascimento ESP do, Cardoso DR. On the Reaction of Lupulones with Hydroxyethyl Radical.pdf. *J Agric Food Chem*. 2012;60(42):10649–56.
108. Sbardella M, Perina DP, Andrade C, Santos CB, Cairo PLG, Marques ELS, et al. Effects of dietary hop -acids or colistin on the performance, nutrient digestibility, and intestinal health of weanling pigs. *Anim Feed Sci Technol*. 2016;217:67–75.
109. Bastos DHM, Oliveira DM, Matsumoto RLT, Carvalho PO, Ribeiro ML. Yerba maté: Pharmacological Properties, Research and Biotechnology. *Med Aromat Plant Sci Biotechnol* [Internet]. 2007;1(1):37–46. Available from: [http://globalsciencebooks.info/JournalsSup/images/0706/MAPSB\\_1\(1\)37-46o.pdf](http://globalsciencebooks.info/JournalsSup/images/0706/MAPSB_1(1)37-46o.pdf)
110. Anti-obesity and anti\_diabetic effects of Yerba Mate in mice.pdf.
111. Fiehn O. Metabolomics - the link between genotypes and phenotypes. *Plant Mol Biol*. 2002;48:155–71.
112. Nicholson JK, Connelly J, Lindon JC, Holmes E. Metabonomics: a platform for studying drug toxicity and gene function. *Nat Rev Drug Discov*. 2002;1(2):153–61.
113. Zhang A, Sun H, Wang X. Serum metabolomics as a novel diagnostic approach for disease: a systematic review. *Anal Bioanal Chem*. 2012;404(4):1239–45.
114. Smolinska A, Blanchet L, Buydens LMC, Wijmenga SS. NMR and pattern recognition methods in metabolomics: From data acquisition to biomarker discovery: A review. *Anal Chim Acta* [Internet]. 2012;750:82–97. Available from: [Go to ISI://WOS:000310409900007](http://www.isinet.com/Go%20to%20ISI/WOS:000310409900007)
115. Roberts LD, Souza AL, Gerszten RE, Clish CB. Targeted Metabolomics. *Curr Protoc Mol Biol*. 2012;(Chapter 30:Unit 30):1–24.
116. Gibney MJ, Walsh M, Brennan L, Roche HM, German B, Ommen B van. Metabolomics in human nutrition:opportunities and challenges. *J Clin Nutr*. 2005;82:497–503.
117. Cevallos-cevallos JM, Etxeberria E, Danyluk MD, Rodrick GE. Metabolomic analysis in food science : a review [Internet]. Vol. 20, Trends in Food Science & Technology. 2009. p. 557–66. Available from: <http://dx.doi.org/10.1016/j.tifs.2009.07.002>
118. Capozzi F, Bordoni A. Foodomics: A new comprehensive approach to food and nutrition. *Genes Nutr*. 2013;8(1):1–4.

119. Gerszten RE, Wang TJ. The search for new cardiovascular biomarkers. *Nature*. 2008;451:949–52.
120. Mar GN La, Horrocks WD, Holm RH. *NMR of Paramagnetic Molecules: Principles and Applications*. Mar GN La, Horrocks WD, Holm RH, editors. Elsevier; 2016.
121. Duynhoven J van, Voda A, Witek M, As H Van. Chapter 3 – Time-Domain NMR Applied to Food Products. In: *Annual Reports on NMR Spectroscopy V*. 2010. p. 145–197.
122. Brereton RG. *Applied chemometrics for scientists*. John Wiley & Sons; 2007.
123. Bro R, Smilde AK. Principal Component Analysis. *Anal Methods*. 2014;6:2812–31.
124. Yu L (Lucy), Cheng Z. Application of electron spin resonance (ESR) spectrometry in nutraceutical and food research. *Mol Nutr Food Res*. 2008;52:62–78.
125. Weil JA, Bolton JR. *Electron paramagnetic resonance: elementary theory and practical applications*. John Wiley & Sons; 2007.
126. Kuriena BT, Scofielda RH. Western Blotting. *Methods*. 2006;38(4):283–93.
127. Dalle-Donne I, Rossi R, Giustarini D, Milzani A, Colombo R. Protein carbonyl groups as biomarkers of oxidative stress. Vol. 329, *Clinica Chimica Acta*. 2003. p. 23–38.
128. Gallagher SR. One-dimensional SDS gel electrophoresis of proteins. In: Wilson K, Walker J, editors. *Current protocols in cell biology*. 2007. p. 6–1.
129. Tsai T-H, Tsai T-H, Wu W-H, Tseng JT-P, Tsai P-J. In vitro antimicrobial and anti-inflammatory effects of herbs against *Propionibacterium acnes*. *Food Chem*. 2010;119(3):964–8.
130. Bolumar T, Skibsted LH, Orlie V. Kinetics of the formation of radicals in meat during high pressure processing. *Food Chem*. 2012 Oct;134(4):2114–20.
131. Corrêa CC, Forato LA, Colnago LA. High-throughput non-destructive nuclear magnetic resonance method to measure intramuscular fat content in beef. *Anal Bioanal Chem*. 2008 Nov;393(4):1357–60.
132. Grossi A, Gkarane V, Otte JA, Ertbjerg P, Orlie V. High pressure treatment of brine enhanced pork affects endopeptidase activity, protein solubility, and peptide formation. *Food Chem*. 2012;134(3):1556–1563.
133. Ezequiel JMB, Galati RL, Mendes AR, Faturi C. Desempenho e características de carcaça de bovinos Nelore em confinamento alimentados com bagaço de cana-de-açúcar e diferentes fontes energéticas Performance and carcass characteristics of feedlot Nelore fed diets contain. *Rev Bras Zootec*. 2006;35(5):2050–7.

134. D'Oliveira; PS. IN do PGTDSESS. Effect of replacing soybean meal with canola meal on the performance of nellore feedlot heifers. *Brazilian J Anim Sci.* 1997;26:568–74.
135. LORENZONI, W. R., CAMPOS, J., GARCIA, J. A.; Silva JFC. Ganho de peso, eficiência alimentar e qualidade da carcaça de novilhos búfalos, Nelores, Holandeses e mestiços Holandês-Zebu. *Brazilian J Anim Sci.* 1986;16(6):486–97.
136. Gonthier M-P, Verny M-A, Besson C, Rémésy C, Scalbert A. Chlorogenic Acid Bioavailability Largely Depends on Its Metabolism by the Gut Microflora in Rats. *J Nutr.* 2003 Jun;133(6):1853–9.
137. Esteve V, Martínez-Granados B, Martínez-Bisbal MC. Pitfalls to be considered on the metabolomic analysis of biological samples by HR-MAS. *Anal Chem.* 2014;2:33.
138. Grossi AB, do Nascimento ESP, Cardoso DR, Skibsted LH. Proteolysis involvement in zinc–protoporphyrin IX formation during Parma ham maturation. *Food Res Int.* 2014 Feb;56:252–9.
139. Want EJ, Masson P, Michopoulos F, Wilson ID, Theodoridis G, Plumb RS, et al. Global metabolic profiling of animal and human tissues via UPLC-MS. *Nat Protoc.* 2013 Jan;8(1):17–32.
140. Mei L, Cromwell GL, Crum AD, Decker EA. Influence of dietary  $\beta$ -alanine and histidine on the oxidative stability of pork. *Meat Sci.* 1998 May;49(1):55–64.
141. Djenane D, Martínez L, Sánchez-Escalante A, Beltrán JA, Roncalés P. Antioxidant effect of carnosine and carnitine in fresh beef steaks stored under modified atmosphere. *Food Chem.* 2004 May;85(3):453–9.
142. Hoppel C. The role of carnitine in normal and altered fatty acid metabolism. *Am J Kidney Dis.* 2003 Apr;41, Supple:S4–12.
143. Fritz IB, McEwen B. Effects of carnitine on fatty-acid oxidation by muscle. *Am Assoc Adv Sci Sci.* 1959;129:334–5.
144. Rasmussen BB, Wolfe RR. Regulation of Fatty Acid Oxidation in Skeletal Muscle. *Annu Rev Nutr.* 1999;19(1):463–84.
145. Trabi M, Keller MD, Jonsson NN. NMR-based metabonomics of bovine blood: an investigation into the effects of long term storage on plasma samples. *Metabolomics.* 2013 Mar;9(5):1041–7.
146. Churchward-Venne TA, Burd NA, Mitchell CJ, West DWD, Philp A, Marcotte GR, et al. Supplementation of a suboptimal protein dose with leucine or essential amino

- acids: effects on myofibrillar protein synthesis at rest and following resistance exercise in men. *J Physiol*. 2012 Jun;590(11):2751–65.
147. Dannert RD, Pearson AM. Concentration of Inosine 5'-Monophosphate in Meat. *J Food Sci*. 1967 Jan;32(1):49–52.
  148. Jones NR. Meat and fish flavors; significance of ribomononucleotides and their metabolites. *J Agric Food Chem*. 1969 Jul;17(4):712–6.
  149. Polovka M (Food RI. EPR spectroscopy: A tool to characterize stability and antioxidant properties of foods. *J Food Nutr Res (Slovak Republic)*. 2006;
  150. Kingston E r., Monahan F j., Buckley D j., Lynch P b. Lipid Oxidation in Cooked Pork as Affected by Vitamin E, Cooking and Storage Conditions. *J Food Sci*. 1998 May;63(3):386–9.
  151. Lee BJ, Hendricks DG, Cornforth DP. Antioxidant Effects of Carnosine and Phytic Acid in a Model Beef System. *J Food Sci [Internet]*. 1998;63(3):394–8. Available from: <http://onlinelibrary.wiley.com/doi/10.1111/j.1365-2621.1998.tb15750.x/abstract>  
[http://onlinelibrary.wiley.com/store/10.1111/j.1365-2621.1998.tb15750.x/asset/j.1365-2621.1998.tb15750.x/pdf?v=1&t=imnygipa&s=cf99be2e9cd75ffa7beb1451b7c1f4445ac0e25a](http://onlinelibrary.wiley.com/store/10.1111/j.1365-2621.1998.tb15750.x/asset/j.1365-2621.1998.tb15750.x.pdf?v=1&t=imnygipa&s=cf99be2e9cd75ffa7beb1451b7c1f4445ac0e25a)
  152. Decker EA, Crum AD. Antioxidant activity of carnosine in cooked ground pork. *Meat Sci*. 1993 Jan;34(2):245–53.
  153. Saiga A, Tanabe S, Nishimura T. Antioxidant Activity of Peptides Obtained from Porcine Myofibrillar Proteins by Protease Treatment. *J Agric Food Chem*. 2003 Jun;51(12):3661–7.
  154. Kohen R, Yamamoto Y, Cundy KC, Ames BN. Antioxidant activity of carnosine, homocarnosine, and anserine present in muscle and brain. *Med Sci*. 1988;85(9):3175–9.
  155. Hayek MG, Han SN, Wu D, Watkins BA, Meydani M, Dorsey JL, et al. Dietary Conjugated Linoleic Acid Influences the Immune Response of Young and Old C57BL/6NCrIBR Mice. *J Nutr*. 1999 Jan;129(1):32–8.
  156. Heuvel JP Vanden. Peroxisome Proliferator–Activated Receptors: A Critical Link among Fatty Acids, Gene Expression and Carcinogenesis. *J Nutr*. 1999 Feb;129(2):575S–580S.
  157. Nicolosi RJ, Rogers EJ, Kritchevsky D, Scimeca JA, Huth PJ. Dietary conjugated linoleic acid reduces plasma lipoproteins and early aortic atherosclerosis in

- hypercholesterolemic hamsters. *Artery*. 1996 Dec;22(5):266–77.
158. Muchenje V, Dzama K, Chimonyo M, Strydom PE, Hugo A, Raats JG. Some biochemical aspects pertaining to beef eating quality and consumer health: A review. *Food Chem*. 2009 Jan;112(2):279–89.
  159. Rodrigues VC, Andrade IF de. Características físico-químicas da carne de bubalinos e de bovinos castrados e inteiros. *Rev Bras Zootec*. 2004;
  160. Huff-Lonergan E, Lonergan SM. Mechanisms of water-holding capacity of meat: The role of postmortem biochemical and structural changes. *Meat Sci*. 2005 Sep;71(1):194–204.
  161. Törnvall U. Pinpointing oxidative modifications in proteins—recent advances in analytical methods. *Anal Methods*. 2010;2:1638–50.
  162. Claeys E, Uytterhaegen L, Buts B, Demeyer D. Quantification of beef myofibrillar proteins by SDS-PAGE. *Meat Sci*. 1995;39(2):177–93.
  163. Pazos M, Andersen ML, Skibsted LH. Amino Acid and Protein Scavenging of Radicals Generated by Iron/Hydroperoxide System: An Electron Spin Resonance Spin Trapping Study. *J Agric Food Chem*. 2006;54(26):10215–10221.
  164. Jongberg S, Lund MN, Waterhouse AL, Skibsted LH. 4-Methylcatechol Inhibits Protein Oxidation in Meat but Not Disulfide Formation. *J Agric Food Chem*. 2011;59(18):10329–10335.
  165. Keszler A, Mason RP, Hogg N. Immuno-spin trapping of hemoglobin and myoglobin radicals derived from nitrite-mediated oxidation. *Free Radic Biol Med*. 2006;40(3):507–515.
  166. Dalle-Donne I, Rossi R, Giustarini D, Gagliano N, Lusini L, Milzani A, et al. Actin carbonylation: From a simple marker of protein oxidation to relevant signs of severe functional impairment. *Free Radic Biol Med*. 2001;31(9):1075–83.
  167. Santé-Lhoutellier V, Engel E, Aubry L, Gatellier P. Effect of animal (lamb) diet and meat storage on myofibrillar protein oxidation and in vitro digestibility. Vol. 79, *Meat Science*. 2008. p. 777–83.
  168. Becker BF. TOWARDS THE PHYSIOLOGICAL FUNCTION OF URIC ACID. *Free Radic Biol Med*. 1993;14:615–31.
  169. Sautin YY, Johnson RJ. Uric acid: the oxidant–antioxidant paradox. *Nucleosides Nucleotides Nucleic Acids*. 2010;27(6):608–19.
  170. Simic MG, Jovanovic S V. Antioxidation mechanisms of uric acid. *J Am Chem Soc*. 1989;111(14):5778–82.

171. Amic A, Markovic Z, Dimitric JM, Luc B, Stepanic V, Amic D. The The 2H+/2e-free free radical scavenging mechanisms of uric acid : thermodynamics of N-H bond cleavage. *Comput Theretical Chem.* 2016;1077:2–10.
172. Chong DP. Theoretical Study of Uric Acid and its Ions in Aqueous Solution. *Theor Comput Sci.* 2013;1(1):1–7.
173. Kelley WN, Rosenbloom FM, Henderson JF, Seegmiller JE. Overproduction of Uric Acid. *Proc Natl Acad Sci.* 1967;57(6):1735–9.
174. Glantzounis GK, Tsimoyiannis EC, Kappas AM, Galaris DA. Uric acid and oxidative stress. *Curr Pharm Des.* 2005;11(32):4145–51.
175. Cameron MA, Sakhae K. Uric Acid Nephrolithiasis. *Urol Clin North Am.* 2007;34(3):335–46.
176. Johnson RJ, Kang DH, Feig D, Kivlighn S, Kanellis J, Watanabe S, et al. Is there a pathogenetic role for uric acid in hypertension and cardiovascular and renal disease? *Hypertension.* 2003;41(6):1183–90.
177. Fang J, Alderman MH. Serum Uric Acid and Cardiovascular Mortality. *Jama* [Internet]. 2000;283(5):2404. Available from: <http://jama.jamanetwork.com/article.aspx?doi=10.1001/jama.283.18.2404>
178. Yu KH, See LC, Huang YC, Yang CH, Sun JH. Dietary Factors Associated with Hyperuricemia in Adults. *Semin Arthritis Rheum.* 2008;37(4):243–50.
179. Lorrain B, Dangles O, Genot C, Dufour C. Chemical modeling of heme-induced lipid oxidation in gastric conditions and inhibition by dietary polyphenols. *J Agric Food Chem.* 2010;58(1):676–83.
180. Lorrain B, Dufour C, Dangles O. Influence of serum albumin and the flavonol quercetin on the peroxidase activity of metmyoglobin. *Free Radic Biol Med.* 2010;48(9):1162–72.
181. Giulivi C, Cadenas E. HEME PROTEIN RADICALS: FORMATION, FATE, AND BIOLOGICAL CONSEQUENCES. *Free Radic Biol Med.* 1998;24(2):269–79.
182. Horner JH, Sheng X, Chandrasena REP, Zhang R, Wan Q, Newcomb M. Compounds I by Photo-Oxidation of Compounds II. *ECS Trans* [Internet]. 2009;19(13):71–80. Available from: <http://ecst.ecsdl.org/content/19/13/71.short>
183. Ames BN, Cathcart R, Schwiers E, Hochstein P. Uric acid provides an antioxidant defense in humans against oxidant- and radical-caused aging and cancer: a hypothesis. *Proc Natl Acad Sci U S A* [Internet]. 1981;78(11):6858–62. Available from:

- <http://www.pubmedcentral.nih.gov/articlerender.fcgi?artid=349151&tool=pmcentrez&rendertype=abstract>
184. Choi HK, Liu S, Curhan G. Intake of purine-rich foods, protein, and dairy products and relationship to serum levels of uric acid: The third national health and nutrition examination survey. *Arthritis Rheum.* 2005;52(1):283–9.
  185. Pai BHS, Swarnalatha G, Ram R, Dakshinamurty K V. Allopurinol for prevention of progression of kidney disease with hyperuricemia. *Indian J Nephrol* [Internet]. 2013;23(4):280–6. Available from: <http://www.pubmedcentral.nih.gov/articlerender.fcgi?artid=3741973&tool=pmcentrez&rendertype=abstract>
  186. Rocha BS, Lundberg JO, Radi R, Laranjinha J. Role of nitrite, urate and pepsin in the gastroprotective effects of saliva. *Redox Biol* [Internet]. 2016;8:407–14. Available from: <http://dx.doi.org/10.1016/j.redox.2016.04.002>
  187. No Title. <http://watcut.uwaterloo.ca/webnotes/Metabolism/Nucleotides.html#sec-nucleotidesPurineDegradationSalvage>.
  188. Telo JP. Radicals derived from uric acid and its methyl derivatives in aqueous solution: an EPR spectroscopy and theoretical study. *Org Biomol Chem* [Internet]. 2003;1(3):588–92. Available from: <http://xlink.rsc.org/?DOI=b208827b>
  189. Bergmann F, Dikstein S. The Relationship between Spectral Shifts and Structural Changes in Uric Acids and Related Compounds. *J Am Chem Soc.* 1955;77(3):691–6.
  190. Wang C, Yuan R, Chai Y, Chen S, Hu F, Zhang M. Simultaneous determination of ascorbic acid, dopamine, uric acid and tryptophan on gold nanoparticles/overoxidized-polyimidazole composite modified glassy carbon electrode. *Anal Chim Acta.* 2012;741:15–20.
  191. Seidel A, Parker H, Turner R, Dickerhof N, Khalilova IS, Wilbanks SM, et al. Uric acid and thiocyanate as competing substrates of lactoperoxidase. *J Biol Chem.* 2014;289(32):21937–49.
  192. Cooper CE, Silaghi-Dumitrescu R, Rukengwa M, Alayash AI, Buehler PW. Peroxidase activity of hemoglobin towards ascorbate and urate: A synergistic protective strategy against toxicity of Hemoglobin-Based Oxygen Carriers (HBOC). *Biochim Biophys Acta - Proteins Proteomics.* 2008;1784(10):1415–20.
  193. Carlsen CU, Kröger-Ohlsen M V., Bellio R, Skibsted LH. Protein binding in deactivation of ferrylmyoglobin by chlorogenate and ascorbate. *J Agric Food Chem.*

- 2000;48(2):204–12.
194. Mikkelsen A, Skibsted LH. Acid-Catalyzed Reduction of Ferrylmyoglobin - Product Distribution and Kinetics of Autoreduction and Reduction By NaDH. *Zeitschrift Fur Leb Und-forsch* [Internet]. 1995;200(3):171–7. Available from: <Go to ISI>://WOS:A1995QM21000002
  195. Libardi SH, Pindstrup H, Amigo JM, Cardoso DR, Skibsted LH. Reduction of ferrylmyoglobin by cysteine as affected by pH. *RSC Adv.* 2014;4(105):60953–8.
  196. Jørgensen L V, Andersen HJ, Skibsted LH. Kinetics of reduction of hypervalent iron in myoglobin by crocin in aqueous solution. *Free Radic Res.* 1997;27(1):73–87.
  197. Reeder BJ, Cutruzzola F, Bigotti MG, Hider RC, Wilson MT. Tyrosine as a redox-active center in electron transfer to ferryl heme in globins. *Free Radic Biol Med.* 2008;44(3):274–83.
  198. Reeder BJ, Grey M, Silaghi-Dumitrescu RL, Svistunenko DA, Bülow L, Cooper CE, et al. Tyrosine residues as redox cofactors in human hemoglobin: Implications for engineering nontoxic blood substitutes. *J Biol Chem.* 2008;283(45):30780–7.
  199. Warren JJ, Tronic TA, Mayer JM. Thermochemistry of proton-coupled electron transfer reagents and its implications. *Chem Rev.* 2010;110(12):6961–7001.
  200. <https://www.photophysics.com/lab/stopped-flow-spectroscopy-beginners-guide>.  
<https://www.photophysics.com/lab/stopped-flow-spectroscopy-beginners-guide>.
  201. Bugnon P, Chott J, Jestin J, Jung B, Laurency G, Maeder M, et al. Second-order globalisation for the determination of activation parameters in kinetics. *Anal Chim Acta.* 1994;298:193–201.
  202. Wilkins RG. Kinetics and mechanism of reactions of transition metal complexes. 2nd ed. Weinheim; 1991.
  203. George BYP, Irvine DH. A Possible Structure for the Higher Oxidation State of Metmyoglobin. *Biochem J.* 1955;60(4):596.
  204. Taylor JF, Morgan VE. Oxidation-reduction potentials of the metmyoglobin-myoglobin system. *J Biol Chem.* 1942;144(1):15–20.
  205. Tsuruga M, Matsuoka A, Sugawara Y. The Molecular Mechanism of Autoxidation for Hemoglobin. *J Biol Chem.* 1998;273(10):8607–15.
  206. Romeros FJ, Ordoñez I, Arduini A, Cadenas E. The Reactivity of Thiols and Disulfides with Different Redox States of Myoglobin. *J Biol Chem.* 1992;267(3):1680–8.
  207. Wilcox WR, Khalaf A, Weinberger A, Kippen I, Klinenberg JR. Solubility of Uric

- Acid and Monosodium Urate. *J Med Biol Eng.* 1972;10:522–31.
208. Litwinienko G, Ingold KU. Solvent Effects on the Rates and Mechanisms of Reaction of Phenols with Free Radicals Solvent Effects on the Rates and Mechanisms of Reaction of Phenols with Free Radicals. *Acc Chem Res.* 2007;40(3):222–30.

## APPENDIX A

**Figure A 1.** (A) Stopped-flow kinetic traces for the reduction of ferryl myoglobin by uric acid and (B) dependence of  $k_{\text{obs}}$  on uric acid concentration at 25 °C. Conditions:  $5 \times 10^3 \text{ mol L}^{-1}$  acetate buffer pH 5.3 containing  $1 \times 10^3 \text{ mol L}^{-1}$  of EDTA;  $[\text{MbFe(IV)=O}]_0 = 15 \times 10^6 \text{ mol L}^{-1}$ . Second-order rate constants found by linear regression was  $826 \pm 42 \text{ L mol}^{-1} \text{ s}^{-1}$ .

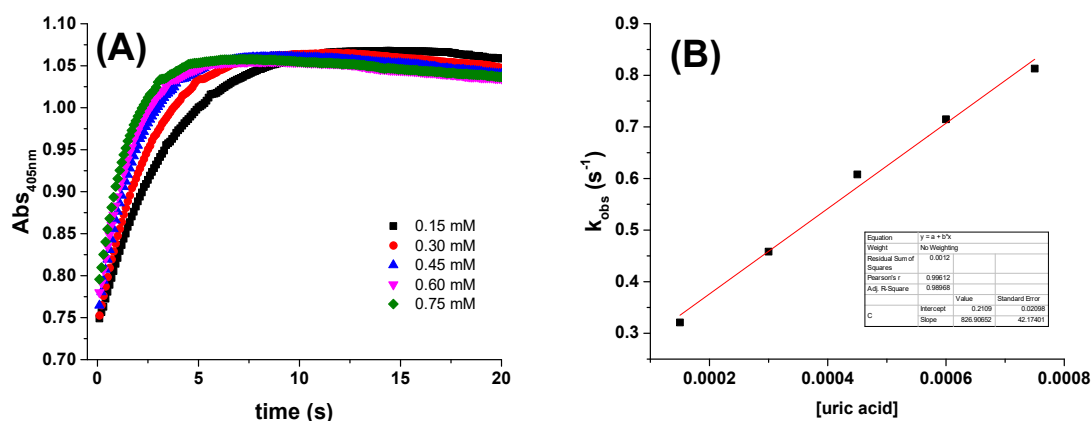


**Figure A 2.** (A) Stopped-flow kinetic traces for the reduction of ferryl myoglobin by uric acid and (B) dependence of  $k_{\text{obs}}$  on uric acid concentration at 25 °C. Conditions:  $5 \times 10^3 \text{ mol L}^{-1}$  acetate buffer pH 5.5 containing  $1 \times 10^3 \text{ mol L}^{-1}$  of EDTA;  $[\text{MbFe(IV)=O}]_0 = 15 \times 10^6 \text{ mol L}^{-1}$ . Second-order rate constants found by linear regression was  $733 \pm 17 \text{ L mol}^{-1} \text{ s}^{-1}$ .

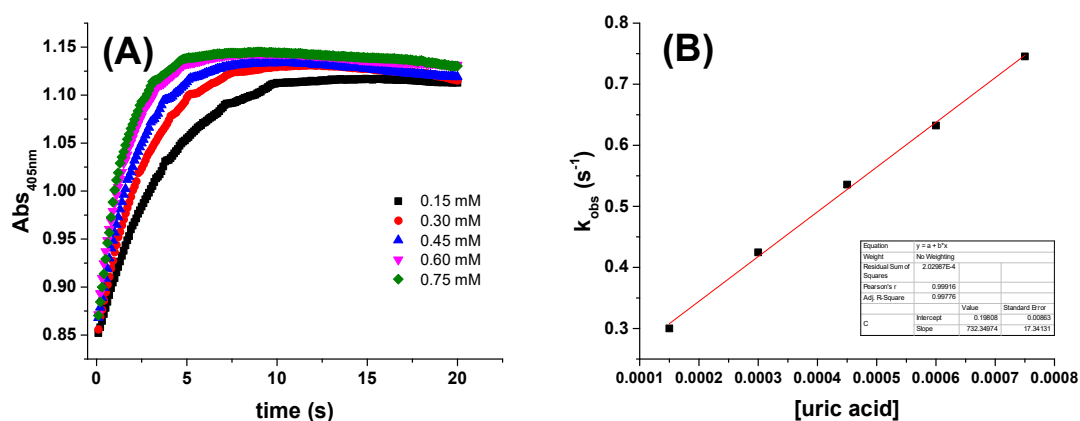


**Figure A 3.** (A) Stopped-flow kinetic traces for the reduction of ferryl myoglobin by uric acid and (B) dependence of  $k_{\text{obs}}$  on uric acid concentration at 25 °C. Conditions:  $5 \times 10^3 \text{ mol L}^{-1}$  acetate buffer pH 5.6 containing  $1 \times 10^3 \text{ mol L}^{-1}$  of EDTA;  $[\text{MbFe(IV)=O}]_0 = 15 \times 10^6 \text{ mol L}^{-1}$ . Second-order rate constants found by linear regression was  $663 \pm 6 \text{ L mol}^{-1} \text{ s}^{-1}$ .

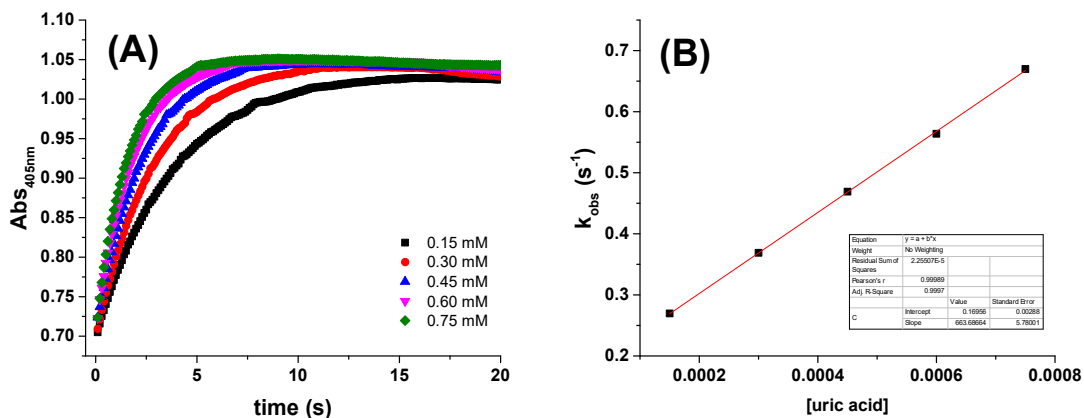


**Figure A 4.** (A) Stopped-flow kinetic traces for the reduction of ferryl myoglobin by uric acid and (B) dependence of  $k_{\text{obs}}$  on uric acid concentration at 25 °C. Conditions:  $5 \times 10^3 \text{ mol L}^{-1}$  phosphate buffer pH 5.8 containing  $1 \times 10^3 \text{ mol L}^{-1}$  of EDTA;  $[\text{MbFe(IV)=O}]_0 = 15 \times 10^6 \text{ mol L}^{-1}$ . Second-order rate constants found by linear regression was  $522 \pm 16 \text{ L mol}^{-1} \text{ s}^{-1}$ .

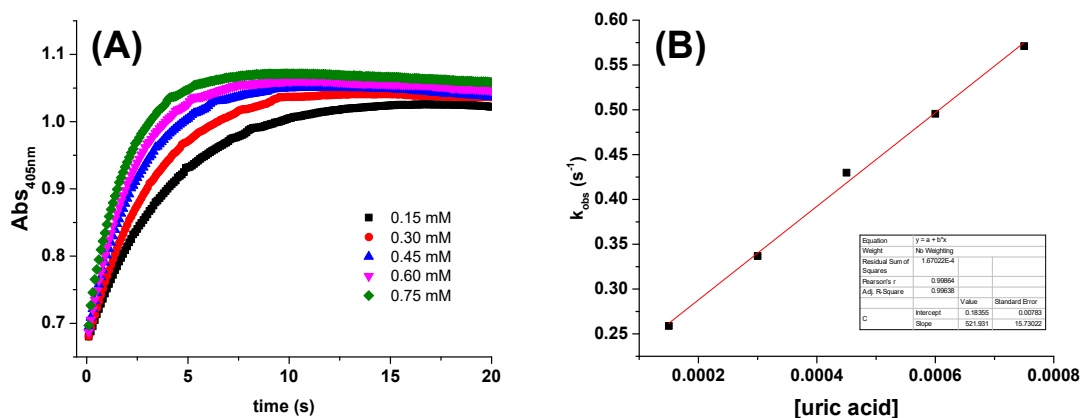


**Figure A 5.** (A) Stopped-flow kinetic traces for the reduction of ferryl myoglobin by uric acid and (B) dependence of  $k_{\text{obs}}$  on uric acid concentration at 25 °C. Conditions:  $5 \times 10^3 \text{ mol L}^{-1}$  phosphate buffer pH 5.9 containing  $1 \times 10^3 \text{ mol L}^{-1}$  of EDTA;  $[\text{MbFe(IV)=O}]_0 = 15 \times 10^6 \text{ mol L}^{-1}$ . Second-order rate constants found by linear regression was  $405 \pm 8 \text{ L mol}^{-1} \text{ s}^{-1}$ .

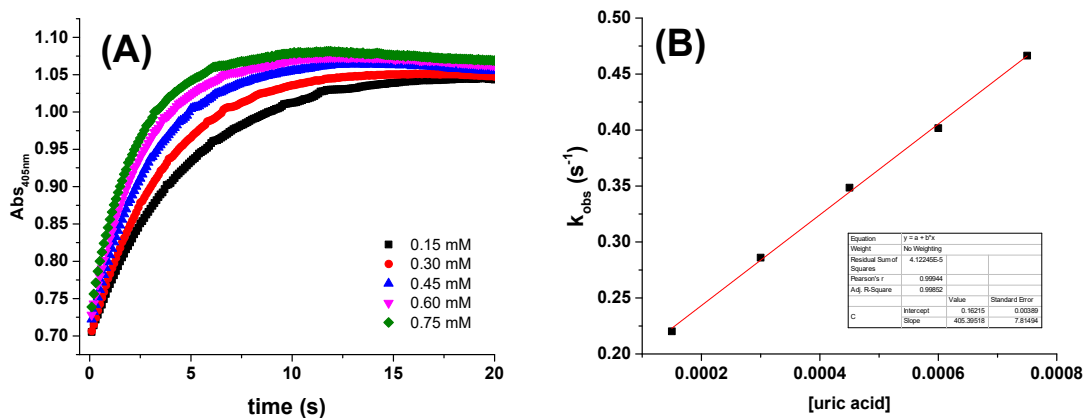


**Figure A 6.** (A) Stopped-flow kinetic traces for the reduction of ferryl myoglobin by uric acid and (B) dependence of  $k_{\text{obs}}$  on uric acid concentration at 25 °C. Conditions:  $5 \times 10^3 \text{ mol L}^{-1}$  phosphate buffer pH 6.1 containing  $1 \times 10^3 \text{ mol L}^{-1}$  of EDTA;  $[\text{MbFe(IV)=O}]_0 = 15 \times 10^6 \text{ mol L}^{-1}$ . Second-order rate constants found by linear regression was  $279 \pm 18 \text{ L mol}^{-1} \text{ s}^{-1}$ .

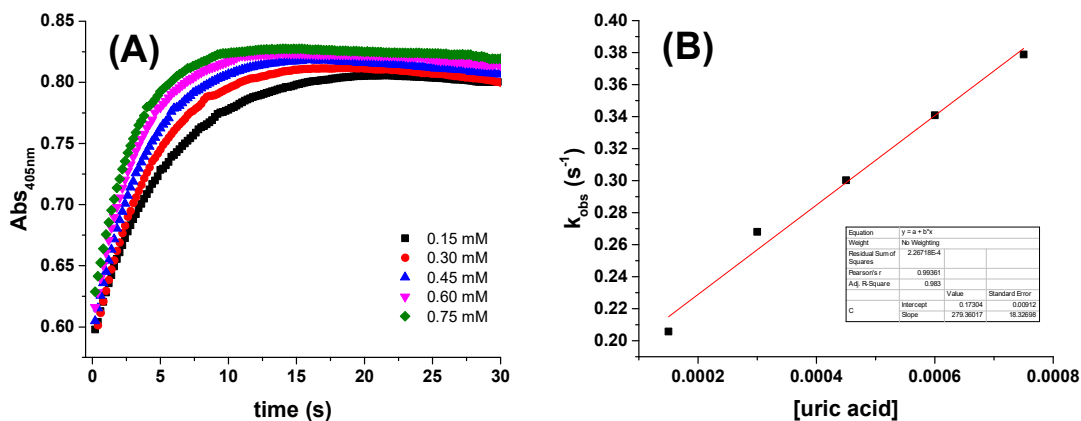


**Figure A 7.** (A) Stopped-flow kinetic traces for the reduction of ferryl myoglobin by uric acid and (B) dependence of  $k_{\text{obs}}$  on uric acid concentration at 25 °C. Conditions:  $5 \times 10^3 \text{ mol L}^{-1}$  phosphate buffer pH 6.5 containing  $1 \times 10^3 \text{ mol L}^{-1}$  of EDTA;  $[\text{MbFe(IV)=O}]_0 = 15 \times 10^6 \text{ mol L}^{-1}$ . Second-order rate constants found by linear regression was  $154 \pm 11 \text{ L mol}^{-1} \text{ s}^{-1}$ .

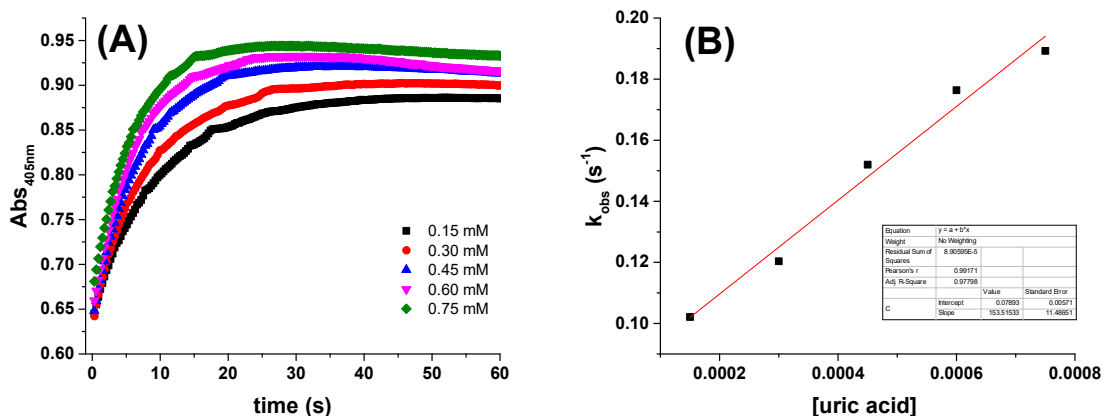


**Figure A 8.** (A) Stopped-flow kinetic traces for the reduction of ferryl myoglobin by uric acid and (B) dependence of  $k_{\text{obs}}$  on uric acid concentration at 25 °C. Conditions:  $5 \times 10^3 \text{ mol L}^{-1}$  phosphate buffer pH 7 containing  $1 \times 10^3 \text{ mol L}^{-1}$  of EDTA;  $[\text{MbFe(IV)=O}]_0 = 15 \times 10^6 \text{ mol L}^{-1}$ . Second-order rate constants found by linear regression was  $30 \pm 2 \text{ L mol}^{-1} \text{ s}^{-1}$ .

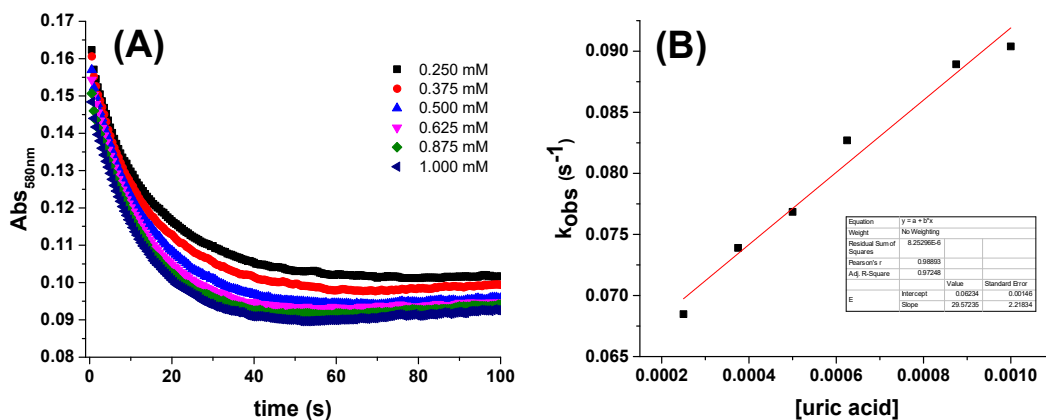


**Figure A 9.**(A) Stopped-flow kinetic traces for the reduction of ferryl myoglobin by uric acid and (B) dependence of  $k_{\text{obs}}$  on uric acid concentration at 25 °C. Conditions:  $5 \times 10^3 \text{ mol L}^{-1}$  phosphate buffer pH 7.5 containing  $1 \times 10^3 \text{ mol L}^{-1}$  of EDTA;  $[\text{MbFe(IV)=O}]_0 = 15 \times 10^6 \text{ mol L}^{-1}$ . Second-order rate constants found by linear regression was  $14 \pm 1 \text{ L mol}^{-1} \text{ s}^{-1}$ .

